Facultad de Ciencias
Departamento de Biología Molecular

Tesis Doctoral

miR-127-3p as a novel mediator in fibrosis development and macrophage polarization in Chronic Kidney Disease

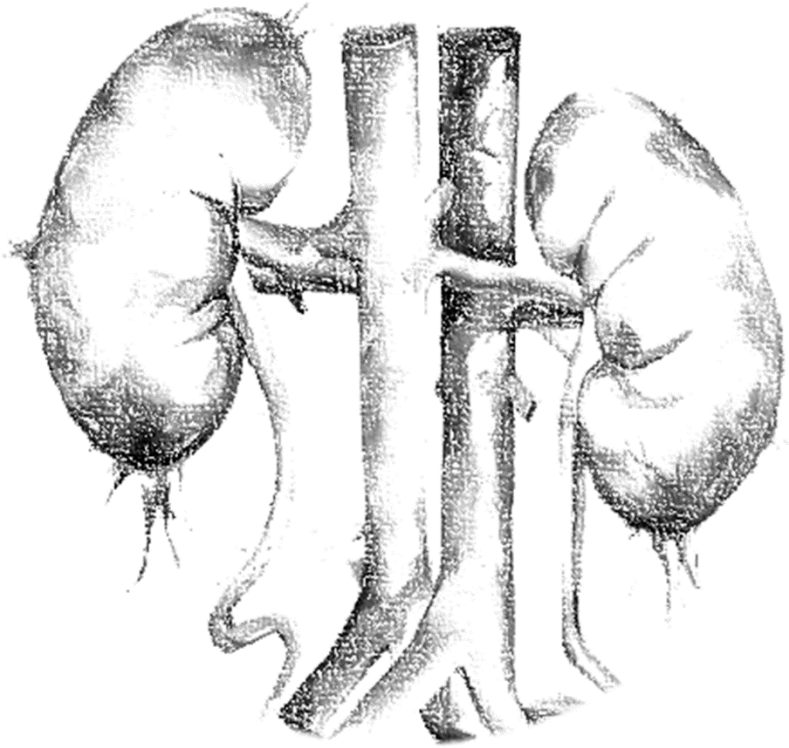

Sara Giménez Moyano

Madrid, 2021

UNIVERSIDAD AUTÓNOMA DE MADRID

FACULTAD DE CIENCIAS

Departamento de Biología Molecular

TESIS DOCTORAL

miR-127-3p as a novel mediator in fibrosis development and macrophage polarization in Chronic Kidney Disease

MEMORIA PARA OPTAR AL GRADO DE DOCTOR

PRESENTADO POR

Sara Giménez Moyano

Graduada en Biología

DIRIGIDO POR

Dra. María Laura García Bermejo (Directora)

Dra. Elisa Conde Moreno (Directora)

Dr. Manuel Fresno Escudero (Tutor)

Instituto Ramón y Cajal de Investigación Sanitaria (IRYCIS)

Hospital Ramón y Cajal

“Para empezar un gran proyecto hace falta valentía. Para terminar un gran proyecto hace falta perseverancia” (Anónimo).

A mis padres,

por ser siempre un apoyo incondicional.

Acknowledgements

Todos aquellos que me conocen, aunque sea sólo un poquito, saben que viajar es una de mis mayores pasiones. Esto no es porque sí, por el mero hecho de "estar de vacaciones" (que también, eso nos gusta a todos), sino porque para mí un viaje es la oportunidad perfecta para conocer nuevos lugares, nuevas personas y nuevas costumbres. También es enfrentarte sólo, o junto con aquellos que te acompañen, a nuevas situaciones, sensaciones y retos. En definitiva, para mí, viajar es crecer, y ese, por encima de todo, constituye el principal motivo por el que amo viajar. Viajar se dice pronto, "viajar, viajo, viajé…", pero conlleva mucho. Un viaje comienza en el momento en el que lo piensas. Luego tienes que prepararte para ello: qué necesitas llevar en tu maleta, qué necesitas saber o aprender antes de llegar a tu destino, y cuáles son los lugares que allí te gustaría visitar. Terminado el proceso de preparación, ahora sí, por fin llega el momento principal, la aventura. Habrá cosas que salgan o sean como las habías pensado, otras no, serán mejor o peor que las expectativas que tenías. A veces, incluso, si el viaje es largo, puedes llegar a echar de menos tus cosas y tu rutina, o incluso pensar que quizá hubiera sido mejor escoger otro destino. Pero sin duda, al volver a casa, la sensación que te invade sobre lo vivido ¡lo merece todo! Pero, además, un viaje no termina aquí, lo cierto es que te acompaña durante toda tu vida, tanto por los recuerdos generados, como por todos los aprendizajes que te aportó, los cuales, sin que te hayas dado mucha cuenta, han contribuido a construir quién eres.

Como ya he dicho, viajar es una de mis pasiones, pero todo esto que escribo aquí tan solo lo hago porque quiero compartir con todos vosotros que para mí la tesis ha sido y creo que será EL VIAJE MÁS ESPECIAL DE MI VIDA.

Tras esta bonita analogía que pone en valor lo importante que ha sido para mí esta etapa, me gustaría comenzar dando el primer "gracias" a la que ha sido (y será, esto ya lo hemos acordado) mi mentora, la Dra. Laura García Bermejo. Podría escribir horas sobre ti y todo lo que tengo que agradecerte. Gracias por confiar en mí y apostar por toda esa motivación y deseo de "ser científica". También por compartir tu laboratorio, tu tiempo, y tu mente extraordinaria conmigo. Por ser una persona cercana, y a la vez una líder capaz de motivar con refuerzo positivo a todos aquellos que estamos a tu alrededor. Es mucho lo que me llevo aprendido de ti. Si tuviera que describirte de alguna manera, sería como una persona que con sus enseñanzas y dedicación es capaz de otorgar fosforescencia a los demás. Haces que la gente brille con luz propia. GRACIAS.

Como no podía ser de otra manera, mi siguiente "gracias" es para la Dra. Elisa Conde Moreno, sin la que este trabajo no hubiera sido posible. Ella ha sido "el ojo que todo lo ve", la persona a la que le debo gran parte del resultado final de esta tesis con sus numerosas aportaciones de ideas, revisiones de resultados, apoyo en la búsqueda de bibliografía, etc. En definitiva, mi "comodín de la llamada y del público" ya que siempre ha estado ahí tanto para dar respuesta a mis dudas, como para tranquilizarme en los momentos de agobio. Además de todo esto, de ti me llevo tu compañerismo, tu capacidad para hacer equipo y para sentir a las personas cuando lo necesitan. Sabes (porque ya te lo he dicho en alguna ocasión), que tienes un conjunto de valores muy bonito, y esto, es una de las cosas, entre otras muchas, por las que tú para mí también eres una líder. GRACIAS.

Por supuesto, el próximo GRACIAS, además INFINITO, es para el resto del "*Integration Lab*". Todas y cada una sois maravillosas. Nada de esto hubiera sido lo mismo sin vosotras. No os podéis imaginar cuanto me ha marcado compartir estos años con vosotras y lo importantes que sois para mí (esto también aplica a las "jefis"). Juntas hemos reído, reído mucho, llorado (de emoción, tristeza, y alegría), nos hemos hasta enfadado unas con otras para volver a reconciliarnos enseguida, porque si algo tiene de especial el laboratorio es que somos una gran familia en la que cada una tiene su lugar y su hueco, y todas somos importantes para las demás. A Maqui, como no, mi compi de mesa y alegría del laboratorio. Hasta en los peores días tienes una sonrisa para todo aquel que esté a tu lado. Hemos compartido muchas cosas juntas, me atrevería a decir que más fuera del trabajo que dentro, has sido y serás confidente y amiga para siempre. Gracias por estar siempre ahí "armando jaleo" y también por tus consejitos de

"mami" siempre que lo he necesitado. A Edurne, gracias por estar siempre dispuesta a echar una mano, por darme tu opinión en momentos clave y por esa mudanza que nos "comimos" mano a mano compartiendo además de cansancio, la alegría de un nuevo espacio. A Lore, mi "kuki", llegaste al labo aportando millones de ideas y con el absoluto deseo de colaborar, eres de las personas que conozco que más se implican e involucran con los demás cuando lo necesitan, poniendo además el corazón en todo lo que haces. Gracias por tu apoyo y ánimos en todo momento. A Carol, qué te voy a contar yo de esta tesis que no sepas Caroli, si has sido mi mano derecha, mi segunda de a bordo estos últimos dos años y ¡mi compañera de fatigas en el "*in vivo*"! Gracias por todo el trabajo con el que me has ayudado, pero sobre todo por haberlo hecho con todo ese mimo, dedicación y constancia que te caracterizan. A Lauri, mi Sali o Salini, gracias por haber sido una compañera diez y un ejemplo a seguir, de ti me llevo la paciencia y templanza que le pones a todo, y por supuesto, los mil y un planes que nos quedan por compartir. A Patri, porque a pesar de que te seguimos llamando "nuevi", llevas ya un añito formando parte de esta familia, y ¡qué añito además! Gracias por adaptarte tan rápido y aportar todos tus conocimientos y ayuda siempre que has podido. A Irene, con la que he podido compartir muy poquito tiempo de trabajo, pero sin duda (alguna, además) sí compartiré muchas aventuras, gracias por apuntarte a un bombardeo. A Silvi, Sil, Silse, Silvitone, Silvitoña, "mi compi predoc", "mi veci", "esa Sagi", mil nombres te puedo poner, tantos como razones para agradecerte todo el tiempo que hemos pasado juntas tanto en el labo como fuera de él. Gracias por haberte cruzado en mi vida, de la cual espero que no salgas nunca. Gracias también por estar siempre dispuesta a ayudar a cualquiera que lo necesite con tu apoyo incondicional, pero sobre todo por la alegría con la que inundas el labo cada día. Por último, quería dar las gracias a los/las que habéis seguido vuestros caminos y ya no estáis en el grupo trabajando, pero sí merecéis un hueco en estas líneas. Elia, gracias por hacerme sentir como en casa cuando he estado tan lejos de ella, por tus súper consejos para entender la "mente estadounidense" y por tus "¿qué tal lo llevas?" que tanto me han animado a continuar. Es increíble como estando tan lejos siempre has conseguido que te sintamos tan cerca. Padi, Jorgi y Martis, gracias por vuestro tiempo compartido conmigo, por vuestro apoyo, y ánimos recibidos, ¡objetivo conseguido!

No podía olvidarme de Kostas, nuestro "as en la manga en biología molecular". GRACIAS por toda la ayuda con los clonajes, diseño de vectores, y por formar parte de ese equipo de apoyo a distancia cuando más lo necesitaba en USA, aportando todo tu conocimiento cuando mi mente "cata-crokeaba" como si de hablar en chino se tratase.

Tampoco podían faltar en estas páginas Bruno y el personal de su laboratorio. A Bruno, muchas GRACIAS por compartir todo tu conocimiento conmigo y orientarme en los momentos clave. También por poner a mi disposición los recursos de tu laboratorio cuando lo hemos necesitado. Espero tus preguntas derivadas de este trabajo, sé a ciencia cierta que aprenderé muchísimo con ellas. A Lala, gracias por tu inestimable ayuda en estos últimos meses.

Una parte importante en esta sección, debe ir dirigida también a la Dra. Gema Juárez, al Dr. Francisco Díaz y al Dr. Javier Villacorta, en resumen "Equipo Vasculitis". Ellos fueron (sin saberlo) mi primera colaboración con clínicos. Gracias a todos y cada uno de vosotros por haberme enseñado cómo de productivo puede ser la interacción entre investigadores y médicos. Para mí sois un ejemplo de grupo clínico con el que colaborar. Pero sobretodo quiero daros las gracias por la buena acogida desde el principio y lo bien que me habéis hecho sentir siempre a la hora de aportar ideas y participar en el grupo. Quiero hacer una mención especial también al gran trabajado realizado por Fran y Jacqueline en el análisis de las muestras de tejido del modelo *in vivo* que se incluye en esta tesis. Valoración que sin duda ha aportado enormemente al trabajo y de la que estoy muy agradecida. Muchas GRACIAS de corazón.

A Silvi, la rubia dicharachera de la -3, ¿puedes contar la de veces que he ido pidiéndote consejo sobre una técnica u otra en estos años? Se me escapan de todas las que han sido. Muchas GRACIAS por tu entera disposición a ayudarme y por todo el cariño con el que siempre me has tratado.

Gracias también al grupo de "Onco", con los que compartimos espacio durante un largo tiempo. Y en especial gracias a Julie, siempre dispuesta a ayudar, y quien me permitía "usurpar" su campana de extracción durante las tardes de los viernes en mis inicios.

El personal del Servicio de Anatomía Patológica y del Servicio de Bioquímica del hospital también se merecen agradecimiento por mi parte, tanto por ayudarme en el análisis de las muestras líquidas de los animales, como por cederme su espacio de trabajo para procesar todos los tejidos de "mis bichitos" como ellos los llamaban, y orientarme en más de una ocasión. Gracias Álex, Tati, Marta (-3), Luis, y resto del equipo.

Por supuesto, un GRACIAS bien grande a todo el personal del Animalario de la Paz, bien merecido por toda su formación, orientación y apoyo durante mis interminables días de "*in vivo*".

Al Dr. Santiago Moreno. A él en especial tengo que agradecerle en buena parte la oportunidad que se me brindó de ir a "investigar a EEUU". Una experiencia con la que desde niña soñaba. Gracias por esto, ¡soñado y cumplido!

Por último, en cuanto a compañeros del hospital se refiere, GRACIAS a todo el personal de la "Funda" por transmitirme que las puertas del IRYCIS estarán siempre abiertas para mí. A Diego y Emma de innovación, con los que tuve la oportunidad de trabajar mano a mano en el Proyecto Caixa Impulse, aprender de ellos, y además… abrir nuevos horizontes…

Of course, thanks to my mates at Victor´s Lab in North Carolina University. I appreciate so much your support and dedication during mi time there. But, specially, I would like to send a huge THANK YOU to "The Caparroquians" people. María, Greg, Sanjeev, Marco, and finally Dorsaf, my partner in crime. I will always be grateful for the warm welcome I had, you made unforgettable my experience there. To Maria "la Española", thanks heartily for being so close to me those months and always has a great advice to give me, I remember you very fondly. And, to finish, to Jarrod. There are not words enough to say "THANK YOU". You were my family there, and I hope my friend forever.

También, quiero darle las gracias a mi amiga Irina, a la que curiosamente siempre siento muy cerca cuanto más lejos estoy yo. Gracias "Irinocito" por las tardes que me acompañaste al teléfono en mis 40 minutos de camino a casa al salir del laboratorio en USA, pero sobre todo por vivir y sentir cada uno de los momentos allí como si fueran tuyos. También por tus "perlitas" diarias con las que me motivabas a distancia, que, por cierto, ¡echo de menos!

Fuera del hospital y de la ciencia, también hay mucha gente a la que le debo mucho:

A Raquel, mi "sister", "mi soul mate", "mi otro yo". No importa cuánto estemos sin vernos porque al final cuando nos juntamos es como si el tiempo no hubiera pasado. Al igual que en muchas experiencias de mi vida, esta como no, también te la conoces al cien por cien. GRACIAS por tu apoyo siempre, ¡a disfrutar de este año, que es tan especial, como siempre juntas!

A mi amiga Eli. Para ti tengo un gran GRACIAS por transmitirme siempre lo orgullosa que estas de mí y de mi trabajo. Por la curiosidad con la que siempre te interesas por lo que hago, y por estar siempre pendiente de cuando este viaje llega a su fin, dándome ánimos. Pero también por compartir durante todos estos años un montón de aventuras, y hacer que mi faceta más "free & wild" siga en mí ¡Nos quedan millones de cosas por vivir juntas!

A la gente de Cani, cada uno de vosotros habéis hecho que me sienta realmente como si de toda la vida perteneciera a estas calles. GRACIAS por ponerlo tan fácil. Cuando inicié este viaje no os conocía todavía, pero sin duda cuento con vuestra compañía para el broche final ¡qué pena no poder celebrarlo con un Jose y luego Momazo! Aun así, hemos sabido reimaginar nuestros planes este año, y he de decir que no lo estamos pasando nada mal. Espero que sigamos sumando.

A toda mi familia, primas y tíos, pero en especial a mi "titi" querida, de la que gracias a sus "achurrukukus", como nos gusta llamar a nuestros abrazos, saco toda la energía para continuar hacia delante en mí carrera. A mis primas, Patri, Ali y Lauri, por haber sido mis hermanas. A mi hermano, ejemplo de constancia y valentía, uno de mis referentes. A Andrea, a la que no me gusta llamar cuñada porque ella, en realidad, es mucho más que eso. A mis suegros Pepa y Pedro, que a día de hoy han ocupado un gran hueco en mi corazón y forman parte de mi familia. Gracias por ser siempre "el apoyo", me hacéis muy afortunada. A mis "pitis", mis gatitos, Bichi y Maui, ellos no se enteran de nada de esto, pero sin saberlo me han hecho mucho más ameno todos esos días de escritura, transmitiéndome su paz y amor incondicional. Y como no, a mi abuelita Candi, que no tiene claro del todo lo que hago, pero sabe trasmitirme lo orgullosa que se siente de mí, y a mi abuelito Gaspar, que desde donde quiera que él nos esté viendo sé que sonríe y también se siente orgulloso.

Llega el momento de agradecer a algunas de las personas más importantes de mi vida. Quiero empezar con Alberto, mi compañero no solo de este, y todos los demás viajes, sino también de vida. GRACIAS por tu paciencia, tu comprensión, tu apoyo, y por todo lo que me has enseñado durante estos años (a pesar de ser el *baby* de la relación). GRACIAS por ser un punto de apoyo desde donde siempre levantarme y crecer. GRACIAS también por seguirme en todas "mis locuras" o al menos animarme a mí a hacerlas. GRACIAS por siempre buscar mi felicidad, pero también por aguantarme en mis momentos de más presión. Para mí representas el lugar donde me siento segura, donde quiero estar, porque haces que todo sea fácil, eres ese lugar clave en el mapa, eres lo que de niños en los juegos llamamos "casa".

Y por encima de todas las cosas, a mis padres. Es absolutamente impensable pensar que podría haber llegado hasta aquí sin vuestro apoyo incondicional. Gracias por estar siempre ahí para todo, y cuando digo todo, es todo, son las risas, los llantos, los consejos, los ánimos, las reprimendas, las felicitaciones, todo. GRACIAS, porque siempre me habéis dado toda la fuerza y confianza necesarias para hacerme pensar que puedo con ¡todo aquello que me proponga y más!, siempre cogiéndome de la mano y dándome el impulso oportuno. Por proyectar cada día todo vuestro amor y admiración que me hacen sentir tan especial. A vosotros os debo la persona en la que me he convertido, y sé que os sentís muy orgullosos de mí, porque me lo transmitís. Pero yo me siento más orgullosa de vosotros. Este momento es de los tres, porque todavía recuerdo como se os iluminaban los ojos cuando os decía ya de bien pequeña que quería ser Doctora en Biología, y cómo siempre me habéis apoyado y sabido motivar para no abandonar ese empeño. Como digo, el mérito no es sólo mío, este título es compartido con vosotros. GRACIAS.

¡GRACIAS A TOD@S POR HABERME ACOMPAÑADO EN ESTE MAGNÍFICO VIAJE!

Summary

Chronic Kidney Disease (CKD) is worldwide recognized as a priority health problem because of its high prevalence and incidence. It courses with a long clinically silent period, therefore diagnosis and treatment occur during advanced stages of the disease. Identification of molecular mechanisms underlying chronic renal injury and searching for early biomarkers of CKD are essential for improving our understanding of CKD pathophysiology and patient management.

microRNAs (miRNAs) are key regulators of gene expression that have emerged as a novel therapeutic target and useful biomarkers for pathology. In our lab we identified a set of miRNAs, including miR-127-3p, that remain altered after an AKI episode. We also demonstrated the protector role of miR-127-3p against ischemic injury in renal tubular cells. Moreover, bibliography has described miR-127-3p as a mediator in macrophage polarization during lung fibrosis. For all above, we aim to investigate the role of miR-127-3p in macrophage polarization during renal fibrosis underlying CKD and its modulation as a novel therapeutic strategy for the disease.

For this, we have studied miR-127-3p expression in a mouse model of renal fibrosis (UUO), and the effect of its exogenous modulation during disease development. We have demonstrated miR-127-3p increases along disease progression in proximal tubules, correlating with fibrosis and the inflammatory response in which macrophages are key cells involved. Besides, we have demonstrated that inhibition of miR-127-3p expression in UUO mice aggravates disease progression and exacerbates associated inflammatory response, including macrophages. Moreover, we have studied the expression of miR-127-3p and the effect of its modulation in naïve murine macrophages (Mϕ) and different induced phenotypes (M1[LPS] and M2[IL-4]). Results have shown that the expression of miR-127-3p does not change depending on the stimulus received. However, NOS2 expression, as a M1 macrophage marker, shows a positive tendency when the miRNA is inhibited in the cells. On the other hand, miRNA over-expression in the M2a [IL-4] phenotype leads to a decrease of NOS2, which suggests that the induction of miR-127-3p expression along the kidney injury modulate macrophages response and contribute to disease outcome. Based on these findings, we have tried different viral-based particles and administration approaches, and finally, we have successfully induced miR-127-3p expression in the renal cortex of mice using lentiviral particles injected through the renal arteria.

Finally, decreased serum levels of miR-146a-3p, miR-27a-3p, and miR-93-3p have been associated with CKD progression. Whereas miR-127-3p, miR-146a-3p, miR-27a-3p, and miR-26b-5p serum levels have demonstrated correlation with renal damage parameters.

In summary, all these results have revealed that miR-127-3p is involved in renal fibrosis as an important mediator of CKD development by affecting macrophages polarization, and therefore its modulation could be a potential therapeutic approach for CKD. Moreover, some studied miRNAs could serve as useful and minimum-invasive biomarkers that contribute to CKD stratification and patient management.

Resumen

La Enfermedad Renal Crónica (ERC) es un problema mundial de salud prioritario por su alta prevalencia e incidencia. Cursa con un largo período silencioso, lo que supone un diagnóstico y tratamiento ya en etapas avanzadas. La identificación de mecanismos moleculares subyacentes a la lesión renal y la búsqueda de biomarcadores precoces es fundamental para mejorar nuestra comprensión de la ERC y el manejo del paciente.

Los microARNs (miARNs) son reguladores de la expresión génica que han emergido como nuevas dianas terapéuticas y biomarcadores en distintas patologías. Previamente, identificamos un conjunto de miARNs, que incluye miR-127-3p, que permanecen alterados tras un episodio de IRA. También demostramos el papel protector de miR-127-3p en la lesión isquémica en células tubulares renales. Además, miR-127-3p se ha descrito como mediador en la polarización de macrófagos en fibrosis pulmonar. Apoyados en lo anterior, el objetivo de este trabajo es investigar el papel de miR-127-3p en la polarización de macrófagos durante la fibrosis renal subyacente a la ERC y determinar el efecto de su modulación como una nueva estrategia terapéutica en esta enfermedad.

Para ello, hemos estudiado la expresión de miR-127-3p en un modelo de ratón de fibrosis renal (UUO) y el efecto de su modulación exógena en la enfermedad. Demostramos que miR-127-3p aumenta con el daño renal en el túbulo proximal, y se correlaciona con el desarrollo de fibrosis y la respuesta inflamatoria. También hemos comprobado que el bloqueo de su expresión en ratones UUO acelera la progresión de la enfermedad y aumenta el infiltrado de macrófagos en el riñón. Además, hemos estudiado *in vitro* la expresión de miR-127-3p y el efecto de su modulación en macrófagos murinos nativos (Mϕ) y diferentes fenotipos inducidos (M1 [LPS] y M2 [IL-4]). Los resultados han mostrado que la expresión del miRNA no cambia dependiendo del estímulo recibido. Sin embargo, la expresión de NOS2, marcador de macrófagos M1, tiende a aumentar cuando se inhibe miR-127-3p en las células, mientras que la sobreexpresión de miR-127-3p en el fenotipo M2a [IL-4] conduce a una disminución de NOS2. Esto sugiere que la inducción del miRNA a lo largo de la lesión renal podría cambiar el curso y el pronóstico de la enfermedad. Basándonos en todo esto, hemos probado diferentes partículas virales y métodos de administración hasta conseguir inducir con éxito la expresión de miR-127-3p en la corteza renal de ratones utilizando partículas lentivirales inyectadas a través de la arteria renal.

Finalmente, demostramos que los niveles séricos de miR-146a-3p, miR-27a-3p y miR-93-3p disminuyen con la progresión del daño renal en pacientes de ERC, y que los niveles séricos de miR-127-3p, miR-146a-3p, miR-27a-3p, and miR-26b-5p se correlacionan con parámetros clínicos relevantes de estos pacientes.

En resumen, miR-127-3p es un importante mediador en la ERC por su implicación en la fibrosis renal y la polarización de macrófagos, por lo que su modulación podría ser una potencial intervención terapéutica en esta enfermedad. Además, los miARNs estudiados podrían servir como biomarcadores útiles para la estratificación y el manejo de pacientes durante la ERC.

Contents

Abbreviations

αSMA	α-smooth muscle actin
A2AR	Adenosine 2A receptor
AAV	Adeno-associated virus
ACEi	Angiotensin converting enzyme inhibition
ACR	Albumin: creatinine ratio
ADMA	Asymmetric dimethylarginine
AER	Albumin excretion rate
AF	Alkaline fosfatase
Ago	Argonaute family protein complex
Akt	Serine/threonine-protein kinases
AKI	Acute Kidney Injury
AngII	Angiotensin II
ARB	Angiotensin receptor blockade
ARG1	Arginase-1
BSA	Bovine serum albumin
CD163	Chitinase-3-like protein 3/Hemoglobin scavenger receptor
CD206	Mannose receptor
CGA	Cause, Glomerular Filtration Rate and Albuminuria
CK	Contralateral kidney
CKD	Chronic Kidney Disease
CKD-MBD	Chronic Kidney Disease-Mineral and Bone Disorder
CPB	Cardiopulmonary bypass
CRF	Chronic Renal Failure
CTs	Crossing points
CVD	Cardiovascular Disease
CXCL4	Chemokine C-X-C motif ligand 4
DAMPs	Damage-associated molecular patterns
DGCR8	DiGeorge syndrome critical region in gene 8
DKK3	Dickkopf-3
DM	Diabetes Mellitus

DMEM	Dulbecco's Modified Eagle Medium
DEPC	Diethylpyrocarbonate
dsRNA	Double stranded RNA
ECM	Extracellular matrix
EGF	Epidermal Growth Factor
eGFR	Estimated GFR
EMT	Epithelial-to-mesenchymal transition
ENCODE	Encyclopedia of DNA Elements
EndMT	Endothelial-to-mesenchymal transition
ESKD	End-Stage kidney disease
EXP5	Exportin-5
FBS	Fetal bovine serum
FFPE	Formalin-fixed and paraffin-embedded
FGF2	Fibroblasts growth factor-2
FIZZ1/RENTLA	Inflammatory zone-1
FN1	Fibronectin-1
GBM	Glomerulus basal membrane
GDF15	Growth Differentiation Factor-15
GFR	Green fluorescence protein
GFP	Glomerular filtration rate
GGT	Gamma glutamyl transferase
GM-CSF	Granulocyte macrophage colony stimulating factor
GPT	Glutamic-pyruvic transaminase
GOT	Glutamate oxaloacetate transaminase
H&E	Hematoxylin and Eosin
HDL	High-density lipoprotein
HIF-1α	Hypoxia-inducible factor 1-alpha
HIV	Human immunodeficiency virus
HIVAN	HIV-associated nephropathy
ICU	Intensive Care Unit

IFNγ	Interferon-γ
IHQ	Immunohistochemistry
IL-10	Interleukin-10
IL-10R	Interleukin-10 receptor
IL-12	Interleukin-12
IL-13	Interleukin-13
IL-1β	Interleukin 1β
IL-23	Interleukin-23
IL-4Rα	Interleukin-4 receptor α
IL-6	Interleukin 6
iNOS	Inducible nitric oxide synthase
IRF	IFN regulatory factor
ISH	*In situ* hybridization
JAK	Janus kinase
K/DOQI	Kidney Disease Outcomes Quality Initiative
KDIGO	Kidney Disease: Improving global Outcomes
KIM1/sKIM1	Kidney injury molecule-1/ soluble kidney injury molecule-1
Lamtor1	Late endosomal/lysosomal adaptor, MAPK and MTOR activator-1
LC	Liposomal clodronate
lincRNAs	Long intervening noncoding RNAs
lncRNAs	Long noncoding RNAs
LPO	Lactoperoxidase
LOX	Lysyl oxidase
LPAR	Lysophosphatidic acid receptor
LPS	Lipopolysaccharide
LV	Lentiviral vector
Mϕ	Macrophages
MAPK	Mitogen-activated protein kinase
MCP1	Monocyte chemotactic protein-1
M-CSF	Macrophage colony stimulating factor

MDB	Mineral Bone Disorder
MHC-1	Major histocompatibility complex-1
miRISC	Effector RNA-induced silencing complex
miRNAs	microRNAs
MMP12	Matrix metalloproteinase-12
MMP7	Matrix metalloproteinase-7
mTOR/mTORC-1	Mammalian target of rapamycin/ Mammalian target of rapamycin complex-1
ncRNAs	Noncoding RNAs
NF-κB	Nuclear factor kB
NGAL	Neutrophil gelatinase-associated lipocalin
NKF	National Kidney Foundation
Nrf2	nuclear erythroid 2-related factor 2
NO	Nitric oxygen
OK	Obstructed kidney
OXID	Oxide nitric synthase
PACT/ PKKRA	Interferon-inducible double-stranded RNA dependent activator
PBS	Phosphate-buffered saline
PBST/TBST	Buffered saline solution with 0.05% v/v Tween-20 added
PCR	Reactive C protein
PCT	Patent Cooperation Treaty
PDGF	Patelet-derived growth factor
PI3K	Fosfoinositol 3-kinase
piRNAs	PIWI-associated RNAs
PPAR	Peroxisome proliferator activated receptors
pre-miRNA	Precursor miRNA
preRISC	Precursor RNA-induced silencing complex
PSG	Penicillin, Streptomycin and Glutamine
PTH	Parathyroid hormone
ROS	Reactive oxygen species
rRNA	Ribosomal RNA

RT	Reverse transcription
qRT-PCR	quantitative real-time polymerase chain reaction
sCr	Serum creatinine
sCysC	Serum cystatin C
SIN	Self-inactivating
siRNAs	Short-interfering RNAs
sKlotho	Soluble Klotho
snoRNA	Small nucleolar RNA
snRNA	Small nuclear RNA
SOC3	Cytokine signaling-3
STAT	Signal transducer and activator of transcription
suPAR	Soluble Urokinase-type plasminogen activator receptor
TAMs	Tumor associated macrophages
TBS	Tris-buffered saline solution
TECs	Tubular epithelial cells
TFEB	Transcription factor EB
TGFβ	Transforming growth factor-β
TLR	Toll-like receptor
TLR4	Toll-like receptor-4
TNF-R	Tumor necrosis factor receptor
TNFα	Tumor necrosis factor-α
TRBP	Trans-activation response RNA-binding protein
Tregs	Regulatory T cells
tRNA	Transfer RNA
UTR	Untranslated region
UUO	Unilateral ureteral obstruction
VEGF	Vascular endothelial growth factor
VIH	Human immunodeficiency virus
YM1	Chitinase-3-like protein 3

Introduction

1. Chronic Kidney Disease (CKD)

1.1 CKD definition and classification

Chronic kidney disease (CKD), also called chronic renal failure (CRF) is an established term that embraces all stages of progressive and non-reversible kidney damage extended over 3 months. kidney damage is defined by a decreased renal function leading to a decrease of glomerular filtration rate (GFR) under 60 ml/min per 1.73 m^2, and/or the appearance of kidney structure abnormalities with implications for health ("K/DOQI Clinical Practice Guidelines for Chronic Kidney Disease: Evaluation, Classification, and Stratification.," 2002).

CKD was introduced as a clinic entity for the first time in 2002 by The National Kidney Foundation (NKF) in its Kidney Disease Outcomes Quality Initiative (K/DOQI) Clinical Practice Guidelines on Chronic Kidney Disease. This consensus document described the disease, including the previous definition and classification in stages of severity from 1 to 5, but merely GFR-based on, and cause-independent (Levey et al., 2005). Years later, the first guideline was consecutively reviewed and modified until the current one was published in July 2017: the KDIGO 2017 Clinical Practice Guideline Update for the Diagnosis, Evaluation, Prevention, and Treatment of Chronic Kidney Disease-Mineral and Bone Disorder (CKD-MBD). Selective updates included in the manuscript were: i) Etiology of damage and injury risk factors taken into account for diagnosis and prognosis. ii) A complete and improved disease classification divided by severity stages from 1 to 5, again GFR-based on (G1 to G5), but together with albumin: creatinine ratio (ACR) categorized from A1 to A3 (**Figure 1**).

Prognosis of CKD by GFR and albuminuria categories: KDIGO 2012

GFR categories (ml/min/1.73 m^2), description and range				Persistent albuminuria categories, description and range		
				A1	A2	A3
				Normal to mildly increased	Moderately increased	Severely increased
				<30 mg/g <3 mg/mmol	30–300 mg/g 3–30 mg/mmol	>300 mg/g >30 mg/mmol
	G1	Normal or high	≥90			
	G2	Mildly decreased	60–89			
	G3a	Mildly to moderately decreased	45–59			
	G3b	Moderately to severely decreased	30–44			
	G4	Severely decreased	15–29			
	G5	Kidney failure	<15			

Figure 1. CKD prognosis by GFR and albuminuria categories established by KDIGO 2012 Guideline. Risk is identified with different colors representing the severity of the damage to evaluate mortality, cardiovascular implications, and progression of the disease in the patients. Green color means low risk and no disease until other markers of kidney damage appear; yellow and orange represent moderate and high risk, respectively; and red indicates very high risk. Risk signature is the result of classifying the patient by a range of persistent albuminuria from low (A1) to moderate (A2) and severe (A3), taken together with the glomerular filtration rate (GFR), from normal (G1) to kidney failure considered level (G5) (KDIGO Guideline 2017 Update).

The new classification guide was abbreviated in CGA from cause, glomerular filtration rate, and albuminuria (KDIGO, 2017) and describes the current routine followed by physicians for patient management, based on **Figure 1**, but also in the appearance of abnormalities in kidney structure and function discovered by urine sediment, electrolytes disorder caused by tubular injury, histology and structural abnormalities detected by imaging. This method allows better patient management, assessment over time of the disease, and an improved classification from stages 1 to 5 in clinical practice for CKD patients.

1.2 Epidemiology and economic impact of CKD

CKD is recognized worldwide as a priority health problem because of its overall high prevalence and increased incidence over the last years, being already considered as a global epidemic that entails a poor life quality of patients and huge economic costs for the health systems (Levey et al., 2011).

Prevalence and incidence of CKD vary among studies between countries around the world, and have high heterogeneity mainly, due to the different lifestyles and the established methods to measure kidney damage. Global prevalence of 13.4% for the all-age population was recorded in 2016. Around 7.4% of that patients belonged to stages 1 and 2, 7.6% of them, was in stage 3, and 0.4% and 0.1% were in stages 4 and 5, respectively (Nathan R Hill et al., 2016) showing that stage 3 was recorded the most common condition for CKD global burden.

Recent data from a fact sheet published last year by the Centers for Disease Control and Prevention in the US, *Chronic Kidney Disease in the United States in 2019*, informed that 1 in 7 of the adult population is estimated suffering from this disease. The rate concurs with Spain´s current prevalence and the majority of developed countries (Gorostidi et al., 2018). CKD prevalence is, in part, due to the sedentary lifestyle and the aging population in these nations, since the disease is most common in people older than 65 years, around 38% (Gorostidi et al., 2018).

Regarding prevalence among genders, many studies have been reported differences between men and women, most of them pointed to females as the most frequent gender suffering from CKD (Bikbov et al., 2020). But it is important to mention that this data varies widely among different studies, demographic areas, and measuring kidney damage methods.

Reports published in 2018 from Vivekanand Jha, Gopesh K Modi, and Yan Xie and colleagues (Jha & Modi, 2018; Y. Xie et al., 2018), suggested that from 1900 to 2016 the global prevalence for CKD concern increased in 86.9% affecting 275.9 million people in 2016 worldwide. The incidence for that period was 88.8% higher, meaning 21.3 million of new cases that year. These rates placed the CKD burden in the 11th position on the depth-cause list.

Nevertheless, all reviews agree on suffering diabetes mellitus (DM), cardiovascular disease (CVD), obesity, previous episodes of renal damage, as well as other renal diseases, are risk factors and the major causes of CKD. Although, human immunodeficiency virus (HIV) infection and genetic or epigenetic alterations are also, etiologies for CKD. But, the importance of kidney diseases lies in the consideration of them as ¨silent diseases¨ since mostly, they don't course with early symptoms and often, people are not conscious of their impaired kidney function, which implies an increased CKD associated risks, and finally, kidney failure that supposes dialysis or kidney transplantation (ASN, Release Press, 2018) increasing mortality, leading to patients´ poor life quality, and huge economic costs for the health systems.

The US Renal Data System announced for 2013, a total of 81.3 billion dollars spent in CKD patients, including end-stage kidney disease (ESKD) ones (Golestaneh et al., 2017). In Spain, stage 5 patients constitute only 1% of total CKD-affected people, but because of their medical requirements, they waste 5% of the total medical annual budget (Gorostidi et al., 2018). For all these reasons, early identification and slowdown of disease progression in CKD patients are critical to prevent mortality and morbidity and to reduce associated CKD costs and outcomes.

1.3 Diagnosis and biomarkers of CKD

According to KDIGO Guidelines and based on CKD definition, the gold standard measurement methods of kidney injury for diagnosis and classification of disease, are i) estimated GFR (eGFR) calculated indirectly as the renal clearance of exogenous filtration markers, such as serum creatinine (sCr) or cystatin C (sCysC) levels, ii) determination of urine albumin excretion rate (AER), and iii) renal biopsy, when it is necessary to confirm kidney structure abnormalities with implication for health.

However, it has been strongly demonstrated that GFR and AER are not able to identify kidney damage in the early stages of the disease, since they are detected when kidney dysfunction already appears (Lopez-Giacoman S & Madero M, 2015; Rysz et al., 2017). And renal biopsy is an invasive technique that involves risks for the patients such as bleeding, hypotension and local pain so, it is generally performed to confirm kidney dysfunction when it is already failing (Bidin et al., 2019). For this reason, CKD courses with a long clinically silent period in which diagnosis, and therefore, treatment, did not occur during early stages, allowing merely, an intervention in advanced stages when life expectancy is shorter and supposes a significant financial investment. Based on that, the search for novel early renal injury biomarkers able to detect a premature condition of CKD, and capable of differentiating between stages has been turned into a significant challenge for the future. In this sense, promising molecules involved in the pathological cellular context of kidney damage are being tested from blood and urine samples of CKD patients. Some of them are ADMA (Asymmetric Dimethylarginine), Uromodulin (Tamm–Horsfall protein), suPAR (Soluble Urokinase-Type Plasminogen Activator Receptor), EGF (Epidermal Growth Factor),

sKlotho (soluble Klotho), TNF-R (Tumor Necrosis Factor Receptor), Galectin-3, DKK3 (Dickkopf-3), GDF15 (Growth Differentiation Factor 15), CKD273, sKIM1 (soluble Kidney Injury Molecule -1), MCP1 (Monocyte chemotactic protein-1), NGAL (Neutrophil Gelatinase-Associated Lipocalin), and different RNA molecules such as miRNAs (microRNAs), ncRNAs (non-coding RNAs), IncRNAs (long non-coding RNAs) and lincRNAs (long intervening non-coding RNAs) (Aguado-Fraile et al., 2015; Rysz et al., 2017; Saucedo AL. et al. 2018; Bidin et al., 2019). However, confirmation of their efficacy, sensitivity and specificity is being investigated or in follow-up period.

1.4 Tissular and cellular features of CKD

Specific features of CKD include progressive destruction of the renal parenchyma and loss of functional nephrons as a direct consequence of cellular processes and molecular mechanisms triggered to compensate for kidney damage and renal dysfunction. Main cells implicated in this pathological context are tubular epithelial cells (TECs), fibroblasts, endothelial cells, podocytes, and inflammatory cells. They are continuously responding to deleterious stimuli and are responsible for the major events that occur in CKD advance, described above, and all of them related each other and over-looped during the progression of renal damage (**Figure 2**) (Djudjaj & Boor, 2019).

- **Tubular epithelial injury:** TECs can be injured by reacting sensitively to a wide range of stress stimuli, including metabolic, toxic, ischemic, mechanic, infectious and immunological stimuli. As a reparative response, they proliferate and increase the expression of pro-inflammatory signaling proteins (e. g. KIM1 and NGAL), pro-fibrotic growth factors (e. g. TGFβ), and cytokines and chemokines that promote inflammation and fibroblasts activation into myofibroblasts (e. g. reactive oxygen species, ROS; interleukin 1β, IL-1β; interleukin 6, IL-6; and tumor necrosis factor α, TNFα) (Djudjaj & Boor, 2019). This scenario leads to tubular atrophy, mainly characterized by significant thickening of tubular basement membrane and lumen dilatation, and strongly associated with loss of epithelial characteristics leading to a partial or total epithelial-to-mesenchymal transition (EMT) of tubular renal cells into differentiated cells which loss their functionality and contribute to interstitial fibrosis development (Djudjaj & Boor, 2019). Many studies highlight the key role of tubular epithelial cells in the development of disease and suggest that they can be restored from slight damage meaning a possible reversible interstitial fibrosis (Matthew & Katalin, 2016).

- **Interstitial fibrosis:** Fibrosis is essential for wound healing providing a scaffold for regeneration after any type of tissue injury (Djudjaj & Boor, 2019), but when the reparative process fails, an interstitial fibrosis appears. It is defined by the accumulation of an abnormal extracellular matrix (ECM) composed of collagen I and IV arranged between tubules and peritubular capillaries. This process is always preceded, accompanied, or stimulated by inflammation (Matthew & Katalin, 2016), fibroblasts proliferation and activation into myofibroblasts, and rarefaction of peritubular capillaries (Rysz et al., 2017). Events that disrupt normal tissue architecture and interfere with organ function, causing a lack of oxygen and nutrients to tubular and

endothelial cells, and contributing to tubular atrophy and vascular rarefaction (Djudjaj & Boor, 2019). During fibrosis, most of fibroblasts express α-smooth muscle actin (αSMA) as a marker of their transformation into myofibroblasts, which reorganize the matrix and increase its density by deposit of collagen, fibronectins, and other glycoproteins (Guzzi et al., 2019). Since fibrosis has been reported within tissue regeneration and inflammation, it is strongly associated with inflammatory infiltrates, mainly lymphocytes and macrophages (Djudjaj & Boor, 2019).

- **Endothelial dysfunction:** Along kidney disease, vascular rarefaction, preceded or produced by tubular injury, fibrosis or/and inflammation, exacerbates the limitation of oxygen and nutrients available to epithelial cells (Matthew & Katalin, 2016) and causes tissue hypoxia and mitochondrial dysfunction (Guzzi et al., 2019). Detachment of podocytes from glomerulus basal membrane (GBM) and their loss, also occur (Rysz et al., 2017), and contribute to vascular functionality changes and sclerosis of the glomerulus. Also, endothelial-to-mesenchymal transition (EndMT) from endothelial cells of peritubular capillaries has been suggested as a source of myofibroblasts during endothelial injury undergoing (Djudjaj & Boor, 2019).

- **Interstitial inflammation:** A low-grade and persistent inflammation is considered a hallmark feature of Chronic Kidney Disease, but if inflammation is a trigger or a result of the disease and how they are related, is still unknown. When kidney damage happens, resident inflammatory cells, among them macrophages and dendritic cells, regulate initial inflammation response by recruiting circulating neutrophils and monocytes (Djudjaj & Boor, 2019), attracted by cytokines, chemokines, and damage-associated molecular patterns (DAMPs) (Gajjala et al., 2015). After that, neutrophils activate monocytes into macrophages, as well as TECs and endothelial cells, whereas DAMPs, build a pro-fibrotic niche supporting the activation of pericytes into myofibroblasts, and leading to a local scenario of inflammatory amplification that causes a permanent inflammation condition as a result of an impaired immune homeostasis, in which macrophages are implicated through their polarization into different phenotypes along the development of disease (Guzzi et al., 2019).

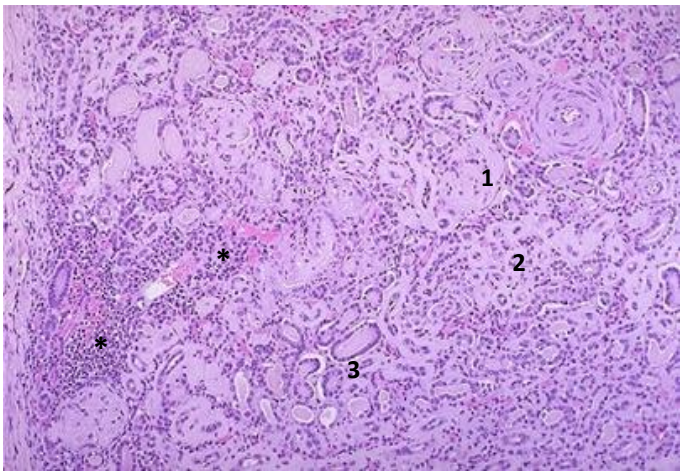

Figure 2. Microscopic appearance of human end-stage kidney damage under hematoxylin and eosin staining. Image shows the representative structure abnormalities in the renal cortex of an end-stage chronic renal damage patient: Inflammatory infiltrates within the renal parenchyma (*****), tubular atrophy (**1**), interstitial fibrosis (**2**), and glomerular sclerosis (**3**) (adapted from Robbins and Cotran Atlas of Pathology, 2015).

1.5 Patient management and therapeutic strategies for CKD

Chronic Kidney Disease could be not considered itself as a diagnosis, since it is rather a consequence of an underlying pathological context given by different deregulated scenarios (Turner et al., 2012). Thereby, currently, patient management is devoted to mitigate associated disorders that are contributing to the disease development, and to slow the progression of kidney damage into advanced stages (Turner et al., 2012; Tomson & Duffy, 2019).

Often, as it was previously cited, patients diagnosed of CKD are suffering from CVD or DM. Therefore, the main approach in these cases is to avoid GFR decline by controlling systemic hypertension by antihypertensive therapy and reducing intraglomerular hypertension (Turner et al., 2012) by angiotensin-converting enzyme inhibition (ACEi), angiotensin receptor blockade (ARB), or a combination of both (Matthew & Katalin, 2016; Tomson & Duffy, 2019). Restrictions in diet, as well as the use of diuretic agents to maintain homeostatic fluids balance, contribute to alleviate glomerular congestion being crucial in slowing kidney injury progression (Vanholder et al., 2018; Kramer, 2019). Also, MBD is a common complication of CKD, meaning abnormalities in the level of calcium and phosphate, parathyroid hormone (PTH), and metabolism of Vitamin D, causing anemia and contributing to neurodegeneration. Treatment in this case is based on phosphorous restriction mainly to recover physiological mineral levels (Webster et al., 2017; Ketteler et al., 2018). Moreover, the degree of kidney fibrosis is often an indicator of future GFR decline thus, inhibition of renal fibrosis and inflammation based on drugs targeting biochemical pathways involved in these processes, are being tested as a potential therapeutic strategy to avoid CKD progression to ESKD. The most relevant anti-fibrotic and anti-inflammatory agents that are being tested in pre-clinical and clinical practice are mainly targeted to inhibit pro-fibrotic factors such as Angiotensin II (AngII), Galectin-3, TGFβ1, and Lysophosphatidic acid receptor (LPAR); to reduce oxidative stress (activators of Nrf2 pathway); and to suppress collagen expression (Pirfenifone, Tranilast, and Lysyl oxidase (LOX) inhibitors) (Turner et al., 2012; Matthew & Katalin, 2016; Tomson & Duffy, 2019).

Furthermore, a significant issue to consider on CKD patient management is that during disease progression, specialists must decide treatment balancing between drug benefits and adverse effects, which implies a continuum monitoring of these multi-disease patients and a huge effort by medical entities (Tomson & Duffy, 2019). Finally, when hopelessly kidney impaired function is established, the next step is to assess and prepare the patient for renal replacement therapy (Turner et al., 2012), dialysis, or kidney transplantation, which are not always possible options due to the compromised health of patients in an advanced stage of kidney disease, as well as allograft immune-compatibility and availability.

Knowing that therapies remain limited and there is no cure for CKD up to date, future efforts have to be devoted to developing improved therapeutic tools that slowdown kidney damage avoiding the progression towards the

final stages of CKD. In this sense, miRNAs, as gene regulators, have emerged in recent years as promising molecules able to modulate the expression of genes involved in cellular processes such as fibrosis and inflammation development, as well as regenerative events, which could turn these molecules into potential therapeutic tools for the treatment of many diseases, among them CKD burden (Rysz et al., 2017).

2. Key mediators of inflammation in CKD: Macrophages

Persistent systemic inflammation has been recognized as an important component of CKD, as was mentioned before. Understanding the role of the key players that contribute to chronic inflammatory status during disease will allow the development of novel therapeutic strategies able to treat and prevent progression and outcomes of CKD (Akchurin & Kaskel, 2015). It is well known that an increased production of pro-inflammatory cytokines, oxidative stress, acidosis, altered metabolism of adipose tissue, and recently discovered, gut microbiota dysbiosis, participate in the setting of an inflammatory milieu (Mihai et al., 2018; Andrade-Oliveira et al., 2019; Yang et al., 2019). This microenvironment strongly influences macrophages response, inflammatory cells that have been recognized as crucial mediators during all phases of kidney disease through their polarization towards different phenotypes and therefore, have been pointed out as interesting target cells for the recovery of homeostasis physiology in CKD (Kim et al., 2015; Pan et al., 2015; Guiteras et al., 2016; Parisi et al., 2018; Engel & Chade, 2019; Meng et al., 2019).

Macrophages are a subtype of leukocytes and constitute crucial cells of innate immunity implicated in homeostasis maintenance and inflammation response through i) phagocytosis of pathogens and clearance of cell debris from senescent/apoptotic cells, ii) recruitment of other inflammatory cells to the inflammation site by the production of different cytokines, iii) antigen presentation, and iv) participation in wound healing and tissue repair (Shapouri-Moghaddam et al., 2018; Lee, 2019). They are present in most body tissues as resident macrophages differently named depends on their emplacement (e. g. alveolar macrophages in the lung, Kupffer cells in the liver, or intraglomerular mesangial cells in the kidney). But they are also recruited to the inflammation site, as blood-peripheral monocytes that scape from the blood flow and migrate into tissues, where they differentiate into macrophages responding to specific signaling (Shapouri-Moghaddam et al., 2018; Y. Wang et al., 2019). The most relevant characteristic of macrophages is their diversification capacity and functional plasticity in response to specific stimuli from the microenvironment, which has been described as macrophage polarization in different phenotypes (Orecchioni et al., 2019). Conventionally, the major phenotypes reported are naïve macrophages (Mϕ), M1 pro-inflammatory macrophages, and M2 anti-inflammatory macrophages. However, it has been reported that *in vivo*, M1 and M2 phenotypes represent the extremes of a spectrum that constitute a continuum of functional subsets with intermediated and overleaped features within many possibilities among M1 and M2

phenotypes, in response to physiological conditions and the local cytokine milieu (Murray, 2017; Y. Wang et al., 2019).

2.1 Macrophage phenotypes and markers

- **Naïve macrophages (Mϕ):** Macrophages differentiated from monocytes and able to polarize into M1 or M2 phenotypes depending on different stimuli (Orekhov et al., 2019).

- **M1-polarized macrophages**: Also called classically activated macrophages or pro-inflammatory macrophages. They are differentiated from monocytes mainly by granulocyte-macrophage colony-stimulating factor (GM-CSF) and activated by interferon-γ (IFNγ) mostly released by lymphocytes, and by lipopolysaccharide (LPS) through toll-like receptor-4 (TLR4). M1 macrophages are characterized by their high expression of pro-inflammatory molecules including TNFα, IL-1β, IL-6, IL-12, IL-13, and ROS (nitric oxygen, NO, and inducible nitric oxide synthase, iNOS) (K. Y. Lee, 2019; Orekhov et al., 2019). They are involved in helper Th1 immune response being critical in the protection against pathogen infections and tumor growth, antigen-presenting functions inducing a humoral immune response, and recruitment and activation of lymphocytes to the inflammation site releasing specific cytokines and chemokines (Orekhov et al., 2019; Y. Wang et al., 2019). Even though M1 are involved in inflammation resolution, they can be harmful for tissue repair suppressing cell proliferation and promoting tissue damage in an exacerbated response (K. Y. Lee, 2019).

- **M2-polarized macrophages:** Also known as alternatively activated macrophages or anti-inflammatory macrophages. They are differentiated from Mϕ or M1 macrophages by IL-4 and IL-13. In the bibliography, anti-inflammatory macrophages were divided into almost four subtypes, M2a, M2b, M2c, and M2d, based on the stimuli received and including specific transcriptional changes between them. But, all of them have signatures in common including high IL-10 and low IL-12 cytokine expression levels, suppressor of cytokine signaling-3 (SOC3), macrophage colony-stimulating factor (M-CSF), CD206, found in inflammatory zone-1 (Fizz1 or RENTLA), chitinase-3-like protein 3 (Ym1 or CD163) and arginase-1 (Arg1) (Y. Wang et al., 2019). Arg1 is especially relevant in M2-like macrophages to deplete L-arginine expression impairing T-cell proliferation and the consequent production of IFNγ, and to compete with iNOS by L-arginine reducing NOS production, avoiding M1 macrophage activation (Orekhov et al., 2019).

  Regarding alternatively activated macrophages subtypes differences, M2a polarization is stimulated by IL-4, IL-13, or parasite infections, through the interleukin-4 receptor α (IL-4Rα) and they are related with Th2 immune response releasing IL-4 together with eosinophils and basophils to encapsulate parasites. M2b macrophages are stimulated by immunoglobulin-complex plus TLR or IL-1R ligands and regulate immune response releasing both pro- and anti-inflammatory cytokines including IL-10, IL-1β, IL-6, and TNFα. In M2c

macrophages, major histocompatibility complex-1 (MHC-1) and CD86 surface marker are up-regulated serving as antigen presentation molecules. These macrophages are stimulated by IL-10 through IL-10 receptor (IL-10R), together with transforming growth factor-β (TGFβ) or glucocorticoid hormones, and they are commonly known for their contribution in tissue remodeling and repair, and extracellular matrix production. Finally, M2d was only described in mice and can be induced by IL-6 and adenosine from M1 macrophages via activation of the adenosine 2A receptor (A2AR). It is characterized by an increased production of vascular endothelial growth factor (VEGF), but it is still mostly unknown (Shapouri-Moghaddam et al., 2018; Lee, 2019; Wang et al., 2019). M2 macrophages control and resolve inflammation through the release of anti-inflammatory cytokines participating in wound healing, post-inflammatory tissue repair, and remodeling promoting cell proliferation. Therefore, they are crucial in tissue repair, but they are also involved in chronic inflammation or infectious diseases when maladaptive repair occurs (Orekhov et al., 2019).

There are other macrophage phenotypes described in the bibliography, including tumor-associated macrophages (TAMs) and human-specific pro-inflammatory M4 macrophages. TAMs are activated by tumors and stimulate cancer cells during carcinogenesis orchestrating several factors in the microenvironment connecting inflammation with the tumor and promoting proliferation, invasion, angiogenesis, and limiting anti-tumor inflammation response (K. Y. Lee, 2019). M4 macrophages have been described as induced by chemokine C-X-C motif ligand 4 (CXCL4) and characterized by their low phagocytic capacity and increased resistance to foam cell formation. Their signature is a down-regulated expression of hemoglobin scavenger receptor (CD163) and an elevated expression of matrix metalloproteinase-7 (MMP7) and -12 (MMP12) (Orekhov et al., 2019).

In recent years, macrophage classification was updated, reflecting the complexity of the identified macrophage subtypes and followed by many laboratories. The proposed nomenclature takes into account the activation signal that drives polarization. In that case, M[IFNγ], M[IL-4], M[Ic], and M[IL-10/TGFβ] correspond to M2a, M2b, and M2c subsets in the old classification (Orekhov et al., 2019).

Despite the scientific community are already knowledgeable of many relevant aspects of macrophages, the main goal in macrophage biology continues being light the specific pathways involved in each phenotype and the molecular mechanisms that trigger M1 and M2 polarization. Terms that continue being controversial due to the lack of defined criteria to score phenotypes within the bibliography. What is inevitable true and well known, is that macrophage polarization is strongly linked with inflammation resolution, successful or impaired, which could be considered as a promising therapeutic approach for dealing with inflammatory diseases (Murray, 2017).

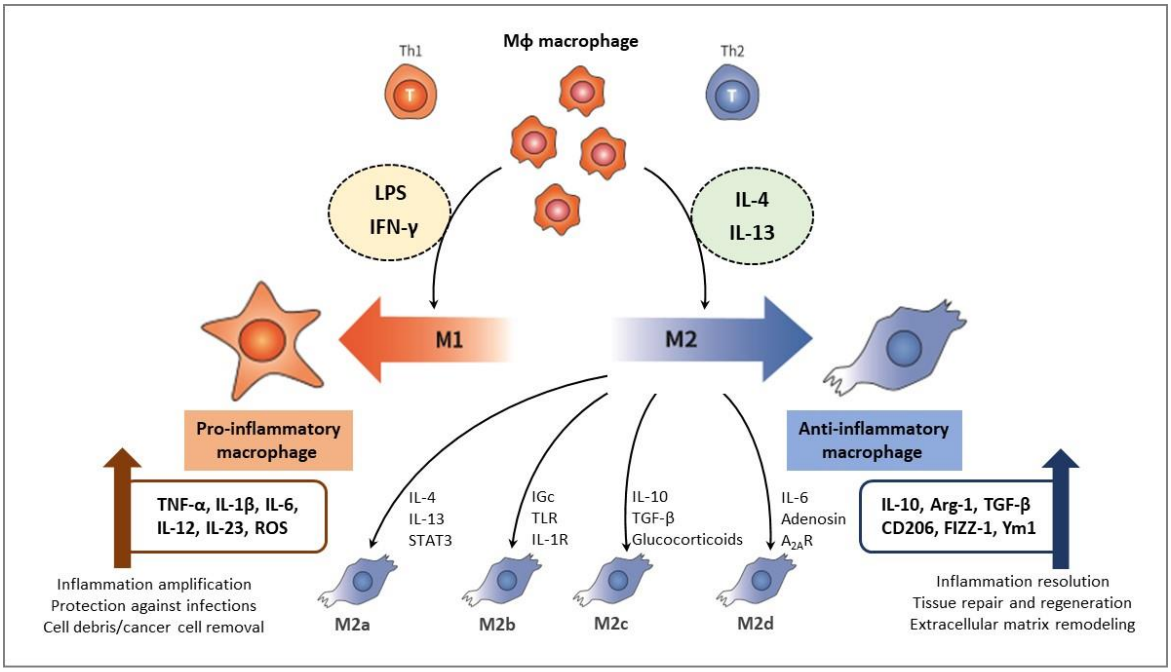

Figure 3. Macrophage polarization phenotypes. M1 and M2 phenotypes are derived from naïve macrophages and they are activated through different mechanisms. M1 or pro-inflammatory macrophages are mainly stimulated by cytokines and molecules involved in the Th1 immune response, including LPS and IFN-γ. These classically-activated macrophages amplify the pro-inflammatory signaling and they are characterized by the high expression of TNF-α, IL-1β, IL-6, IL-12, IL-23, and ROS. In contrast, M2 or anti-inflammatory macrophages are generally activated by IL-4 and IL-13 and participate in the Th2 immune response. They are characterized to express high amounts of IL-10, Arg-1, TGF-β, CD206, FIZZ1, and Ym1, and they can be divided into four subtypes of alternatively-activated macrophages, M2a, M2b, M2c, and M2b, each one differently activated and with a particular biological function. Pro-inflammatory macrophages are involved in inflammation response, protection against infections and cell debris, and cancer cell removal. Whereas anti-inflammatory macrophages have been described as involved in inflammation resolution, wound healing and tissue repair, and extracellular matrix remodeling (adapted from Lee, 2019).

2.2 Macrophage polarization process and molecular mechanisms involved

Macrophages adopt different phenotypes, switching between M1-like or M2-like depending on the signals received from the microenvironment that trigger key transcription factors in the cell, which cross-interact and activate diverse signaling pathways that promote changes in cell transcriptome and proteome and finally, cause the conversion of macrophages into specific phenotypes with different biological activities (Murray, 2017; Shapouri-Moghaddam et al., 2018; Y. Wang et al., 2019).

Among molecular mechanisms involved in this process, IRF/STAT signaling pathway is considered a key modulator in the control of macrophage polarization. A predominant activation of STAT1 and NF-κB by IFN-γ and TLRs induces the expression of transcription factors like IRF-1/IRF-5 that promote M1 differentiation. Whereas STAT-3/STAT-6 signaling and IRF-3/IRF-4 expression by stimulation of IL-4/IL-13 and IL-10, contribute to M2 phenotype

polarization (N. Wang et al., 2014; Essandoh et al., 2016; Lee, 2019). Pathways like PI3K/AKt, MAPK, PPAR, and JAK/STAT also seem to be implicated in this process but, the major molecular mechanisms that govern the switch of phenotype in macrophages continue being an issue under intensive review, and many aspects related remain completely understood (Y. Wang et al., 2019).

Macrophage polarization is also modulated by other relevant conditions present in many diseases, such as hypoxia, where the increased expression of HIF-1α promotes M1 pro-inflammatory macrophages differentiation (N. Wang et al., 2014). But also, post-transcriptional modifications by miRNAs and epigenetic changes through histone modifications are implicated in phenotype changes (Shapouri-Moghaddam et al., 2018; Orliaguet et al., 2020).

Moreover, arginine metabolism was identified as the main difference between M1 and M2 phenotype functions that influence their polarization. M1 uses arginine to generate NO molecule, widely used to damage and kill pathogens through peroxynitrite production. In contrast, M2 uses arginine to generate ornithine as a repair molecule through the synthesis of proline and polyamines (Orekhov et al., 2019).

It is important to mention that different phenotypes can coexist in the same population in a determinate space and time and that polarization states can change or reverse responding to microenvironment stimuli to regulate macrophage function (Murray, 2017; Chen et al., 2019; Orekhov et al., 2019). Therefore, polarization of Mϕ into either the M1 or M2 phenotype has become a promising therapeutic approach for dealing with inflammatory diseases (Y. Wang et al., 2019).

2.3 Role of macrophages in CKD

Macrophages, as key regulators of tissue homeostasis and immune response, have been reported highly involved in renal injury and fibrosis development in many experimental models and human renal biopsies of kidney diseases (Meng et al., 2019). In the last decade, macrophage polarization has emerged as a critical player in the progression of CKD (Engel & Chade, 2019), since the evidence shows that during the initial stages of kidney damage, M1 macrophages are predominant and contribute to kidney injury, but ongoing the progression of kidney disease, they switch into M2 phenotype, which is related with tissue repair and wound healing but also, with fibrosis development (Meng et al., 2019). However, the relationship between this process and the pathological context is still controversial and change among kidney diseases.

During the early stages of CKD when the kidney is injured, monocytes are recruited to the inflammation site induced by a local production of chemokines. Then, they differentiate into M1 macrophages in response to pro-inflammatory mediators, including IFNγ, and factors like DAMPs and immune complexes, released by Th1/17 cells and NK cells (Meng et al., 2019). Activated M1 macrophages produce high amounts of pro-inflammatory cytokines

IL-1β, IL-6, and TNFα, and factors such as ROS, that cause endothelial dysfunction and death of healthy renal cells exacerbating inflammation signaling and contributing to tissue injury (Guiteras et al., 2016). This scenario extended over a long period, leads to the progression of renal injury, and contribute to the decline renal function (Engel & Chade, 2019).

Detailed studies identified that after this initial inflammation phase, macrophages undergo a phenotypic change that confers a protective and reparative role, leading to an inflammation resolution and tissue repair stage (Guiteras et al., 2016). During this recovery period, it has been reported that Th2 cells and Tregs are recruited to the renal parenchyma, where they secrete cytokines such as IL-4 and IL-13, able to polarized M1 macrophages toward the M2 phenotype, which predominates during this stage of kidney disease as essential players for inflammation management and wound healing (T. Chen et al., 2019). The major M2 subsets described orchestrating this phase are M2a and M2b phenotypes. M2a macrophages express high levels of anti-inflammatory mediators like mannose receptor (CD206), IL-10, and TGFβ, which promote tubular cell proliferation and regeneration. Whereas M2b macrophages additionally have up-regulated antigen presentation, acting as a cross-talk with B cells and being involved in the deactivation of T cells and pro-inflammatory macrophages. Moreover, M2c macrophages are stimulated by IL-10 and TGFβ released by M2a and M2b, and also contribute to tissue repair and matrix remodeling. Theoretically, M2 subsets working together, play an immunoregulatory role in alleviating renal inflammation, stimulating angiogenesis and endothelial repair, and contributing to wound healing and ECM remodeling (T. Chen et al., 2019)(Guiteras et al., 2016).

Unilateral ureteral obstruction (UUO) nephropathy is an extended animal model that mimics CKD in humans and constitute the most well-characterized *in vivo* model to investigate kidney fibrosis development. In consonance with the previously described, many studies demonstrated that depletion of macrophages by liposomal clodronate (LC) during early stages of kidney damage in the UUO model in mice, prevent the progression of kidney injury, indicating a pathogenic role of M1 macrophage phenotype during early stages of kidney disease (Meng et al., 2019). Moreover, it was reported in the same animal model, that once the disease is already triggered, depletion of macrophages does not allow tissue regeneration and results in prejudicial, aggravating fibrosis development (Engel & Chade, 2019), however the transfer of M2 polarized macrophages into the injury site, enhances the repair process. This data suggests an important role of M2 phenotype in the resolution of kidney disease, and that a failure of polarization from M1 macrophages toward M2 ones, could lead to renal inflammation and fibrosis development, contributing to CKD progression (Meng et al., 2019).

Nevertheless, kidney damage and renal fibrosis may not only be triggered by pro-inflammatory M1 macrophages, but also, M2 macrophages described as pro-fibrotic, have been associated with fibrosis during CKD progression, which is controversial with the repair role associated to this phenotype (T. Chen et al., 2019). This fact is based on

constant M2 macrophage infiltration could result in a continuous production of tissue repair and matrix remodeling growth factors and molecules, including TGF-β1, fibroblasts growth factor-2 (FGF2), PDGF, Gal-3, fibronectin-1 (FN1) and MMPs, which activate myofibroblasts, and induce EMT and EndoMT, contributing to an abnormal extracellular matrix (ECM) deposition, wound healing failure and blockage of inflammation resolution (Meng et al., 2019). According to that, some *in vivo* studies revealed that due to a chronic M2 phenotype activation during later stages of kidney damage, a persistent injury and inflammation appear and consequently cause the recruitment of M1 macrophages to the inflamed site, increasing the M1:M2 ratio, which amplifies pro-inflammatory signaling again and reduce M2 polarization. Thus, mechanisms initially reparative, may subsequently become harmful and results in an irreversible fibrosis and progressive kidney tissue destruction (Guiteras et al., 2016).

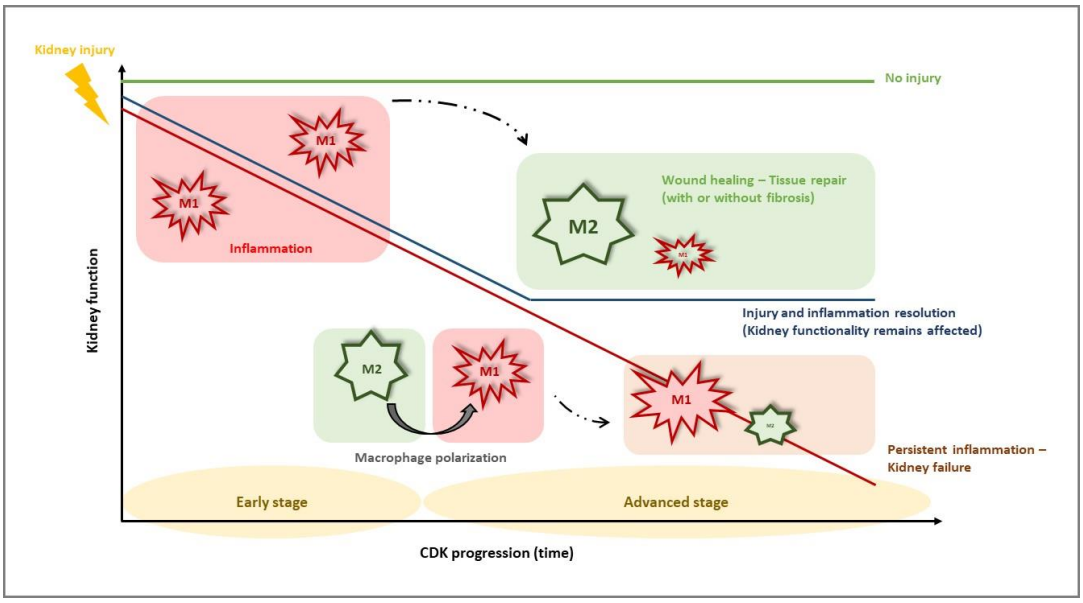

Figure 4. M1 and M2 balance during chronic kidney disease progression. During the early stages of CKD, when kidney injury happens, there is an infiltration of M1 macrophages which release pro-inflammatory cytokines and promote an inflammation state. After that, a recovery phase begins characterized by the polarization of M1 macrophages toward the M2 phenotype, which leads to a wound healing, that may conclude with injury resolution and tissue repair, with or without fibrosis, even though kidney functionality remains affected. However, if injury resolution does not occur, polarization toward M2 phenotype fails, and M1 macrophages persist at injured sites, increasing the M1:M2 ratio and causing a continuous inflammatory state promoting renal fibrosis and failure (adapted from Guiteras R et al., 2016).

In summary, since macrophages seem to play pathogenic and protective roles during kidney disease progression, they could serve as potential targets to ameliorate renal injury through manipulation of their polarization (Engel & Chade, 2019). Nevertheless, macrophage dynamics during the different phases of CKD progression are not fully understood and more studies about macrophage polarization and their contribution during disease may be relevant in terms of defining the type of therapy (Guiteras et al., 2016).

3. MicroRNAs

Protein-coding sequences have been the most investigated DNA region during the last decades, even though they occupy only ~1.5% of the human entire genome. The remaining portion was considered ¨junk¨ DNA during a long period, a term that was popularized in the '60s referring to the non-functionality of this ~98% non-coding region, which besides, about 59% of its, constitute repeated sequences. However, a recent analysis published by the Encyclopedia of DNA Elements (ENCODE) project suggested that almost ~80% of the genome does not codify for proteins, but produces different sized transcripts which participate in essential biological functions being involved in cellular processes by gene regulation, what could be a reason why it is highly conserved among animal kingdom (Fu, 2014; Barahona, 2019).

These RNA transcripts are termed non-coding RNAs (ncRNAs) and have been classified by size in long non-coding RNAs (lncRNAs), which have more than ~200 nucleotides (nt), and small non-coding RNAs, smaller in length. Likewise, small RNAs have been divided into functional and regulatory ncRNAs. Functional RNA molecules are directly involved in processing and translation, and because of that, are considered housekeeping molecules, since they are abundantly and ubiquitously expressed in all cell types in the organisms (Fu, 2014). Most popular among them are ribosomal RNA (rRNA) and transfer RNA (tRNA), both indispensable molecules for protein synthesis. Small nuclear RNA (snRNA) and small nucleolar RNA (snoRNA), also belong to this cluster and they are involved in splicing events and modification of other small RNAs, respectively (Hombach & Kretz, 2016; Shanmugam et al., 2017). Regulatory small ncRNAs were discovered more recently in mammals and have been intensively investigated and reviewed to be key regulators of gene expression in many different cellular pathways (Hombach & Kretz, 2016). Most relevant are PIWI-associated RNAs (piRNAs), short interfering RNAs (siRNAs), and microRNAs (miRNAs) (Fu, 2014).

In this work, we focused on miRNAs to be potential regulators of most human mRNAs involved in cell differentiation (predicted two-third of human mRNAs) (Salloum-Asfar et al., 2019), development and homeostasis maintenance, and which deregulation has been strongly associated with human pathological contexts (Gebert & MacRae, 2019). The first miRNA was discovered in 1993, from *Caenorhabditis elegans*, an invertebrate model organism, and it was named lin-4 because it participated in the regulation of LIN-14 protein expression in this nematode (Bartel, 2018). Further, let-7 miRNA was recognized in humans and other bilateral animals, and since then, the number of discovered miRNAs has exponentially increased thanks to the development of sequencing technologies, and computational and bioinformatics prediction methods, which has enhanced miRNAs research, mRNAs targeted, and possible functions (Bartel, 2018; Barahona, 2019). Currently, it has been identified more than 2.500 miRNAs in humans, and many of them, and also their mRNAs targets, are highly conserved among species (http://www.mirbase.org/).

3.1 Biogenesis and action mechanism of miRNAs

MicroRNAs (miRNAs) are endogenous non-coding RNA molecules of ~22 nt that negatively regulate gene expression in a post-transcriptional manner by targeting specific mRNAs for degradation or translation repression (Mohr & Mott, 2015).

The synthesis of miRNAs constitutes a several steps process that starts with the transcription of miRNAs genes from the genome, mostly by RNA polymerase II enzyme (Pol II), to produce the primary miRNA (pri-miRNA), a transcript of several kilobases in length that contains a stem-loop structure (Wahid et al., 2010). Major miRNAs have been described residing into intergenic regions (intergenic miRNAs), but in lower frequency, they are found into intronic regions (intronic miRNAs), close to other miRNAs building clusters (poly-cistronic miRNAs), or transcribed from their own promoter (mono-cistronic miRNAs or mirtron), which requires the intervention of the spliceosome to generate the primary transcript (Wahid et al., 2010; Barahona, 2019). The next step takes place in the nucleus and it is led by Drosha, a class 2 RNase III enzyme that requires the DiGeorge syndrome critical region in gene 8 (DGCR8) to form the microprocessor complex, to cleave the stem of the loop structure of the pri-miRNA transcribed by Pol II, and release a ~70 nt hairpin shaped structure, known as precursor miRNA (pre-miRNA). After that, the resulting pre-miRNA is translocated into the cytoplasm by the RanGTP-dependent nuclear transport receptor exportin-5 (EXP-5). The transport occurs through nuclear pore complexes when EXP-5 recognizes the double-stranded RNA (dsRNA) stem-loop and leads it out of the nucleus where hydrolysis of GTP occurs. Once in the cytoplasm, pre-miRNA is subsequently processed by Dicer protein, an endonuclease cytoplasmic RNase III enzyme, which becomes the pre-miRNA in a mature miRNA duplex. Dicer protein, in a highly specific manner, removes the terminal miRNA loop, leaving a 22 nt double-stranded structure. In humans, Dicer protein is associated with two proteins, trans-activation response RNA-binding protein (TRBP) and protein kinase, interferon-inducible double-stranded RNA dependent activator (PKKRA, also known as PACT), which contribute to the construction of the effector RNA-induced silencing complex (miRISC). According to the current model, once the 22 nt double-stranded mature miRNA is generated, it is loaded into the Argonaute family protein complex (Ago) in an ATP-dependent manner to produce the precursor RNA-induced silencing complex (preRISC). After that, the degradation of one strand of the miRNA (passenger strand), whereas the other strand (guide strand) remains bound to Ago, constitutes the final mature miRNA, which assemblies the (miRISC). Strand selection for the cleavage of the dsRNA is based on thermodynamic stability, most stable remains, while the other is degraded.

Finally, mature miRNA guides RISC to its target sites in the 3´ untranslated region (UTR) of the mRNA which is silenced by translation repression or degradation (Wahid et al., 2010; Bartel, 2018; Gebert & MacRae, 2019).

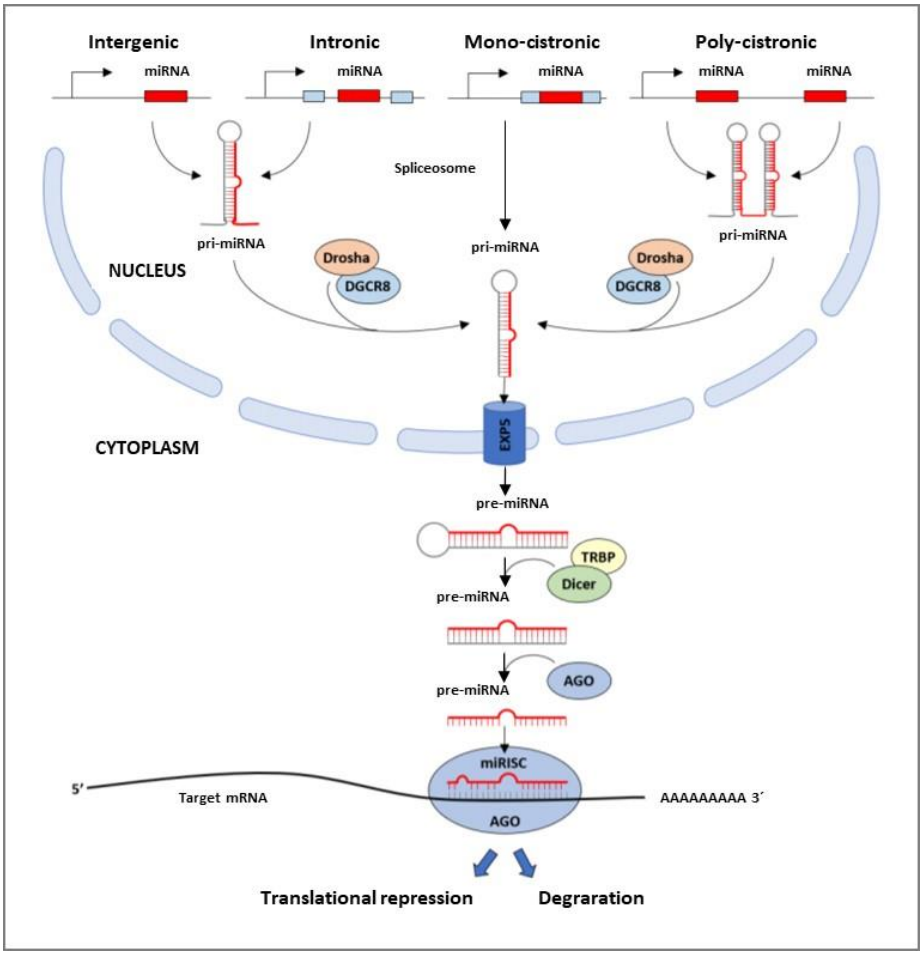

Figure 5. Biogenesis of miRNAs. miRNAs are transcribed by Pol II from intergenic, intronic, and poly-cistronic regions of the genome, or by spliceosome in the case of mono-cystronic miRNAs, to generate stem-loop structures called pri-miRNAs, which are processed in the nucleus by Drosha-DGCR8 into pre-miRNAs. After that, the hairpin shaped structures are exported to the cytoplasm by EXP-5, in a GTP-dependent manner, where they are processed by Dicer-TRBP to generate a duplex miRNA by the removal of the loop structure. The dsRNA structure is loaded into the AGO protein family, which eliminates the passenger strand remaining the most stable one. Finally, mature miRNA single-stranded and Ago constitute the miRISC.A complex in which miRNA guides the recognition of the mRNA target and RISC inhibits the gene expression by translational repression or degradation depending on cell requirement (adapted from Rivera-Barahona A, 2019).

Recognition of mRNA targets and gene expression silencing by translational repression or degradation occurs through an essential sequence mostly situated between nucleotides 2 to 7 (counting from the 5' end) of the mature miRNAs known as ¨seed sequence¨, which is complementary to the binding site in the 3´UTR of the target mRNA (Mohr & Mott, 2015; Bartel, 2018). The pairing between the seed sequence and the target site of the mRNA is crucial to determine the silencing method, degradation, or translational repression (Mohr & Mott, 2015). Degradation occurs when the seed sequence matches perfectly with the targeted transcript allowing, a method commonly reported in plants. But, if the seed sequence-binding to the transcript was not complete, as usually occurs in animals, slicing of the mRNA does not occur, and miRISC could only block the initiation of the translation process making it less efficient, and subsequently repressing translation of the mRNA target. However, it has been demonstrated that in mismatched-bindings, the adaptor protein TNRC6 can be recruited by Ago and interacts with deadenylase complexes to clip the poly(A) tail of the mRNA target causing mRNA destabilization that derivate into degradation of the mRNA target (Bartel, 2018; Barahona, 2019; Gebert & MacRae, 2019). Therefore, it could be that degradation or translational repression of the targeted mRNA depends on the cell requirement and its extracellular communication, and not necessarily because of a perfect binding (Mohr & Mott, 2015).

To finalize, it is well established that miRNAs exhibit tissue and cell specificity expression patterns and they are grouped in families based on the similarity of their seed sequences forming complex networks of interactions allowing one miRNA can target many different mRNAs, and one mRNA can be regulated by many different miRNAs to interfere and regulate biological pathways (Gebert & MacRae, 2019) involved in many biological functions such as developmental timings, cell differentiation, embryogenesis, metabolism, organogenesis, and apoptosis (Saliminejad et al., 2019). Because of that, their deregulation and aberrant expression patterns have been strongly associated with many diseases and could serve as interesting indicators of pathology (O'Brien et al., 2018).

3.2 miRNAs as useful biomarkers and therapeutic strategy in pathology

Numerous studies demonstrate that miRNAs are released from the cells into extracellular fluids including urine, serum, cerebrospinal fluid, and preservation solutions, among others, serving as signaling molecules that mediate in cell-cell communication, acting as regulators, able to modulate cellular activities (Saliminejad et al., 2019). They can be found circulating in vesicles such as exosomes, microvesicles, apoptotic bodies, or associated with molecules like high-density lipoprotein (HDL) or proteins like Ago2 (Sohel, 2016; Saliminejad et al., 2019; Salloum-Asfar et al., 2019) (**Figure 6**).

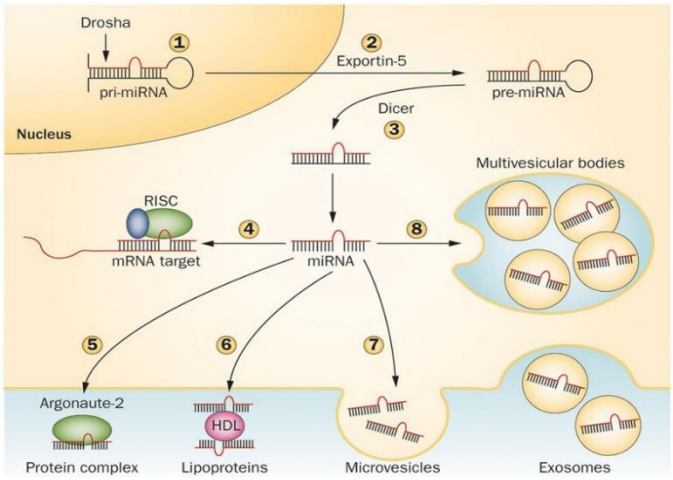

Figure 6. Circulating miRNAs released from the cells into extracellular fluids. Mature miRNAs already synthesized (**1-4**) can be released into the extracellular microenvironment to target other cells serving as signaling molecules and regulators. They are carried out by RNA-binding proteins like Ago2 (**5**), associated with lipoproteins, such as HDL (**6**), or vehiculized by vesicles including exosomes, microvesicles (**7**), and Multivesicular bodies (**8**) (Guay, C. & Regazzi, R., 2013).

In contrast to other cellular RNA species, miRNAs are highly stable against degradation, thus they resist room temperatures several days, and also conditions as boiling, multiple freeze-thaw cycles, and high or low pH. Based on these features, circulating miRNAs have been widely reported as potential and excellent biomarkers that indicate the presence of different pathologies and even, stage and progression of many diseases (Huang W, 2017; O'Brien et al., 2018; Hanna et al., 2019). Regarding that, our lab has previously identified and published under intellectual property protection, a set of serum microRNAs, including miR-101-3p, miR-127-3p, miR-210-3p, miR-126-3p, miR-26b-5p, miR-29a-3p, miR-146a-5p, miR-27a-3p, miR-93-3p and miR-10a-5p, able to diagnose Acute Kidney Injury (AKI) at Intensive Care Unit (ICU) and associated to cardiopulmonary bypass (CPB), in comparison to

control patients (Aguado-Fraile et al., 2015), contributing to demonstrate the value of microRNAs as biomarkers of disease in clinical practice.

Furthermore, many studies have confirmed that extracellular miRNAs can regulate biological functions in platelet cells, acting as intercellular signaling molecules and regulating molecular pathways (Riffo-campos et al., 2016; O'Brien et al., 2018). Also, it has been demonstrated that the return of the altered miRNA pattern expression to normal levels can restore homeostasis in animal models and even eliminate certain malignancies (Wahid et al., 2010). Based on that, miRNAs have been unleashed as novel targets for developing therapies, against diseases (Huang W, 2017). Moreover, *in vivo* delivery vehicles for miRNAs overexpression, or anti-miRs constructs, able to block miRNAs function in the cells, have been developed and successfully achieved in animal models. The most extended methods used for *in vivo* miRNA overexpression are based on viral particles, lentivirus (LV) or adeno-associated virus (AAV), containing the pre-miRNA sequence. Also, liposomes and polymers conjugated with the miRNA sequence are being validated as useful tools for this purpose.

Currently, the major miRNAs-based therapies are in the pre-clinical stage. Remarkably some of them, including Miravirsen, an intramuscular inhibitor of miR-122 for the treatment of Hepatitis C, systemic delivery of miR-34 mimic as a potential therapy for liver cancer, or the recovery of miR-21 renal expression in Alport syndrome patients, are already being tested in clinical trials and constitute the most advanced miRNA-based therapeutics to date (Saliminejad et al., 2019)(www.clinicaltrials.gov).On the other hand, clinical validation of miRNA signatures for early diagnostic use of many diseases are already ongoing and its offered to clinicians and covered by major insurance companies (Bonneau et al., 2019).

3.3 miRNAs in CKD and macrophage polarization

Healthy kidneys have a tissue-specific miRNAs expression pattern that constitutes a renal physiology signature. miR-192, miR-194, miR-204, miR-215, and miR-216 were the first miRNAs reported abundantly expressed in human kidneys (Sun et al., 2004; Ichii & Horino, 2018). Many studies later suggested the expression of other miRNAs in this organ and, not all of them equally expressed along the different renal compartments in homeostasis conditions. For example, miR-192 and miR-194 were reported highly expressed in the cortex, whereas miR-27b expression was characteristic of the medulla. However, miRNAs expression can be differently altered during the progression of kidney injury depending on the etiology of the damage (Lorenzen et al., 2011).

To date, many miRNAs have been associated with CKD in humans and animal models. One of the first was the up-regulated expression of miR-21 associated with renal pathogenesis in human biopsies of IgA and diabetic nephropathies, both extended etiologies of CKD (Zarjou et al., 2011). miR-21 targets molecules including p-53, SMAD7, TGFβ-R2, TIMP331, ERK/MAPK, PTEN, PPARα, among others, which could be key mediators in the

development of disease (Ichii & Horino, 2018). miR-192 was reported also markedly increased in human biopsies of diabetic nephropathy correlating with tubulointerstitial fibrosis and impaired kidney function, through targeting TGFβ1 signaling (Kato et al., 2007). In contrast, the miR-200 family has been published downregulated in IgA nephropathy, whereas miR-141 and miR-205, also were found upregulated. All of them correlating with proteinuria, GFR decline, and loss of E-Cadherin expression (a cell epithelial marker) (Lorenzen et al., 2011). In UUO mice elevated expression of miR-433, miR-382, and miR-491 were recorded in the tubulointerstitial, inner and outer area, and glomerulus or epithelial cells respectively (Zhou et al., 2010Li et al., 2013; Kriegel et al., 2020), and miR-34c also was reported increased in this mouse model, having as downstream factors CTGF, αSMA, collagen type 1, collagen type 3, and fibronectin, involved in fibrosis development (Morizane et al., 2014).Besides, *in vitro* experiments in human proximal tubular epithelial cells (HK-2 cells) treated with high TGFβ1 levels (a fibrosis development contributor) demonstrated a downregulation of miR-29a expression in the cells. miRNA that bioinformatics approaches predict to be involved in the regulation of many genes related to extracellular matrix formation, such as collagen genes, MMP2, and integrin-1β (Ichii & Horino, 2018). These are only few studies published showing evidences that miRNAs deregulation is intimately related to fibrosis development underlying CKD.

Regarding that, unpublished results in our lab demonstrated that the induced expression of miR-127-3p in HK-2 cells submitted to high levels of TGFβ1 as a pro-fibrotic agent, maintains an epithelial phenotype and blocks TEM, targeting MMP13 mRNA. Moreover, the culture of human fibroblasts in the medium from HK-2 cells in which miR-127-3p expression was up-regulated, induced toxicity, and reduced its activation into myofibroblasts, a process underlying fibrosis. miR-127-3p expression also correlated with the progression of CKD in renal tissue biopsies from patients. Thus, all these data together could suggest that miR-127-3p could be involved in the progression of CKD orchestrating mechanisms underlying fibrosis and maybe inflammation response (unpublished data).

As it was previously described, fibrosis is considered a process strongly associated with inflammation resolution, in which the switch of macrophages between different phenotypes plays a pivotal role in the progression of CKD. miRNAs have been reported as key mediators in macrophage phenotype polarization, and their deregulation has been extensively linked to an excessive or impaired inflammatory response of macrophages during disease (N. Wang et al., 2014). In this context, various studies have analyzed miRNAs profile in different polarized macrophage phenotypes to determine miRNAs expression in M1 and M2 conditions in humans and mice, and their functional role in the polarization process. miR-9, miR-155-5p and miR-125b are some examples of miRNAs consistently reported able to promote pro-inflammatory M1 macrophages (Thulin et al., 2013; Zhang et al., 2013; Cobos Jiménez et al., 2014). Interestingly, miR-127-3p also has been reported as an enhancer of M1 macrophages polarization, since stimulation with LPS elevates miR-127 expression in macrophages, which inhibits Bcl6 expression and leads to an increase in the phosphorylation of JNK, promoting M1 polarization and amplifying pro-

inflammatory signaling in acute lung inflammation (Ying et al., 2015). However, miR-124, miR-223, miR-34a, let-7c, miR-132, miR-146a, and miR-125a-5p have been identified with anti-inflammatory responses and M2 polarized macrophages by several studies (Q. Chen et al., 2012; Banerjee et al., 2013; Yang Sun et al., 2013; Vergadi et al., 2014; Liu et al., 2015; W. Zhang et al., 2015; Essandoh et al., 2016).

The functional role of miRNAs implicated in the polarization process has been mainly related to the target of various transcription factors involved in IRF/STAT signaling, which is considered the major pathway controlling the switch of macrophage phenotype (Essandoh et al., 2016). But, it is important to consider that miRNA expression profiles in polarized macrophages could differ depending on the location and stimulation received by the local microenvironment (Essandoh et al., 2016). Even though, some miRNAs have been reported associated with different phenotypes depending on the inflammatory stage (Sheedy, 2015). For example, miR-21 has been described targeting STAT3 and thereby promoting M1 phenotype during early stages of inflammation, while at inflammation resolution phase, it had been reported downstream CSF-1R, being involved in M2 polarization and the suppression of M1 macrophages (Caescu et al., 2015).

Modulating inflammatory response always has been a very interesting topic for basic and clinical research to control the progression of many diseases. In this context, as mediators in cellular response, miRNAs have demonstrated in the last decade that they could serve as a potential therapeutic strategy for the treatment of many pathological contexts.

To summarize, it is important to highlight that CKD is an unresolved worldwide health problem affecting around 15% of the world population, lacking accurate biomarkers for early diagnosis and efficient therapies to block or reverse progression. As a consequence, CKD runs silently for a long time until its detection, when kidney damage is already irreversible and finally, patients need substitutive therapy which implies a poor quality of life for them and high economic cost for the health systems. All this highlights the urgent clinical need of characterizing and validating new molecular targets for novel therapeutic approaches for CKD, including miRNAs, lately emerging as potentially useful biomarkers of disease and suitable for modulation as an efficient strategy for CKD treatment.

It is also important to mention that although intensive research has been recently done in CKD, most of the publications describe experimental therapies devoted to mitigate disease symptoms or to improve patients´ life quality, lacking knowledge in mechanisms underlying disease trigger and development. Remarkably, in this work, we study miRNAs as key elements in the critical relationship between inflammation and fibrosis development, considering fibrosis as a consequence of an impairment in inflammation resolution and suggesting macrophage polarization as a critical cellular process implicated in this impaired resolution. Therefore, whether results support this rationale, miRNAs modulation could be considered as an efficient and novel therapeutic approach to CKD.

Objectives

Previous data from our lab demonstrate that miR-127-3p expression increases in HK-2 cells treated with TGFβ, a classical pro-fibrotic stimulus that induces EMT in the context of renal diseases, and that this miRNA correlates with damage severity in biopsies from CKD patients, strongly suggesting that could be involved in the cellular processes that contribute to fibrosis development underlying CKD (Martín-Gómez, Ph.D. Dissertation, October 2018). Furthermore, our lab also contribute to unveil microRNAs as potential useful biomarkers in AKI and CKD (Aguado-Fraile et al., 2015; Martín-Gómez, Ph.D. Dissertation, October 2018). Moreover, it has been widely described that macrophage polarization has a crucial role in renal injury and fibrosis development during CKD progression (Engel & Chade, 2019). Additionally, it has been reported that miR-127-3p promotes M1 macrophage polarization amplifying pro-inflammatory response in acute lung inflammation (Ying et al., 2015).

Based on the state of the art and our previous results, we propose as the **hypothesis** of this work that **miR-127-3p could play an important role in CKD establishment and progression by modulating the inflammatory macrophage response and fibrosis development during the progression of the disease, among other mechanisms, therefore, miR-127-3p could also be considered a potential biomarker in this pathology context**.

To confirm or refuse this hypothesis, we will address as the **principal objective** of this work to **characterize the role of miR-127-3p in the renal fibrosis underlying CKD and the associated macrophage polarization during the disease development and to address the usefulness of miR-127-3p as biomarker in this clinical context.**

To achieve this goal, we propose the following **partial objectives**:

1. Characterize miR-127-3p expression in an experimental murine model that mimics human CKD (UUO model) and investigate the role of this miRNA in the progression of kidney damage by modulating the miRNA expression *in vivo*.

2. Characterize miR-127-3p expression in different macrophage phenotypes obtained by exogenous stimulation (M1[LPS] and M2a[IL-4]) and the role of this miRNA in the polarization process by modulating the miRNA expression *in vitro*.

3. Determine the serum expression of an associated renal damage set of miRNAs (miR-127-3p, miR-126-3p, miR-146a-3p, miR-26b-5p, miR-27a-3p and miR-93-3p) in CKD patients exhibiting different severity, and correlate serum miRNA levels with the main clinical features of the patients.

Material and methods

Applied methods and material required to achieve the objectives proposed in this work will be described in this section. Conditions of each method are detailed bellow allowing reproducibility. Used material has been specified for each technique.

1. Unilateral ureteral obstruction (UUO) animal model mimicking human CKD

1.1 UUO animal model description: procedure and animals used

UUO animal model is the most widely accepted experimental model to mimic human CKD in an accelerated manner, and useful to study pathogenesis, mechanisms, and effects of drug intervention during disease (Martínez-Klimova et al., 2019b). The experimental procedure consists of a ligation of the ureter of one kidney, usually the left, and commonly with a 5.0 silk thread, 1 cm below the renal pelvis. The kidney in which the ligation was performed is named obstructed kidney (OK), and the other one, is named contralateral kidney (CK) and can be used as negative control. The intervention reduces the renal blood flow and declines the GFR in the OK within 24h after the urine flow obstruction, which causes tubulointerstitial injury, accompanied by vasculature damage, and the recruitment of an inflammatory infiltrate, mainly composed by macrophages. On day 7 after surgery, tubular dilation and atrophy appear together with an established renal fibrosis in the obstructed organ. Finally, OK reaches an estimated human end-stage by around 2 weeks, whereas CK supposedly remains histology unaffected and functional (Arvaniti et al., 2016; Martínez-Klimova et al., 2019b). UUO animal model has advantages including easy performance, good reproducibility, and short time-course. The possibility to choose between rat and mice, and no specific strain dependence, are also relevant properties of this pre-clinical model. However, disadvantages include the non-accurate estimation of renal function by estimation of serum creatinine and urea, and proteinuria analysis, because the ligation on the left ureter prevents the waste of urine from the operated kidney (H. C. Yang et al., 2010a) and contralateral non operated kidney can compensate renal function.

4- to 6-week-old male C57BL/6j mice weighing 20-25 g were purchased from Charles River Laboratories and settled in the animal facility, being divided by a maximum of 5 animals per cage with standard conditions (12h light/dark cycle, constant temperature, 24 ± 0.2°C, and free access to rodent chow and water). The UUO procedure was developed in the left kidney, as it was described previously, under total anaesthesia by inhaled 2% mixture of isoflurane/oxygen. During the surgery, mice were positioned on a heated surface to maintain an optimal body temperature, and a dose of 20 mg/kg of Tramadol was subcutaneously administrated pre- and 24h post-surgery as analgesia, to minimize surgical pain. Animals were sacrificed by terminal cardiac puncture under anaesthesia at the end point of the model. All *in vivo* experiments were performed in accordance to the Ethics Committee for Animal Wellbeing (CEEA, for the Spanish acronym of ´*Comitée de Experimentación Ético Animal*´) of the Animal

Facility of IdiPAZ, were they were carried out, and authorized by the Autonomous Community of Madrid (CAM, for the Spanish acronym of *´Comunidad Autónoma de Madrid´*) (PROEX 161/17).

1.1.1 Experimental animal groups

- **UUO-mice:** In these animals, UUO model was performed to obtain Obstructed Kidney (OK) and Contralateral Kidney (CK). Stablished sacrificed times were 3, 5, 7, 10, and 15 days after surgery.
- ***Sham*-mice:** Control group in which the same intervention was performed, but without clamping the ureter, therefore, any kidney resulted affected (*Sham* kidneys). Sacrificed time for these animals was established at 5 days after the surgical procedure.

1.1.2 Sample collection

Urine (pre- and post-intervention): Basal samples were collected during the 24h before UUO or *sham* procedure, and post-intervention samples were obtained 24h before the sacrifice, both using metabolic cages. ~0.5 to 1 ml of urine was obtained per animal, and centrifuged at 1,500 rpm for 5 min at 4°C to remove waste particles before they were saved in freezing tubes at -80°C for future analysis.

Blood/serum: ~1 ml of blood was obtained per animal by the cardiac puncture performed at sacrifice time. For serum extraction, blood was collected in a Vacutainer EDTA/separator gel tube (BD) and maintenance at room temperature for 30 min. Then they were centrifuged at 2,500 rpm for 10 min at 4°C and saved frozen at -80°C for future analysis.

Kidneys: Kidneys were removed by dissection of renal pedicles and weighted. Half of each kidney was directly frozen in liquid nitrogen for RNA and protein extraction, and the other half was fixed in 4% formalin and paraffin-embedded for further analysis.

2. *In vivo* miR-127-3p modulation in the UUO murine model

miR-127-3p expression was modulated in the UUO mouse model during this work. To address that, a miRNA Inhibitor was used to block miR-127-3p expression, while the overexpression of the miRNA was tried by viral constructions. The procedure and material and methods applied for these interventions are detailed below.

2.1 miR-127-3p inhibition in the UUO murine model

miR-127-3p expression was inhibited in mice by subcutaneous injection of mmu-miR-127-3p miRCURY LNA miRNA Inhibitor from Qiagen, diluted in sodium chloride. A Negative Control acquired from the same company was used as Scrambled control. **Table 1** describes the specifications of the probes purchased for this procedure.

To establish the adequate dose of miRNA Inhibitor, mice in which UUO was performed were randomly divided into groups of 2 animals, and treated with different doses of mmu-miR-127-3p Inhibitor following the manufacturer's recommendation: 20 mg/Kg, 10 mg/kg, and 5 mg/kg were the doses for miRNA Inhibitor groups, and 100 µl of sodium chloride, was used as a vehicle control group. 7 days after surgery, mice were sacrificed and kidneys were harvested to monitored miRNA modulation in the renal tissue by qRT-PCR. Finally, 10 mg/kg was the established dose for showing the highest miRNA interference results during the experiment, in a safe manner.

Table 1. miRNAs interference probes used for *in vivo* miR-127-3p inhibition. Product specification and use.

Product name	Product group	Sequence Number	Sequence 5´-3´	Use	Reference
mmu-miR-127-3p	miRCURY LNA miRNA Inhibitor	MIMAT0000139	UCGGAUCCGUCUGAGCUUGGCU	miRNA inhibition	Cat. Num. 339203 PER-YCI0199249-FZA
Negative Control A	miRCURY LNA miRNA Inhibitor	-	ACGTCTATACGCCCA	Scrambled control	Cat. Num. 339203 PER-YCI0201588-FZA

Considering UUO murine model procedure together with the interference miRNA conditions explained before, the experimental mice groups designed for this procedure were:

- **miR-127-3p inhibited UUO-mice:** UUO-mice in which miR-127-3p Inhibitor probe was administered to obtain miRNA-modulated Obstructed kidney (OK) and Contralateral kidney (CK) samples. Sacrificed times were established at 3, 5, 7, and 15 days after surgery.
- **miR-127-3p inhibited *Sham*-mice:** *Sham* group with non-intervened *sham* kidneys in which miR-127-3p expression was modulated. Sacrificed time for these animals was established at 5 days after the surgical procedure.
- **Scrambled UUO-mice:** UUO-mice in which Negative Control A was administered to obtain Scrambled Obstructed kidney (OK) and Contralateral kidney (CK) samples. Sacrificed times were established at 3, 5, 7, and 15 days after surgery.
- **Scrambled *Sham*-mice:** *Sham* group with non-intervened kidneys in which Negative Control A probe was administered to obtain Scrambled *Sham* kidneys. Sacrificed time for these animals was established at 5 days after the surgical procedure.

To ensure an efficient inhibition of miR-127-3p expression, treatment doses were differently administered in mice along the UUO experimental model depending on the sacrificed time. **Figure 7** summarized the *in vivo* administration of the treatment scheme followed during the experimental procedure.

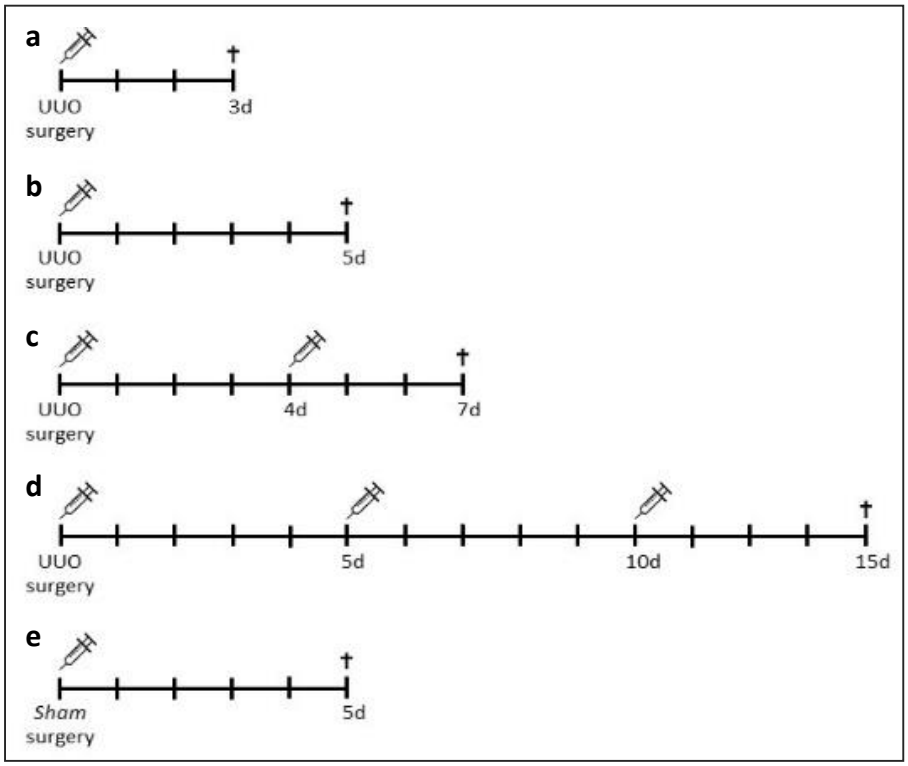

Figure 7. Scheme for treatment administration in the experimental UUO mouse model to inhibit miR-127-3p expression. First dose of the corresponding treatment (miR-127-3p Inhibitor or Negative control) was injected after performing the surgery (UUO or *sham*) for the entire experimental groups. For 3d-UUO, 5d-UUO, and *sham* mice, the first dose was unique until the sacrifice (**a**, **b, and e**). In 7d-UUO mice, a second dose was administered on day 4 after surgery (**c**). Finally, 15d-UUO mice groups were treated beside the initial dose, at day 5 and day 10 after surgery (**d**).

Sample collection from UUO miR-127-3p inhibited mouse model was carried out as it was described before in this section.

2.2 miR-127-3p over-expression in UUO mice

miR-127-3p overexpression along the UUO model in mice was addressed by the administration of different viral vehicles containing the pre-miR-127-3p sequence or a Scrambled sequence as negative control of miRNA expression. Moreover, for each vehicle, we tested several vias and/or dosages.

2.2.1 Adeno-Associated Viral (AAV) constructs

Adeno-associated virus constructs were given up by the Department of Biochemistry and Molecular Biology of *Universitat Autònoma de Barcelona* (UAB), where they were produced by the Virus Unit Core Facility led by Doctor Chillón Rodríguez. **Table 2** specifies the constructs tested in mice for *in vivo* overexpression of miR-127-3p.

Table 2. Adeno-associated constructs tested for *in vivo* miR-127-3p overexpression in mice. Specifications showed in this table were provided by the producer laboratory (Virus Unit Core Facility) based on their research background. AAV doses are specified in GC/ml (genomic copies per milliliter).

Vector name	Construct	Titer (GC/ml)	Vol. injected/mice
AAV1-CMV-GFP	UPV-629	2.5×10^{12}	100 µl AAV stock + 100 µl vehicle
AAV2-CMV-GFP	AAV2-GFP	1.6×10^{12}	130 µl AAV stock + 70 µl vehicle
AAV8-CMV-GFP	UPV-1044	6.12×10^{12}	41 µl AAV stock + 159 µl vehicle
AAV9-CMV-GFP	UPV-1075	1.16×10^{13}	21.3 µl AAV stock + 178.5 µl vehicle
AAV10-CMV-GFP	AAV10-GFP	1.9×10^{13}	14.3 µl AAV stock + 185.7 µl vehicle

AVV dose was administered in mice by retro-orbital injection using sodium chloride as a vehicle. One mouse per AVV construct was employed in this experimental procedure. Since this experiment aims to determine whether any of the AVVs have kidney tropism, no UUO surgery was performed, nor did the adeno-associated constructs used contain the miRNA sequence. Sacrificed time was established on the eleventh-day post-intervention and major organs were harvested for acquiring fluorescent images under an IVIS Imaging System. The radiance (photon emission per unit area) of a region-of-interest (ROI) was acquired by the viewer image software.

2.2.2 Lentiviral-vector (LV) particles

Third generation self-inactivating (SIN) lentiviral vectors used to produce viral particles enable to infect mice were acquired from System Biosciences in bacterial stocks. **Figure 8** specifies the backbone employed in this experiment containing the **mmu-pre-miR127-3p** plasmid to induce miR-127 expression, or **mmu-pre-000** one, as Scrambled Control hairpin, both with approximately 100 bp. The backbone is a human immunodeficiency virus (VIH) lentiviral vector with around 8,000 bp named CD513, that contains a copGFP reporter and a Puromycin resistant gene under the control of an EF1 promoter where the plasmid is cloned under the control of a CMV promoter.

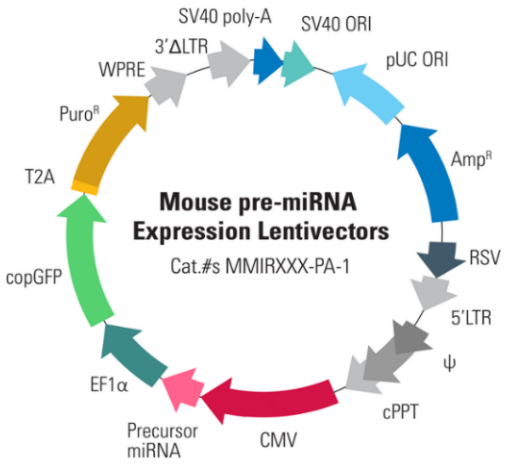

Figure 8. Mouse pre-miRNA expression lentivector backbone used for miR-127-3p overexpression in mice. The HIV-1 derived pMIRNA1/pCD513 vector contains a WPRE element to enhance CMV-driven transcripts translation. SV40 origin enables efficient termination of transcription. Hybrid RSV-5'LTR promoter provides a high-level expression of the viral transcripts in HEK293 cells. cPPT, GAG, LTRs genetic elements are necessaries for packaging, transducing, and integrating the viral expression construct into genomic DNA. pUC origin copies replication in *Escherichia coli* cells. Ampicillin resistance gene for bacteria selection is also included as well as CopGFP as fluorescent marker to monitor positive transfection and transduction. Product Catalog Number MMIRXXX-PA-1 from System Biosciences.

Plasmid amplification

Bacterial stocks with the constructs streaked were plated with Lennox L Agar (#22700025, Invitrogen) containing 100 ng/ml of ampicillin (#69-53-4, Sigma-Aldrich), and incubated overnight at 30°C in a stove. Next day, single colonies were picked and incubated in 3 ml of Miller's LB Broth Base (#12795027, Invitrogen) shaking overnight at 30°C (mini-cultures). After this time, 2,500 µl of the mini-cultures were added in 1 l of LB Broth medium with 100 ng/ml of ampicillin in an Erlenmeyer flask and incubated shaking overnight at 30°C (maxi-cultures). To continue, DNA was extracted from maxi-cultures using an EndoFree Plasmid Maxi Kit (#12362, Qiagen), following the manufacturer's instructions. Concentration and purity of the obtained DNA were estimated in µg/µl with a Nanodrop 2,000 device (Thermo Fisher) and considering the A260/280 and A260/230 ratios. Finally, correct plasmid sequences were verified by sequencing in the *Parque Científico de Madrid*.

Lentivirus particles production

24h hours before starting the transfection protocol, HEK293T/17 cells from ATCC (#CRL-11268) were seeded in 20 dishes (per plasmid) of 100 mm ($5 \cdot 10^6$ cells/dish) and incubated overnight at 37°C in 5% CO_2 with DMEM (Dulbecco's Modified Eagle Medium) (#31885-023, Gibco) supplemented by 15% fetal bovine serum (FBS) (#10099-141, Gibco) non-heat treated, 1.5% Penicillin (10,000 U/ml), Streptomycin (10,000 µg/ml) and L-Glutamine (29.2 mg/ml) (PSG) (#10378-016, Gibco), and 1.5% HEPES Buffer (#15630-049, Gibco). Next day, 2h before continuing with the protocol, media from plates were replaced with 7 ml of fresh DMEM w/o PSG, and incubated again at 37°C until their use. Meanwhile, Lipofectamine and DNA mix required for the transfection of each plasmid were prepared following the next protocols:

- Lipofectamine Mix: 750 µl of Lipofectamine 2,000 Transfection Reagent (#11668-027, Invitrogen) were added into 10 ml of DMEM. Mixture (one per plasmid) was incubated at room temperature until their use.
- DNA Mix: 130 µg of DNA extracted from maxi-cultures (each plasmid has to be prepared separately) were added into 10 ml of DMEM, together with 37 µg of pMD2.G DNA (#12259, AddGene) and 73 µg of psPAX2 DNA (#12260, AddGene), both necessaries for virus packaging. Mixes were incubated for 5 min at room temperature.

Lipofectamine Mix was added into DNA Mix for each plasmid by dropping. Solutions were gently mixed and incubated for 20 min at room temperature to enable the formation of transfection complexes. After this time, 1 ml of the transfection solution was added per plate (20 plates per plasmid) drop-wise, distributed by gently swirling, and incubated overnight at 37°C. The day after, medium was replaced and cells were again incubated overnight at 37°C. Finally, the virion-containing media was harvested 48h post-transfection and filtered through a

45-mm filter (#146615, Biolab) to remove cell debris. The viral supernatant was purified by ultracentrifugation (2h, 28,000 rpm, 4°C) using a 20% sucrose cushion. Virus pellets were re-suspended overnight in 100 µl of PBS and stored at 4°C. A second harvest was performed by adding fresh medium to the virus-producing cells and the supernatant was collected again, ultracentrifuged, and re-suspended the following day. The concentrated virus was stored at 80°C in 100 µl aliquots until their use.

Lentiviral particles tittering

To determine lentiviral particle concentration, the day before starting the titer protocol, $0.076 \cdot 10^6$ HEK293T cells per well were seeded in a 24-well plate (one plate per plasmid). Next day, the lentivirus stocks were diluted in 10-folds serial dilutions from 10^{-2} to 10^{-6}, into a final volume of 1 ml of DMEM supplemented by 15% of FBS non-heat treated, 1.5% of PSG, and 1.5% HEPES Buffer, containing 8 µg/ml of polybrene (#H9268, Sigma-Aldrich). Plates were incubated at 37°C. 48h post-infection, percentage of fluorescent cells positive for GFP were counted using flow cytometry (Beckman Coulter). Finally, the lentivirus titer was estimated in well in which 1-10% of the cells were expressing GFP and following this formulation: (N seeded cells) x (Dilution Factor) x (% of GFP positive cells/100) / (Final transfection Volume).

Lentivirus administration in mice

To establish the adequate protocol that ensures the infection of kidney cells with the lentivirus particles able to induce miR-127-3p expression in mice, and avoiding side effects, after an intensively search in the bibliography, different protocols were selected to be tested in the animals (**Table 3**).

Table 3. Administration vias and dosages tested for *in vivo* miR-127-3p induction by lentiviral particles. Vias/ways for lentivirus administration in mice were found in the bibliography from different publications. Lentivirus doses for each method are specified in TU/ml (transduction units per microliter). Sacrificed times were chosen based on our previous experience.

Administration route	Lentivirus dose	Sacrificed times
Renal arteria (H. H. Chen et al., 2016)	10^6 TU/ml in 100 µl LV stock	3d, 5d and 10d
Renal parenchyma (D. Chen et al., 2017)	10^6 TU/ml in 100 µl LV stock	3d, 5d and 10d
Retro-orbital (systemic) (Fierro-Fernández et al., 2020)	10^8 TU/ml in 100 µl LV stock + 100 µl vehicle	5d, 10d and 15d

One mouse per administration route and sacrifice time were employed in this experimental procedure, and UUO surgery did not be performed in these animals to be an initial test. Besides, 2 *sham* mice were included as a control

to further compare results. Moreover, *s*ample collection was different from the *in vivo* experiments previously described. In this experiment, all the biological material was discarded, except kidneys, which were harvested and divided into two halves, one was placed in 30% of sucrose overnight before being embedded in Tissue-Tek® OCT (#4582, Sakura) cryo embedding compound, and frozen at -80°C; and the other half was fixed in 4% formalin and paraffin-embedded for further analysis.

3. Techniques for histological studies

Formalin-fixed and paraffin-embedded (FFPE) tissues were sectioned into 3-4 µm thick slices using a microtome (Microm HM 325, Thermo Scientific) and placed into polysyne covered microscopic-slides *(#K802021-2, Dako*). To perform histological staining, tissues were deparaffinized in an oven for 1 h at 60°C, and sequentially incubate for 10 min at room temperature in xylene, 100% alcohol, 95% alcohol, 70% alcohol solutions, and finally, in water for 20 min, to rehydrate the tissue.

After the subsequent stain, the slides were observed under a phase-contrast optical microscope and evaluated by a pathologist specialized in renal diseases. Tissue images were acquired using a digital camera incorporated into a Nikon Eclipse TE2000-U microscope.

3.1 Hematoxylin and eosin (H&E) staining

H&E is the gold standard method used by pathologists to evaluate structure of tissue and its alterations for clinical evaluation. In this work, H&E stain was performed in an automated system (CoverStainer, Dako) following the standard protocol established for patient's biopsies, in which after rehydration, tissues are submerged in Hematoxylin (Dako) for 250 s, followed by a wash in abundant distilled water, and submerged again in Eosin (Dako) for 250 s. Finally, samples were evaluated scoring the damage observed into the endothelial, glomerular, tubular, and interstitial renal compartments (Khalid U et al., 2016).

3.2 Masson´s trichrome (Masson) staining

Masson is a three-color staining protocol used in tissue fibrosis evaluation since it allows pathologists to distinguish cells from connective tissue composed by deposits of collagen I, stained in blue color, which are an accepted sign of tissue fibrosis development. Masson protocol in rehydrated tissues was performed using a Masson Staining Kit (ArtisanLink, Dako) and following the manufacturer´s recommendation.

3.3 Immunohistochemistry (IHC)

Immunohistochemistry was performed to visualize protein content and localization in tissue samples through detection of specific epitope-antibody interactions, also labelled. First, FFPE rehydrated samples were heat-treated using a pressure cooker to unmask the antigenic epitopes. Antigen retrieval solution and boiling time suitable for each antibody are specified in **Table 4**. Then, slides were tempering for 20 min immersed in the preferred retrieval solution, and washed for 5 min in 1X phosphate-buffered saline (PBS) or tris-buffered saline (TBS) solution, depending on antibody recommendations (**Table 4**). Second, tissue-endogenous peroxidase activity was blocked to avoid non-specific signal during immuno-detection activity, by incubating slides in the Peroxidase Blocking Solution (#S2023, Dako) for 30 min at room temperature, in a humidified chamber. To continue, they were washed three times in the 1X buffered saline solution preferred with 0.05% v/v Tween-20 added (PBST or TBST). After that, tissues were treated with 1X PBS or TBS with 1% v/v bovine serum albumin (BSA, #A7906, Sigma-Aldrich) solution for 30 min at room temperature to avoid non-specific antibody binding. Third, samples were incubated with the primary antibody diluted following the specification of the data sheet (**Table 4**), overnight at 4°C in a humidified chamber. Next day, slides were washed three times in 1X PBST or TBST for 5 min before incubating them with the secondary antibody, usually HRP-conjugated (**Table 4**), for 30 min at room temperature. Then, after three more washes of 5 min in 1X PBST or 1X TBST, signal was developed using a detection kit containing DAB substrate as chromogen (#GV82511-2, Dako). Reaction during this step was stop when tissues appears colored applying water. To finalize, a counterstain with Harris' Hematoxylin Solution (#1.09253.0500, Merk), 2 min at room temperature, was performed in the samples to distinguish cellular compartments in the stained tissues. Tissues were dehydrated incubating them in the xylene and alcohol solutions sequence described before, but starting in alcohol and finishing in xylene, and mounting with DEPEX medium (#3808600E, Laica Byosystems) to be analysed and evaluated under the microscope.

Table 4. Primary antibody used for immunohistochemistry staining. Product specification, procedure followed, and IHC-related product used for each one.

Primary Antibody	Source	Reference	Dilution	Wash Solution	Antigen Retrieval Solution	Antigen Retrieval Time	Secondary Antibody	Dilution
Anti-α-Smooth	Mouse monoclonal	Ab7817 Abcam	1,5/1000	PBS	Citrate, pH6	10 min	EnVision Dako, K4065	No diluted
Anti-CD3	Rabbit monoclonal	Ab16669 Abcam	1/100	PBS	Citrate, pH6	10 min	EnVision Dako, K465	No diluted
Anti-CD68	Rabbit polyclonal	Ab125212 Abcam	1/100	PBS	Citrate, pH6	10 min	EnVision Dako, K465	No diluted
Anti-YM1	Goat polyclonal	AF2446 RyD	1/50	PBS	Citrate, pH6	10 min	Anti-Goat Sigma, A5420	1/50

3.4 miRNAs *in situ* hybridization (ISH)

In situ hybridization uses a complementary RNA probe to localize a specific RNA sequence, in this case, a miRNA, in the tissue. To start the protocol, deparaffinized and rehydrated kidney sections were treated with Proteinase K (158918, Qiagen) diluted in 1X PBS (3 µl/ml) for 15 min at 37°C to digest the tissue and allow the probe to penetrate in the cells. Then, they were washed with diethylpyrocarbonate-treated (DEPC-treated) water for 5 min at room temperature to remove the exceeded product. After that, 25 µl of the specific probe solution was added over tissue sections to detect the studied miRNA, or the internal control (housekeeping) (**Table 5**), diluted in Formamide-free microRNA ISH Buffer (#90-012, Exiqon) and DEPC-treated water (probe solution: 1 µl of the probe (studied miRNA or housekeeping)/250 µl of DEPC-treated water/250 µl of Formamide-free microRNA ISH Buffer). Slides were covered and sealed with Fixogum rubber cement (#290110001, Marabu) to avoid evaporation, and incubated overnight at 37°C in a humidified chamber. Next day, samples were washed in 5X SSC for 5 min at 60°C and incubated in 1X Blocking Reagent Solution (#11096176001, Roche) for 5 min at room temperature. Later, 200 µl of DIG-AP antibody (#11093274910, Roche) (1:800) was added in each slide diluted in 1X Blocking Reagent Solution with 10% of sheep serum (S2263, Sigma-Aldrich) and incubated for 1h at room temperature. After two washes in PBST 0.1% v/v for 5 min each one, slides were treated with 150 µl of chromogen solution: 200 µl of NBT-BICP Stock Solution (#11681451001, Roche) diluted in 10 ml of 0.1 M Tris HCl/NaCl pH 9.5, for 2h at 37°C, again in a humidified chamber. Over this time, tissue sections were washed again in PBST for 5 min at room temperature two times, and two more in DEPC-treated water. Finally, nuclei in the tissue sections were stained by incubation with Nuclear Fast Red solution (#N3020, Sigma-Aldrich) for 1h at room temperature. Stain excess was removed under running water before dehydration in the xylene and alcohol solutions sequence described before, but starting in alcohol and finishing in xylene, and mounting with FLUKA Eukitt mounting medium (#03989, Fluka) to be analysed and evaluated under the microscope.

Table 5. Detection probes used for *in situ* hybridization. Product specification and miRNA targeted.

Product name	Target	Product group	Sequence 5´-3´	Use	Reference
hsa-miR-127-3p	miR-127-3p	miRCURY LNA miRNA Detection	/5DiGN/AGCCAAGCTCAGACGGATC/3DiG_N/	miRNA studied detection	339111 YD00611784-BCG Qiagen
hsa-mmurno-U6	Control Probe	miRCURY LNA Control Probe	-	Housekeeping	99002-15 Exiqon

4. Renal function estimation

To study renal function in the experimental mouse model, serum and urine samples collected as it was previously described were provided to the Biochemical Department of *Hospital Ramón y Cajal*, where renal parameters including creatinine, urea, proteins, uric acid, phosphorous, and cystatin were estimated, using the same techniques and equipment's than the regular clinical practice for determining impaired renal function in humans.

5. Human serum samples collection and storage

Human serum samples used in this work for miRNA expression analysis were kindly provided by the Hospital Fundación Alcorcón. Samples belong to the PRONEDI collection (**Annex 1**), including 100 patients diagnosed in different stages of CKD classified following KDIGO Guidelines, and recruited after signing the consent document. At disease diagnosis, when blood samples were collected, 21 patients were in stage 2 of kidney damage, 63 were in stage 3, and 16 in stage 4.

Serum was obtained from blood samples by centrifugation at 2,500 rpm for 10 minutes at 4°C and stored in freezing tubes at -80°C according to the quality standards of the Biobank Facility of *Hospital Fundación Alcorcón*, where they were stored until their use. Each sample is anonymous and identified by an unmistakable code that is associated with a document containing all processing information, and also relevant clinical data and experimental research data obtained for the study.

All experimental designs including human samples have been revised and approved by The Clinical Investigation Ethical Committee of the Community of Madrid (CEIC-R) (PI031707).

6. Cell culture procedures

6.1 Differentiation and culture of murine macrophages

In vitro experiments were developed in primary murine macrophages differentiated from monocytes. To obtain them, monocytes were extracted from the bone marrow of the femur and the tibiae of mice and cultured in macrophage differentiation media in a humidified atmosphere with 5% of CO_2 at 37°C. Macrophage differentiation media consists in DMEM containing 10% of FBS (#DE14-801F, batch 9SB024, Lonza), 4,500 mg/L of glucose (#37966-047, Invitrogen), 100 U/ml penicillin and 100 µg/ml streptomycin (#15070-063, Invitrogen), 25% of HEPES

Solution Buffer pH 7.5 (#17-737E, Biowhittaker), and 10 ng/ml of Recombinant Mouse M-CSF (#315-02-B, PeproTech).

After 5 days, the monocytes were differentiated into macrophages. Erythrocytes and other unattached cells were removed by washing with PBS, and then media was replaced with fresh macrophage differentiation media. It is of utmost significance for culturing these cells to consider that as an inflammatory cell type, they can activate themselves by any stimuli like temperature change or traces from pathogens.

6.2 *In vitro* stimulation for macrophage polarization induction

To induce polarization in the murine macrophages towards different phenotypes, approximately 4 x 10^5 cells/well were seeded in 24 well plates and incubated at standard conditions 24h with complete DMEM media in which polarization factors were added. Cells were stimulated with LPS (20 ng/ml) (#L2654, Sigma-Aldrich) to promote M1 phenotype and with IL-4 (10 ng/ml) (#214-14, Peprotech) to promote M2a phenotype.

6.3 *In vitro* modulation of miR-127-3p in murine macrophages

miR-127-3p expression was modulated in cultured murine macrophages by transient transfection with Pre-miR-127-3p (hsa-miR-127-3p, mirVanaTM, microRNA mimic, #4464066, Ambion) to overexpress miRNA, and Anti-miR-127-3p (hsa-miR-127-3p, mirVana, miRNA Inhibitor, #4464085, Ambion) to inhibit the miRNA expression. Pre-miR-Scrambled (mirVanaTM, microRNA mimic Negative Control #1, #4464088, Ambion) and Anti-miR-Scrambled (mirVana, miRNA Inhibitor Negative Control #1, #4464077, Ambion) were used as negative control tools of transfection. Transfection reagent and medium were SiPORT NeoFX (#AM4511, Invitrogen) and standard DMEM, respectively. Volumes and final concentrations plate used for each transfection are specified in **Table 6**. Conditions were established after setting experiments and checking miR-127-3p expression by qRT-PCR.

Following the manufacturer´s instructions, transfection reagent was added into DMEM and incubated for 10 min at room temperature. Next, miRNAs were mixed at the chosen concentrations with DMEM, and also incubated for 10 min at room temperature. Then, Transfection Reagent mix was added into miRNAs mixes. Solutions were incubated for 20 min at room temperature to allow the formation of transfection complexes and after this time, different condition mixes were added in the corresponding wells/dishes. Finally, plates were incubated at standard conditions overnight, and after 24h, supernatants and cells were harvested and stored at -80°C for further analyses.

It is important to mention that in this work, *in vitro* modulation of miR-127-3p expression was performed after murine macrophages were stimulated towards different phenotypes following the protocol described above.

Table 6. Established conditions for miR-127-3p transfection in murine macrophages. Final concentration and volume of the reagents according to the size recipient in which transfection was performed. Cf: final concentration; Vol.: volume; Vf: final volume.

Plate size	miRNA modulators (Cf)		SiPORT NeoFX (Vol.)	DMEM (Vf)
24 well	Pre-miRs	10 µM	1 µl/well	500 µl
	Anti-miRs	50 µM	2.5 µl/well	
100 cm^2	Pre-miRs	10 µM	5 µl/dish	5 ml
	Anti-miRs	50 µM	7.5 µl/dish	

7. Techniques for nucleic-acid studies

7.1 RNA isolation

7.1.1 Total RNA extraction from cell culture and fresh renal tissue

Total RNA was extracted with guanidine thiocyanate-phenol-chloroform method using Tripure Isolation Reagent (#11667165001, Roche) following the manufacturer's instructions: mechanical lysis for cell cultures, and the use of a Tissue Lyser device (Qiagen) in renal tissues for a high-throughput samples disruption and homogenization, followed in both cases by phenol/chloroform extraction, and subsequent alcohols precipitation. Mouse kidney tissues were previously manually dissected containing a high proportion of renal cortex, where proximal tubules are located. Besides, to maximize the efficiency of RNA isolation in murine macrophages, glycogen (#10814010, Invitrogen) was added into Tripure Isolation Reagent [20 µl/ml], and linear acrylamide (#AM9520, Invitrogen) was used in the alcohol precipitation step (3µl/tube).

7.1.2 Serum total RNA extraction

Before RNA isolation, 1,25 µl of MS2-phages RNA (#10165948001, Roche) and 1 µl of synthetic RNA (Spike-in) Sp2 (#339390, Qiagen) were added per serum sample. After that, isolation of total RNA was done in 200 µl of sample using the miRNeasy Serum/Plasma Advanced Kit (#217304, Qiagen) from aliquots of 250 µl previously centrifuged at 2,500 rpm during 10 min at 4°C to discard cell debris.

7.1.3 Total RNA extraction from FFPE tissues

Total RNA from FFPE tissue samples was purified using the miRNeasy FFPE Kit (#217504, Qiagen) and following the manufacturer's instructions. After optimizing the protocol, the sample amount chosen to include in the kit was 5 sections of 10 µm per block.

7.2 RNA quantification and integrity study by electrophoresis

Concentration and purity of the obtained RNA were estimated in µg/µl with a Nanodrop 2000 device (Thermo Fisher) and considering the A260/280 and A260/230 ratios. RNA integrity, was checked by electrophoresis in agarose gel loading a solution mix composed of 1 µl of total RNA, 1 µl of NonTox DNA-Dye (A9555, PanReac AppliChem), and 5 µl of nuclease–free water PCR-grade. After electrophoresis, RNA bands were visualized under a UV-transilluminator, ChemiDoc MP Imaging System (BioRad), and contrasted with an RNA integrity control marker. Finally, RNA was stored at -80 ºC until its use.

7.3 Quantitative Real-time Polymerase Chain Reaction (qRT-PCR)

7.3.1 qRT-PCR for messenger expression

Reverse transcription (RT) to obtain cDNA from the isolated RNA was performed using a Transcriptor First Strand cDNA Synthesis Kit (#04897030001, Roche). Following the manufacturer's instructions, 2 µg of RNA from each sample were used for the reaction. Once reverse transcription finished, 1 µl of the obtained cDNA was used as a template for the qRT-PCR, together with SYBR Green I Master Mix (#04887352001, Roche). Amplification was carried out in a Light Cycler 480 thermal cycler (Roche) with the following temperature protocol: 40 cycles at 95°C for 10s, 60°C for 20s, and 72°C for 20s. All reactions were performed in triplicate for each sample, and 28S ribosomal gene was selected as an internal control (housekeeping gene) for data normalization. Besides, cDNA samples were diluted 1/100 with sterile nuclease-free water to 28S gene amplification, and no diluted for the rest of the genes studied. Results were expressed calculating quantification crossing points (CTs) with the 2nd derivative method (Light Cycler 480 Software 1.5, Roche) and data analysis for gene expression values was presented as ΔCTs obtained as follows: ΔCT = Gene CT − housekeeping CT, or folds, using the $2^{-\Delta\Delta CT}$ formula. Specific primers (oligonucleotides) employed are detailed in **Table 7** (*included at the end of this section*). They were synthetized by TIB Molbiol in a 100 µM stock concentration and diluted in a use concentration of 1:10 in nuclease-free water.

7.3.2 qRT-PCR for miRNA expression

cDNA for miRNAs expression study was generated using the miRCURY LNA Universal RT microRNA, Polyadenylation, and cDNA Synthesis Kit II (#339340, EXIQON). Drown from manufacturer´s recommendations, 200 ng of isolated RNA from cells or paraffin-embedded tissue, or 4 µl in the case of serum samples, were used to follow the protocol. Besides, cel-miR-39-3p was employed as an external control to monitored cDNA synthesis efficiency. Later, 4 µl of the obtained cDNA, 1/11 diluted in nuclease-free water, were added as a template for the qRT-PCR in each reaction sample, with 6 µl of master mix including 5 µl of SYBR Green and 1 µl of specific LNA probes for each selected miRNA (#339347, Qiagen). Amplification was performed in a Light Cycler 480 thermal cycler (Roche) following the next temperature protocol: enzyme activation at 95°C for 10 min, 45 cycles at 95°C for 15s, and finishing with 60°C for 60s. All reactions were carried out in triplicate using a Light Cycler 480 instrument (Roche) and Ct values were calculated using a 2nd derivative method (Light Cycler 480 Software 1.5, Roche). miRNA expression values are presented as ΔCTs obtained as follows: ΔCT = miRNA CT − housekeeping CT, or folds, using the $2^{-\Delta\Delta CT}$ formula. Normfinder and Bestkeeper software were used to determine the most stable housekeeping miRNAs. miR-191-3p was finally selected as housekeeping for data normalization in case of cell and tissue samples.

All LNA miRNAs probes used in this work were obtained from Qiagen and used at a final concentration of 10 µM (**Table 8**) (*included at the end of this section*).

8. Statistical analyses

Statistical analyses were performed with GraphPad Prism 8 (La Jolla, CA) and data were presented as mean±s.e.m. A one-way ANOVA test was used to find differences among groups by Kruskal-Wallis-test as a non-parametric one. When significant differences were found between groups, a non-parametric t-test U-Mann-Whitney was performed to analyze the differences. In the case of human serum samples, additionally, the Shapiro-Wilk test was first performed to confirm or reject normal distribution, and the Spearman correlation coefficient was calculated to determine the strength and direction of the relation between groups. Differences observed among groups were considered statistically significant following the next p-values: * < 0,05, ** < 0,01, and *** < 0,001.

Table 7. Oligonucleotides used for messenger expression analyses. Product specifications and sequences.

Gene primers (mRNA)			
Gen	**Specie**	**Forward sequence 5´-3´**	**Reverse sequence 5´-3´**
28S	Human/Mouse	CAGTACGAATACAGACCG	GGCAACAACACATCATCAG
LNC2 (NGAL)	Mouse	ATGTCACCTCCATCCTGGTCAG	GCCACTTGCACATTGTAGCTCTG
KIM1	Mouse	TCAGATTCAAGTCTTCATTTCAGG	ACCACCCCCTTTACTTCCA
TGFβ1	Mouse	CACCATCCATGACATGAACC	CCGCACACAGCAGTTCTTC
FSP1	Mouse	GGAGCTGCCTAGCTTCCTG	TCCTGGAAGTCAACTTCATTGTC
NOS2	Mouse	AGACCTCAACAGAGCCCTCA	AAGGTGAGCTGAACGAGGAG
ARG1	Mouse	GAATCTGCATGGGCAACC	GAATCCTGGTACATCTGGGAAC
TNFα	Mouse	TGCCTATGTCTCAGCCTCTTC	GAGGCCATTTGGGAACTTCT
IFNγ	Mouse	ATCTGGAGGAACTGGCAAAA	TTCAAGACTTCAAAGAGTCTGAGGTA
IL1β	Mouse	TGTAATGAAAGACGGCACACC	TCTTCTTTGGGTATTGCTTGG
IL4	Mouse	GAGAGATCATCGGCATTTTGA	AGCCCTACAGACGAGCTCAC
IL10	Mouse	AAGGACCAGCTGGACAACAT	TCATTTCCGATAAGGCTTGG

Table 8. Oligonucleotides (LNA miRNAs probes) used for miRNA expression analyses. Product specifications and sequences.

miRNAs primers		
miRNA	**LNA name**	**Reference number**
Cel39	cel-39-3p	YP00203952
Sp2	UniSp2	YP00203950
miR-191	hsa-miR-191-5p	YP00204306
miR-127	hsa-miR-127-3p	YP00204048
miR-146	hsa-miR-146a-5p	YP00204688
miR-93	hsa-miR-93-3p	YP00204470
miR-126	hsa-miR-126-3p	YP00204227
miR-26b	hsa-miR-26b-5p	YP00204172
miR-27a	hsa-miR-27a-3p	YP000206038

Results

1. Unilateral ureteral obstruction (UUO) mice model: mimicking CKD in humans

Characterization of histopathological and functional damage during CKD development and progression in an appropriated animal model is crucial for results translation to clinical practice. To aim that, we have set up and performed the UUO model, a widely recognized mice model reproducing chronic renal damage in humans. We have used 33 mice divided into the experimental groups already described in the material and methods section. **UUO-mice**: 5 animals per sacrifice time established (3, 5, 7, 10, and 15 days) formed this group. ***Sham*-mice**: 8 mice constituted the *sham* control group.

1.1. Structural damage and fibrosis development evaluation

Disorganization of kidney tissue and fibrosis appearance are unequivocal signs of chronic renal damage (Nogueira et al., 2017). First step in this work was to characterize the histopathological damage in kidney sections from mice, by H&E and Masson staining, and subsequent evaluation by expert Pathologists in a double-blind manner.

H&E stained kidney tissues revealed a tightening of the renal cortex compartment and ablation of the medulla since day 7 post-surgery, and even its vanishing at day 15 after UUO (**Figure 9**), which are considered very characteristic features of end-stage kidney damage (Yamashita SM *et al.,* 2015). Besides, the quantification of the histological parameters by this stain (**Table 9**) shows the evidence of progressive structural damage in the renal cortex of the obstructed kidneys since day 3 after surgery, mainly characterized by the appearance of inflammatory infiltrates, tubular atrophy and dilatation, glomeruli hypertrophy, and interstitial distortion (representative images in **Figure 10A)**. These alterations severely increase until the end of the model, compared with contralateral kidneys at each point and *sham* mice samples, which exhibit normal morphology, indicating that kidney affection is associated with the disease's severity. Furthermore, the histological damage during the UUO model also includes the appearance of collagen fibers within the renal parenchyma, as a deposition of an abnormal peritubular and periglomerular ECM, observed by Masson staining and quantification (**Table 9**) demonstrating fibrosis development in the injured renal tissue, as expected in chronic renal diseases. Representative images are shown in **Figure 10B**

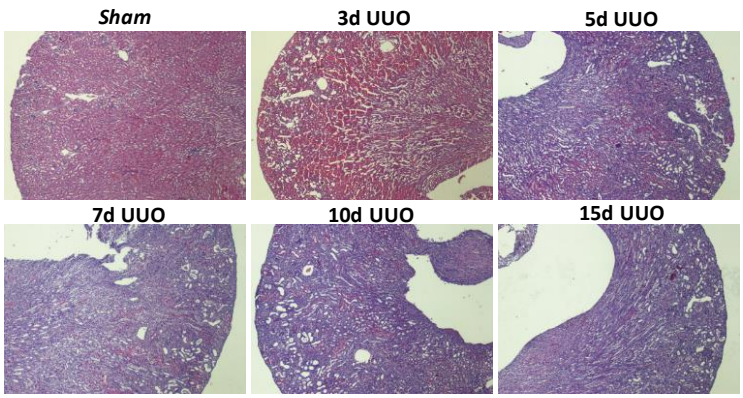

Figure 9. Kidney tissue losses normal structure along UUO model. H&E stain images demonstrate that obstructed kidneys exhibit medulla ablation and pathological renal cortex remodeling, which become more severe with the time of the UUO. In contrast, *sham* kidney remains unaffected (image zoom: x40).

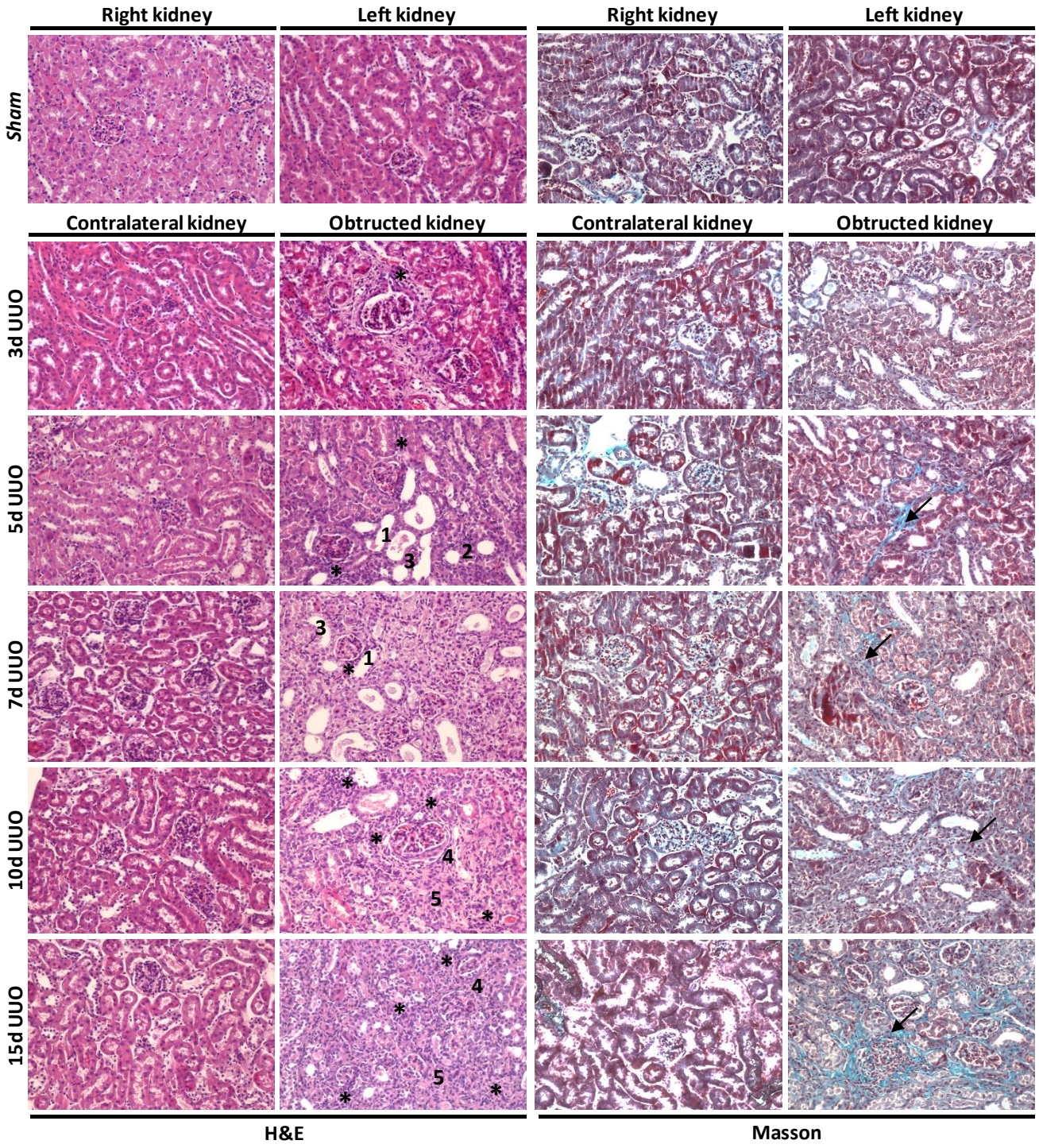

Figure 10. Histological alterations and fibrosis development in kidney tissue from UUO mice. A) H&E stain images (x200) show a sequential increase of tissue injury in the obstructed kidneys from day 3 after UUO to the end of the model, whereas contralateral kidneys and *sham* mouse display a normal histoarchitecture. Damage evidences are indicated in the pictures by **numbers** and **asterisks,** and include: inflammatory infiltrates (*****), loss of brush border integrity (**1**), thickened basement membrane (**2**), lumen dilatation (**3**) in atrophied proximal tubules, glomeruli rarefaction and thickness of their Bowman´s Capsule (**4**), and finally, interstitial distortion **(5). B)** Masson stain images (x200) display a gradual fibrosis development in obstructed kidneys from day 3 post-surgery to the end-point of the experimental model (day 15), in comparison with *sham* kidney as control tissue. Collagen deposition in the interstitium as abnormal ECM can easily be observed stained in blue color (**arrows**).

	Sham	3d UUO	5d UUO	7d UUO	15d UUO
Tubular atrophy (%)	0	0	0	5	5-10
Tubular dilatation (%)	-	Cortical	Cortical	Cortical/Medullar	Cortical/Medullar
Interstitial fibrosis (%)	0	1	5	5-10	10
Interstitial inflammation (%)	0	0	5	5	10
Tubular vacuolization	No	No	No	No	Yes
Tubular necrosis	No	No	No	No	Yes
Glomerular hypertrophy	No	No	No	No	Yes
Tubular inflammation	No	No	Yes	Yes	Yes

Table 9. Double-blind evaluation of tissue damage and inflammation along the UUO experimental model. Data demonstrate an increased tissue injury during the disease, based on the appearance of tubular atrophy, dilatation, vacuolization and necrosis, accompanied by interstitial fibrosis and inflammation in the UUO mice samples, in comparison with the *sham* mice group.

Moreover, and to further characterize fibrosis development, we studied the expression of α-Smooth muscle actin (αSMA) through immunohistochemistry in kidney sections from UUO mice. αSMA is a standard marker of fibroblasts activation into myofibroblasts, which are responsible for generating an abnormal ECM that contributes to kidney damage, as it was already described in the introduction of this work. As a result, **Figure 11** shows an induced peritubular expression of this protein during kidney disease, from day 5 of kidney damage until the end of the model (day 15), when staining shows an interstitial myofibroblasts network that involves tubules and glomeruli modifying the normal renal histo-architecture. In comparison, *sham* mice only display muscular actin protein signaling from small blood vessel cells and not from fibroblast activation.

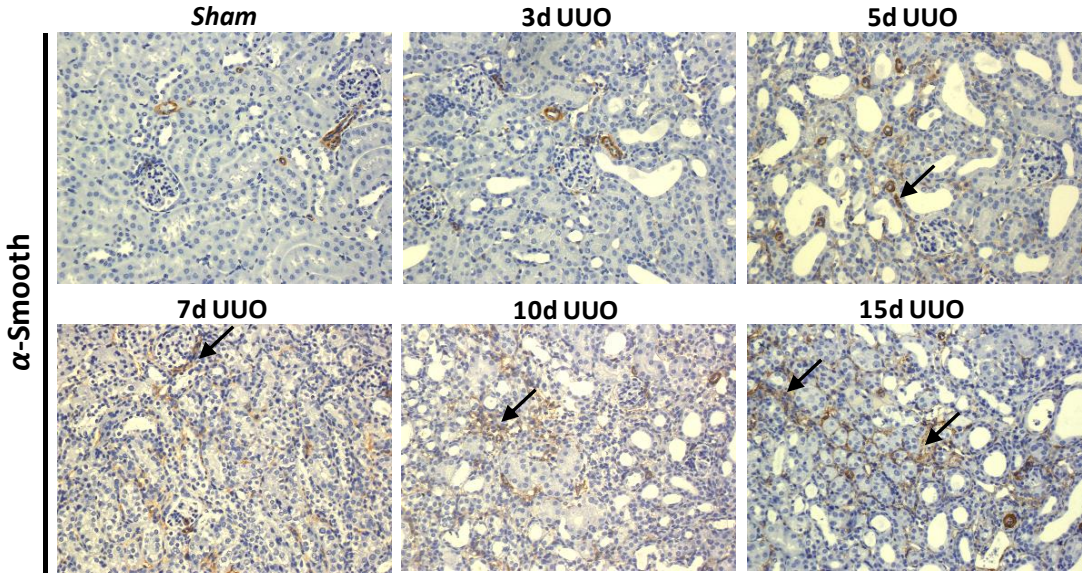

Figure 11. Immunostaining of α-Smooth muscle actin protein, to evaluate fibroblasts activation in obstructed kidneys sections from UUO mice. Pictures show an increased expression of α-Smooth actin protein from day 5 of kidney damage until the end of the model (day 15) (**arrows**), when the protein reaches the maximum expression levels, correlating with damage severity. In comparison, *sham* mouse does not exhibit staining that corresponds with fibroblasts activation (Images zoom: x200).

To complete the evaluation of structural damage and fibrosis development, we investigated the expression of classical tubular damage markers, NGAL and KIM1, and fibrosis related genes, FSP1 and TGFβ, by qRT-PCR, in kidney tissue from experimental mice groups. **Figure 12** presents these data expressed as fold change values and using the *sham* group as control reference. As we can observe in the graphics, UUO intervention leads to a progressively increased expression levels of all studied genes since days 3-5 of UUO, correlating with the morphological alterations and fibrosis development previously evaluated by H&E and Masson staining and α-SMA immunohistochemistry. All these features faithfully reproduce CKD progression in humans.

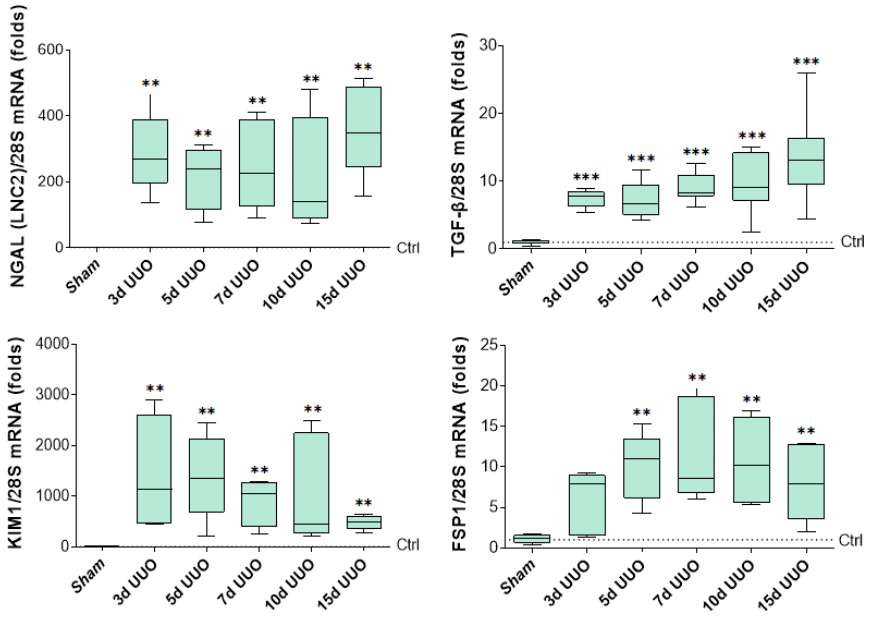

Figure 12. Tubular damage and fibrosis markers expression evaluated in kidney tissue by qRT-PCR. Graphics show an increased expression of tubular damage markers, NGAL, KIM1 and TGFβ, from day 3 of disease, followed by the increased expression of fibrosis gene FSP1 from day 5 of UUO, in comparison with control mice (*sham* group). Data are presented as mean ± SD. UUO-mice N=5, *Sham*-mice N=6. Significant differences from *sham* control group as fold change values are indicated by *(P<0.05); **(P<0.01); ***(P<0.001).

1.2 Inflammatory infiltrate characterization

As it was described in the introduction, an inflammatory response accompanies damage severity along CKD progression. Related with that, H&E staining in kidney sections from UUO mice revealed the presence of an inflammatory infiltrate within the renal parenchyma.

To characterize essential cells involved in the inflammatory response observed during kidney disease progression in the UUO animal model, we performed immunohistochemistry in kidney tissue to visualized T lymphocyte infiltrates by CD3, and the presence of macrophages and the M2 subtype by CD68 and YM1, respectively. Images in **Figure 13** indicate an abundant inflammatory infiltrate composed of T lymphocytes and macrophages in the renal cortex from day 3 after surgery and increasing during the UUO model's progression. Moreover, YM1 expression, as an M2 macrophage marker, appears in the renal cortex around day 5 post-surgery and increases its expression until the end of the model, according to tubular damage. Furthermore, we observed a high expression of YM1 marker in proximal tubular epithelial cells from *sham* mice and its vanishing with the severity of the damage along the experimental model.

To complete the inflammatory response characterization in UUO mice, we studied in renal tissue, by qRT-PCR, the expression of NOS2, a standard M1 macrophage marker, and ARG1 and FIZZ1, as M2 ones (**Figure 14A**), together with inflammatory cytokines related with macrophage functionality. i.e.: TNFα, IFNγ, IL-1β, IL-4, and IL-10 (**Figure 14B**). Gene expression analyses demonstrated that NOS2 expression, as an M1 marker, increases from day 5 after surgery and reaches its maximum at day 7-10 until the end of the model, which indicates recruitment of classically activated macrophages to renal tissue since injury begins. M2 markers, ARG1 and FIZZ1, also show expression from day 3 and 5 respectively after injury in UUO mice, but remarkably, FIZZ1 exhibits a relevant increased expression at the end of the model. Finally, the increased expression of pro-inflammatory cytokines, TNFα and IL-1β, from day 3 of the experimental model corroborates an exacerbated pro-inflammatory (M1) response induced in the early stages of injury and show the same pattern than NOS2 expression, as M1 marker. Besides, the late increase of IL-4 and IL-10 expression indicates a shift in the inflammatory response.

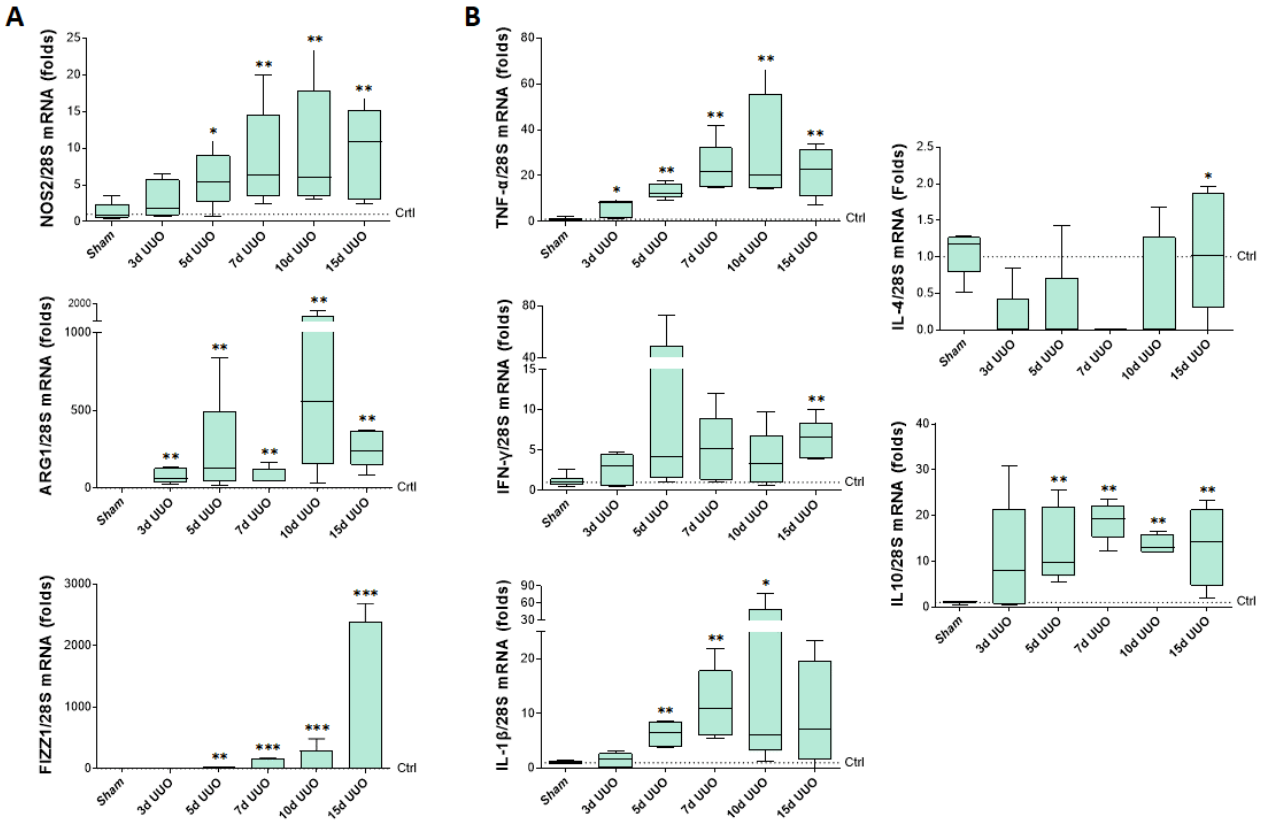

Figure 6. Macrophage markers and cytokines studied in kidney tissue by qRT-PCR. A) NOS2 and ARG1 expressions were induced from days 5 and 3 of kidney damage, respectively, in UUO mice indicating the presence of macrophages since the early stages of renal injury. However, FIZZ1 expression remarkably, reaches high levels at the end of the model which demonstrates most M2 phenotype at this time. **B)** TNFα and IL-1β are induced since the beginning of the experimental model and show the same expression pattern than the M1 marker NOS2. On the other hand, IL-4 increase its expression later matching the highest expression of FIZZ1 and also when kidney damage is more severe**.** Data are presented as mean ± SD. UUO-mice N=5, *Sham*-mice N=6. Significant differences from *sham* control group as fold change values are indicated by *($P < 0.05$; **P<0.01).

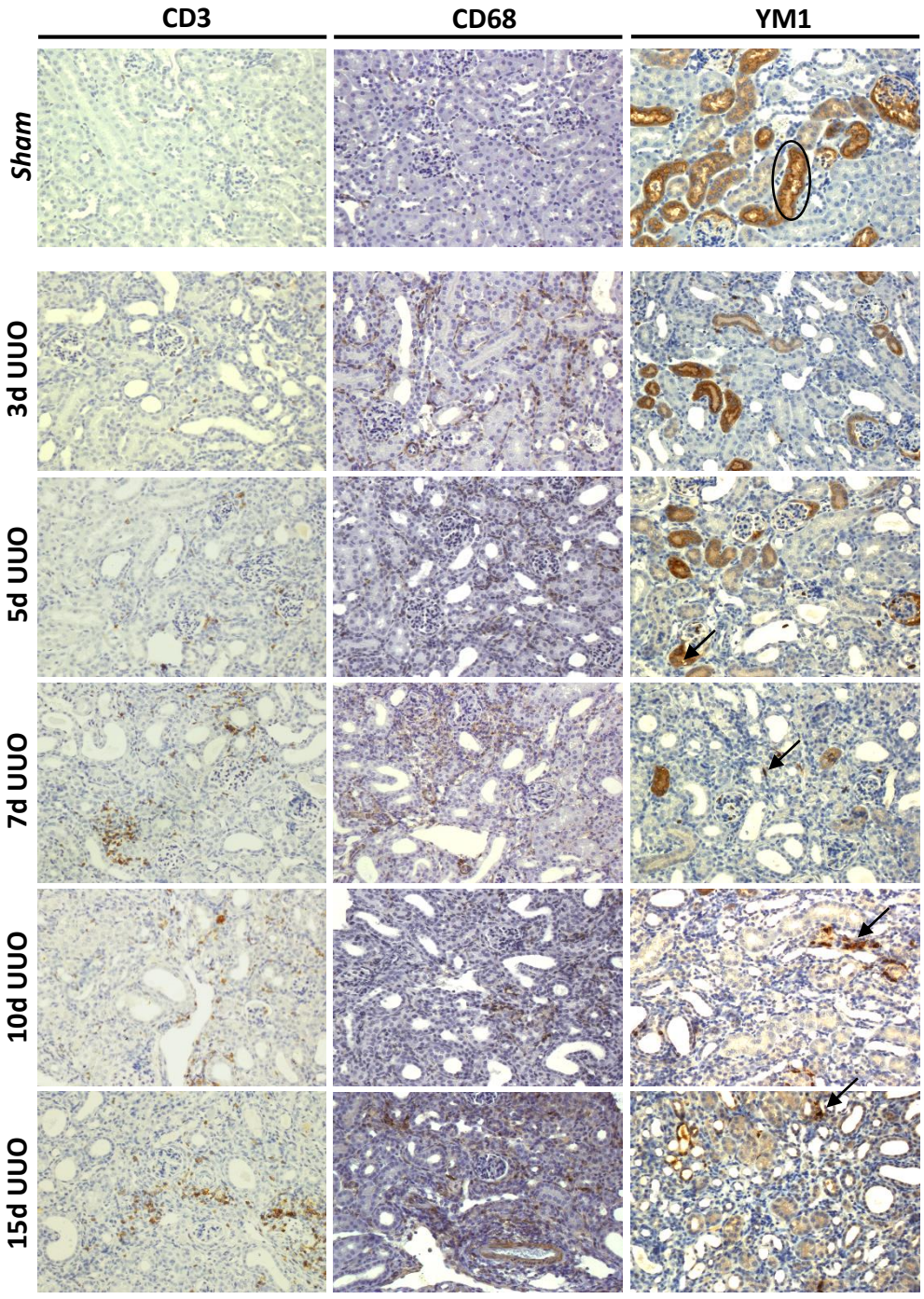

Figure 13. Immunostaining of CD3, CD68, and YM1 to characterize the inflammatory infiltrate and macrophage polarization during renal disease in obstructed kidney sections from UUO mice, in comparison with *sham* control mice. Stained tissues show CD3 and CD68 proteins from day 3 after UUO surgery until the end-point of the experimental model, which indicates the presence of peritubular infiltrates composed by T lymphocytes and macrophages associated to the progression of the disease. YM1 molecule expressed in undamaged proximal tubule cells (**circle**), is vanishing along the disease, while this molecule as alternative activated macrophages marker (**arrows**) indicates an increase of M2 phenotype from day 5 after surgery until the end of the experimental model. (Images zoom: x200).

1.4 Renal function evaluation in urine and serum samples

Histopathological alterations and fibrosis development in kidney tissue are accompanied by organ dysfunction during disease progression in CKD patients, as it was described in the introduction of this work. Currently used clinical parameters, including creatinine, urea, cystatin, uric acid, proteins, and phosphorous, were analyzed in serum and urine samples from mice to evaluate kidney function after UUO intervention.

We can observe in **Figure 15** any of the serum and urine parameters measured show significant differences between experimental groups of the UUO model compared with *sham* mice, except serum urea and uric acid, which are higher at days 10 and 3 after surgery, respectively. Overall, these data do not indicate the alteration in the renal function intended from the histological damage observed in UUO mice, as might be expected. This discordance was already explained in the mouse model described in the material and methods section.

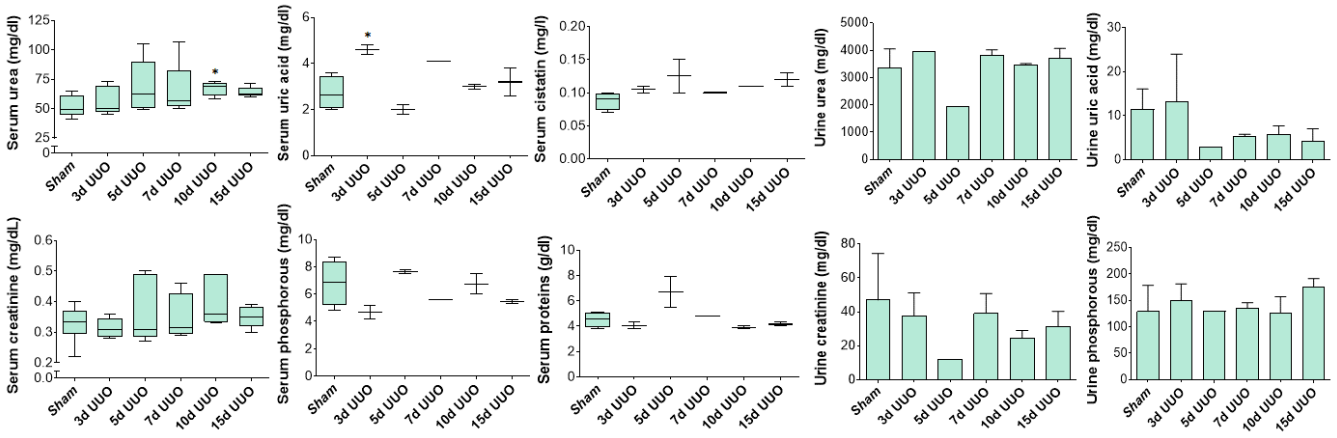

Figure 15. Analysis of serum and urine levels of clinical parameters currently used to evaluate renal function. Graphics show that serum urea and uric acid are significantly higher at day 10 and 3 of UUO, respectively, both in comparison with the *sham* control group. The rest of the parameters measured do not exhibit differences between experimental groups. Data are presented as mean ± SD. UUO-mice N=5, *Sham*-mice N=6. Significant differences from *sham* control group are indicated by *(P<0.05).

Taken together, data obtained from UUO mouse model characterization study demonstrate that this *in vivo* experimental model reproduced the main issues of fibrosis development and kidney damage observed in human CKD, accordingly to the bibliography, therefore being suitable for studying the role of miR-127-3p in the progression of chronic renal damage.

2. Study of renal miR-127-3p expression in the UUO mouse model during disease progression

As it was largely described in the introduction of this work, miRNAs are considered key regulators of cell response to several stimuli and stress. Previous research in our lab demonstrated that miR-127-3p expression increased in human proximal tubular cells (HK-2) treated with TGFβ, a classical pro-fibrotic stimulus that induces EMT. miR-127-3p expression also correlated with damage severity in biopsies from CKD patients, and it was localized in epithelial tubular cells from renal cortex, demonstrating that this miRNA could be involved in the cellular processes that contribute to fibrosis development underlying CKD (Martin-Gómez, Ph.D. Dissertation, October 2017). Based on these results and following the main objective of this work, we study miR-127-3p expression and in kidney tissue from UUO mice during the experimental model by qRT-PCR (**Figure 16A**). Furthermore, we also tested by ISH that miR-127-3p expression was localized in tubular cells reproducing human data describe above (**Figure 16B**).

Graphic from **Figure 16A** shows miR-127-3p expression in kidney tissues from UUO mice model is induced after kidney injury and increases its expression along the experimental model, exhibiting the highest level at day 5 after surgery. Besides, image from **Figure 16B** shows miRNA expression is mostly localized at the cytoplasm of proximal tubular cells, in the renal cortex, as we have expected.

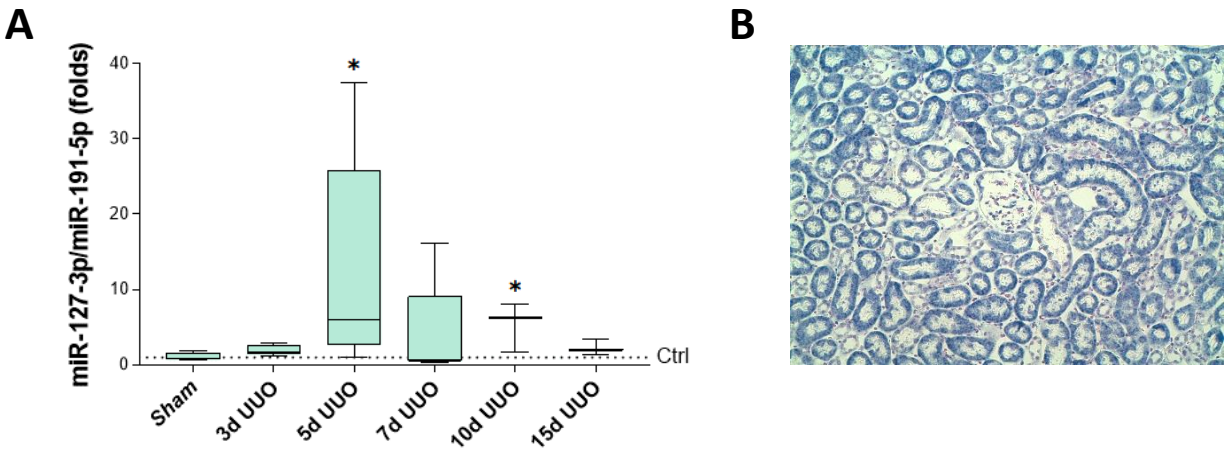

Figure 16. Study of miR-127-3p expression in kidney tissue from UUO mice. A) miR-127-3p expression is induced during UUO mouse model, exhibiting the highest expression at day 5 after kidney damage. Results from qRT-PCR are presented as mean ± SD. UUO-mice N=5, *Sham*-mice N=8. Significant differences from *sham* control group as fold change values are indicated by *(P<0.05). **B)** miR-127-3p expression is localized in the cytoplasm of tubular cells which reproduces results previously obtained in our lab in human samples of CKD patients. miR-127-3p signaling is visualized in purple (Image zoom: x200).

It is essential to highlight that miR-127-3p induction correlates with the elevated expression of classical tubular damage and fibrosis development markers, and the inflammatory response associated with UUO kidney damage previously showed in this section.

3. Modulation of miR-127-3p expression in the UUO mouse model

Once we demonstrated miR-127-3p expression increases during the progression of kidney damage along UUO mouse model, we went further into the biological significance of this miRNA by exogenous modulation of its expression in the UUO mouse model, following the protocol described in the material and methods section, using *in vivo* miRNA inhibition and over-expression procedures.

3.1 miR-127-3p inhibition in the UUO mouse model

For the *in vivo* miR-127-3p inhibition procedure, we divided 74 mice into the following groups (already described in material and methods section): **miR-127-3p inhibited UUO-mice**: 8 animals per sacrifice time established (3, 5, 7, and 15 days). **miR-127-3p inhibited *Sham*-mice:** 5 mice composed the *sham* control group for miR-127-3p inhibited mice. **Scrambled UUO-mice**: 8 animals per sacrifice time established (3, 5, 7, and 15 days). **Scrambled *Sham*-mice:** 5 mice composed the *sham* control group for Scrambled mice.

First, we studied the expression of miR-127-3p by qRT-PCR in kidney tissue from mice to evaluate the efficiency of inhibition. Results are presented in **Figure 18**; in which we can observe that the miRNA expression was abrogated in miR-127-inhibited mice along the UUO model compared to Scrambled mice.

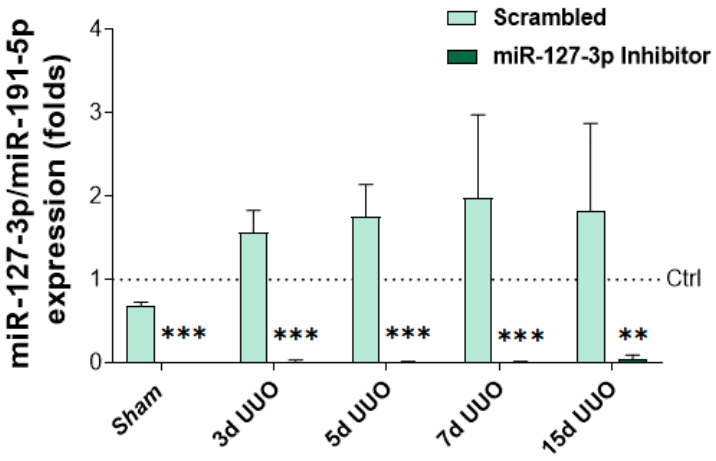

Figure 18. miR-127-3p analysis in kidney tissue from UUO mice in which miR-127-3p inhibitor or Scrambled sequence were administered. As shown, the expression of miR-127-3p was inhibited along UUO model in those mice in which miR-127-3p inhibitor was administered, in comparison with Scrambled mice. Results from qRT-PCR are presented as mean ± SD. UUO-mice N=8, *Sham*-mice N=5. Significant differences from Scrambled control group as fold change values are indicated by *(P<0.05); **(P<0.01); *** (P<0.001).

3.1.1 Histopathology and gene expression study in kidney tissue from miR-127-3p inhibited UUO mice

Renal histopathology was studied in all the experimental groups to determine whether the inhibition of miR-127-3p expression affects renal disease progression. Methods and parameters analyzed for this purpose were the same as the previously described for UUO mouse model characterization.

3.1.1.1 Structural damage and fibrosis development evaluation

To study the role of miR-127 in tissue damage and fibrosis development in UUO mice, we evaluated structural injury and collagen fibers deposit within the renal parenchyma by H&E and Masson staining, respectively, in kidney sections from mice, representative images are shown in **Figure 19A**. Tissues from mice experimental groups were double-blind evaluated by expert Pathologists (**Figure 19B**).

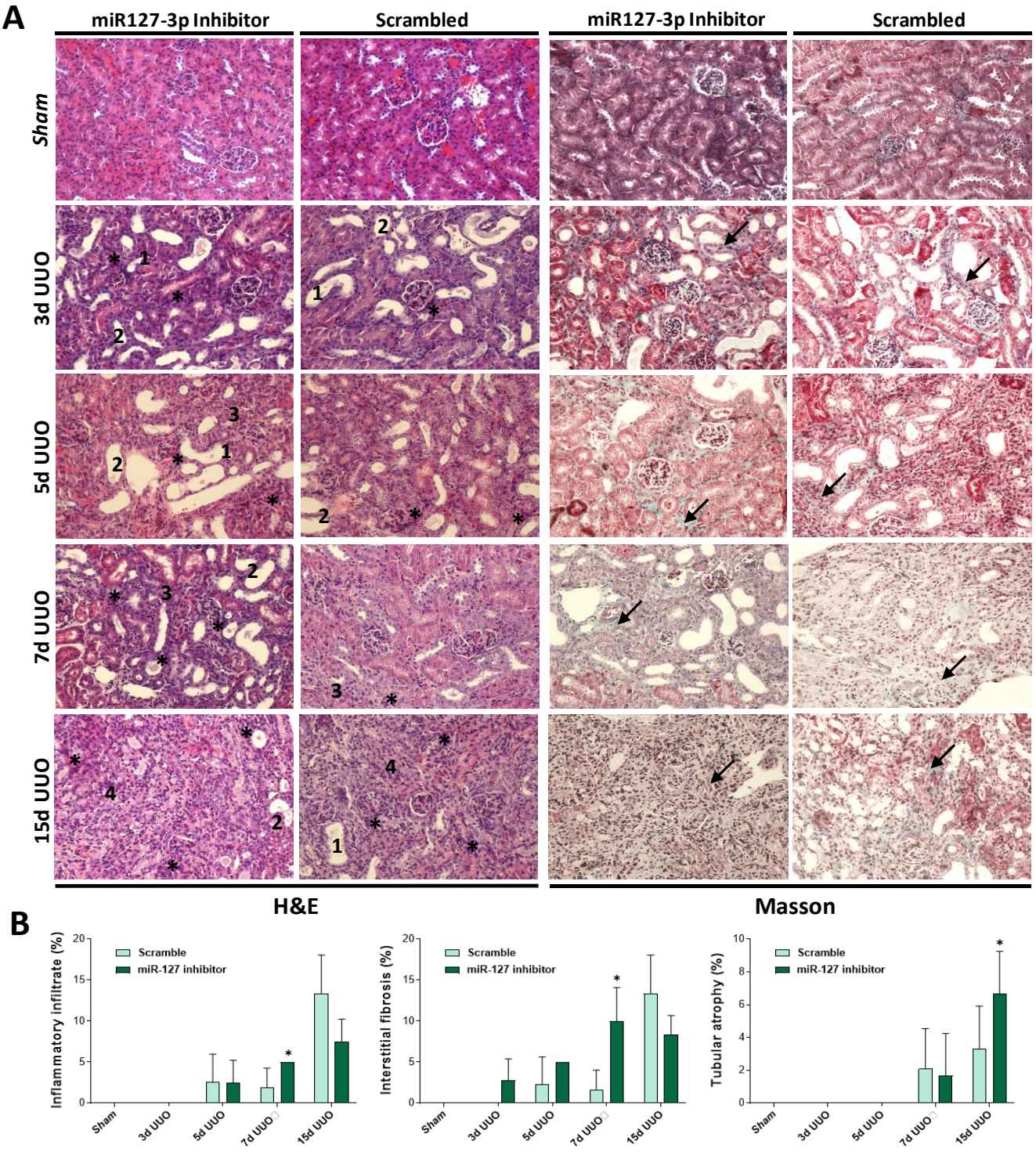

Figure 19. Histological damage and fibrosis development evaluation in obstructed kidneys from miR-127-3p-inhibited and Scrambled UUO mice. A) H&E and Masson stained images (x200) show an increase of tissue injury and fibrosis development from day 3 after UUO to the end of the model in both groups. Evidences are highlighted in H&E samples including: inflammatory infiltrates (*****), loss of brush border integrity (**1**), thickened basement membrane (**2**), lumen dilatation (**3**) in atrophied proximal tubules, and interstitial distortion **(4)**. Collagen deposition in the interstitium as abnormal ECM can easily be observed stained in blue color (**arrows**) in Masson stained samples. **B)** Statistical study of the stained images evaluation shows that the percentages of inflammatory infiltrate and interstitial fibrosis, at day 7 post-surgery, and tubular atrophy, at the end of the model (day 15), are higher in miR-127-3p inhibited UUO mice compared to the Scrambled UUO ones. Data are presented as mean ± SD. UUO miR-1273-p inhibited mice N=8, Scrambled mice N=5. Significant differences between experimental groups are indicated by *(P<0.05). (*Description from figure shows in the previous page*).

H&E and Masson staining and subsequent quantification show statistically significantly higher inflammatory infiltrate and interstitial fibrosis, at day 7 after UUO, and tubular atrophy, at day 15, in miR-127-3p inhibited mice compared to the Scrambled ones.

Following this, we determined α-Smooth muscle actin (αSMA) by immunohistochemistry, as a fibrosis marker already studied for the UUO mouse model characterization. Again, samples were analyzed by expert Pathologists in all conditions (**Figure 20**). Related images show an interstitial expression of this molecule in the tissues from the beginning of damage at day 3, until the end of the experimental model, at day 15 in both conditions studied, but no differences between experimental groups.

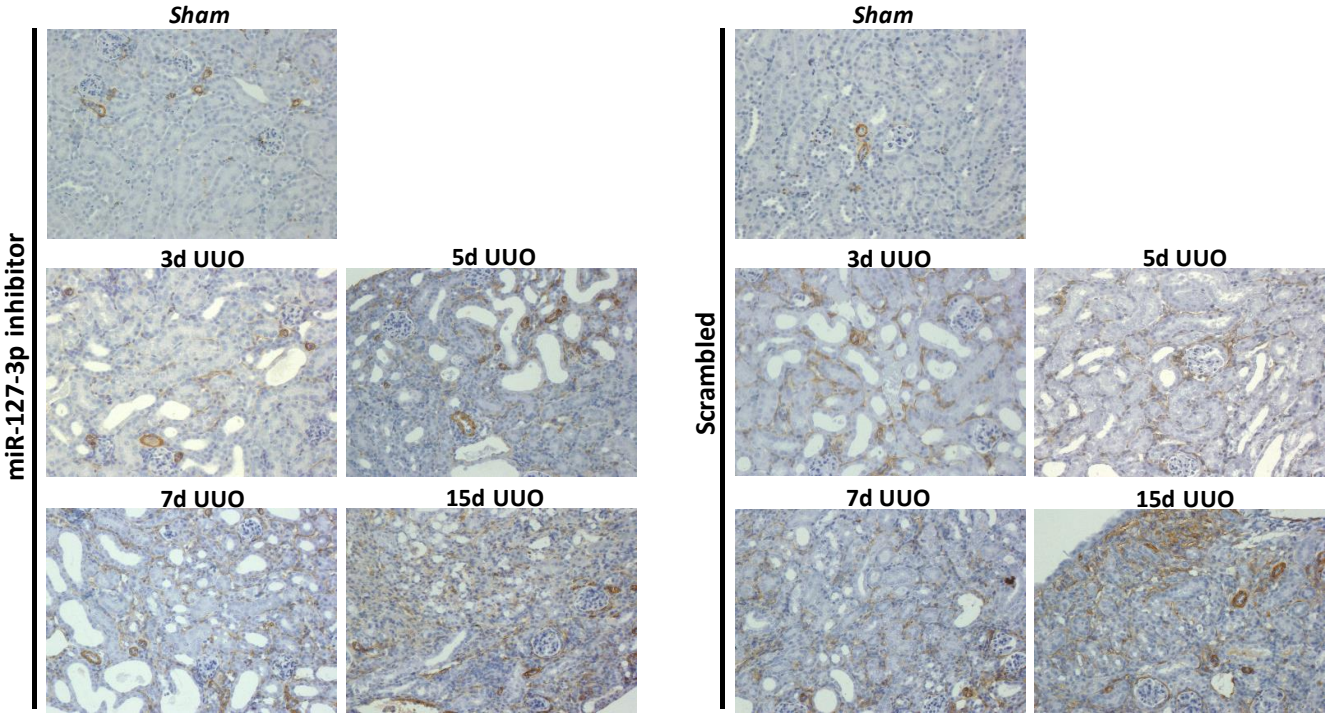

Figure 20. *α*-Smooth immunostaining to evaluate fibroblasts activation in obstructed kidneys sections from experimental mice groups. Pictures show an increase *α*-Smooth actin protein expression in the tissue since day 3 of kidney damage until the end of the model, following the expression pattern already described along UUO experimental model. Differences are not evidenced between studied conditions (Images zoom: x200).

To support the obtained results, we analyzed NGAL, KIM1, TGFβ, and FSP1 molecules related to tubular damage and fibrosis development by qRT-PCR in kidney tissues from miR-127-3p inhibited and Scrambled UUO mice. Results of each condition were first normalized by their *sham* group (miR-127-inhibited *sham*-mice and Scrambled *sham*-mice) and then, compared between them to analyze differences.

Figure 21 shows a higher expression of all the genes studied at days 3, 5, and 7 after surgery in animals in which the miRNA was inhibited, compared to Scrambled group.

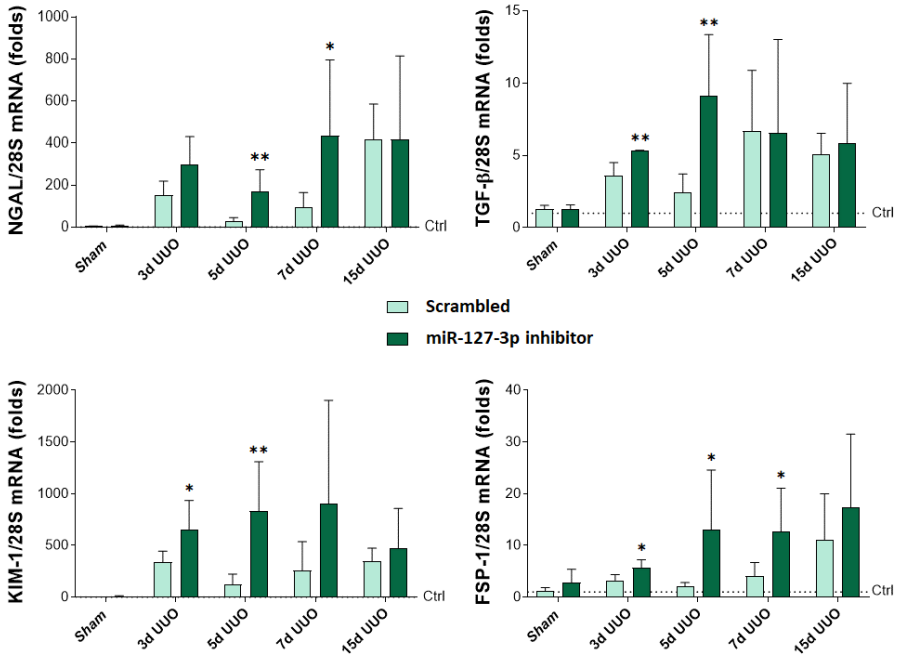

Figure 21. Tubular damage and fibrosis markers expression evaluated in kidney tissue by qRT-PCR. Graphics show a higher expression of KIM1, TGFβ, and FSP1 from day 3 of disease, and NGAL, from day 5 after surgery, in miR-127-3p inhibited mice in comparison with Scrambled group. At day 15 after surgery all the studied markers showed differences between experimental conditions. Data are presented as mean ± SD. UUO-mice N=8, *Sham*-mice N=5. Significant differences between experimental groups, miR-127-3p inhibited and Scrambled mice, as fold change values are indicated by *(P<0.05); **(P<0.01).

On the whole, data assessing structural damage and fibrosis development collectively demonstrate that miR-127-3p inhibition leads to more severe renal injury and an earlier fibrosis development during the UUO experimental model.

3.1.1.2 Macrophage phenotypes evaluation

Following the objectives of this work, we investigated the role of miR-127-3p in macrophage polarization and whether it affects the progression of renal damage.

To this purpose, we characterized macrophage phenotypes along the UUO model in kidney tissue from experimental groups by immunostaining and subsequent quantification of CD68 and YM1 proteins. Results are shown in **Figure 22A** and **22B**.

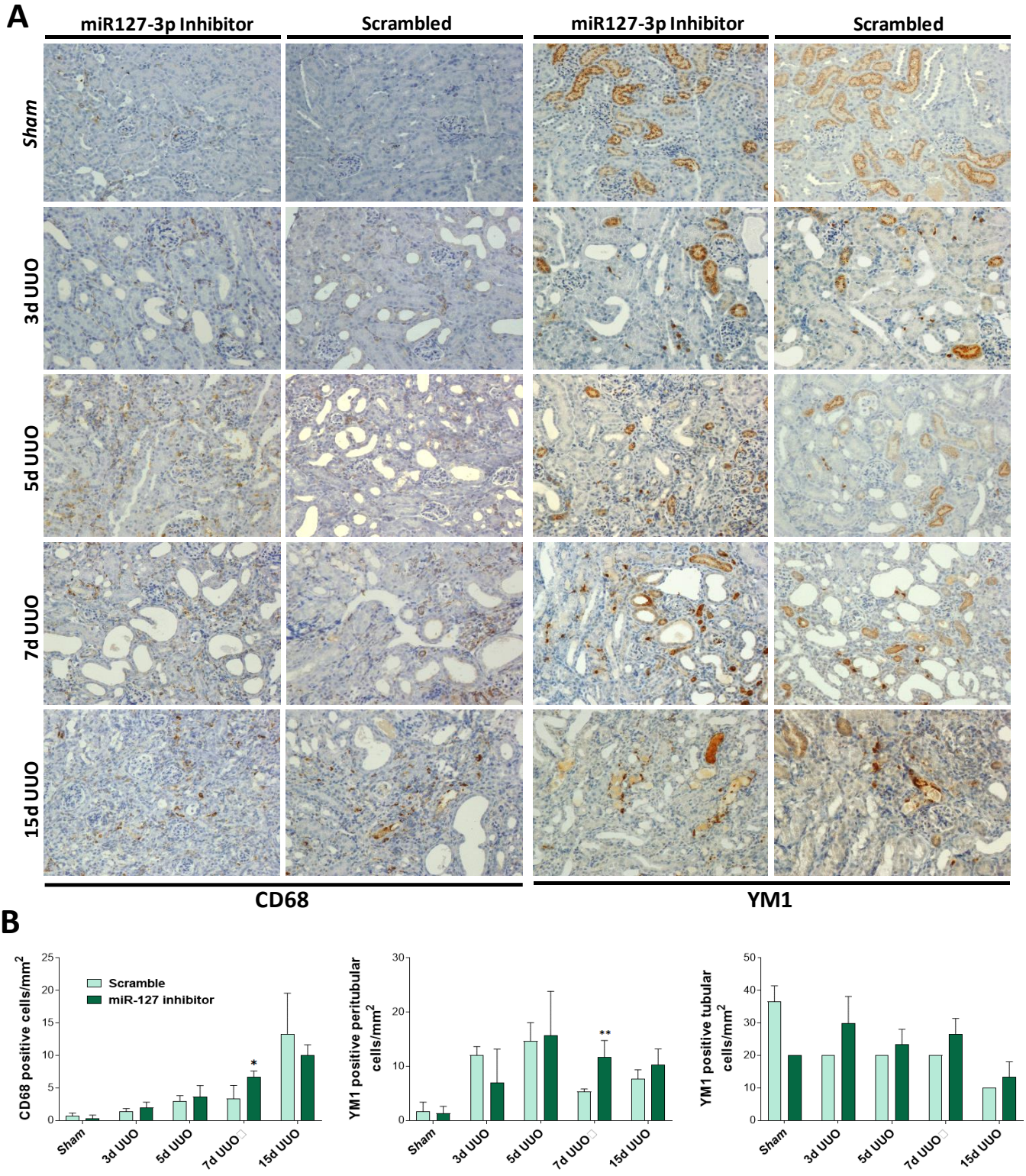

Figure 22. Macrophage markers analysis during renal disease in obstructed kidneys sections from experimental mice groups. CD68 and YM1 peritubular expression proteins and its quantification show the same expression pattern along disease in both conditions as the already described in the UUO mouse model characterization, but also demonstrate more presence of macrophages infiltrate, and M2 phenotype in miR-127-3p inhibited mice at day 7 after surgery, compared to Scrambled UUO mice. Besides, YM1 staining in undamaged proximal tubules did not show robust differences between groups along the disease´s progression. Images zoom: x200. Data from graphics are presented as mean ± SD. UUO miR-1273-p inhibited mice N=8, Scrambled mice N=5. Significant differences between experimental groups are indicated by *(P<0.05); **(P<0.01).

Immunostaining of CD68 protein and its quantification show the same expression pattern in both experimental groups than the already described during UUO model characterization, but also demonstrate a higher presence of peritubular macrophages in miR-127-3p inhibited UUO mice at day 7 after surgery, in comparison with the Scrambled ones. Moreover, results about YM1 protein expression, as an alternative activated macrophage marker (peritubular staining), show more M2 macrophages within the renal parenchyma in miR-127-3p inhibited mice at day 7 after UUO, in comparison with the Scrambled group. However, YM1 protein staining in undamaged proximal tubules did not show differences between experimental groups along the progression of the renal disease.

Taken together, these data firmly demonstrate that infiltrated macrophages are higher at day 7 after UUO when miR-127-3p is inhibited, and that there is an increase in macrophage polarization towards M2 phenotype at this time in those mice.

To further evaluate the involvement of miR-127 in macrophage polarization changes between experimental conditions along renal disease, we studied the expression of markers and inflammatory cytokines related to different macrophage phenotypes, as it was previously indicated. The analysis of these results are presented in **Figure 23**, in which graphics indicate no differences between miR-127 inhibited and Scrambled groups along the UUO model in the expression of NOS2 molecule, as M1 macrophage marker, and ARG1 and FIZZ1 molecules, as M2 markers. However, the expression of TNFα and IL-1β cytokines demonstrate an exacerbated pro-inflammatory response induced in miR-127-3p inhibited mice at days 5 and 7 after UUO, compared to Scrambled group. Moreover, no significant differences were found in IL-10 cytokine expression between conditions, although an increase tendency is observed.

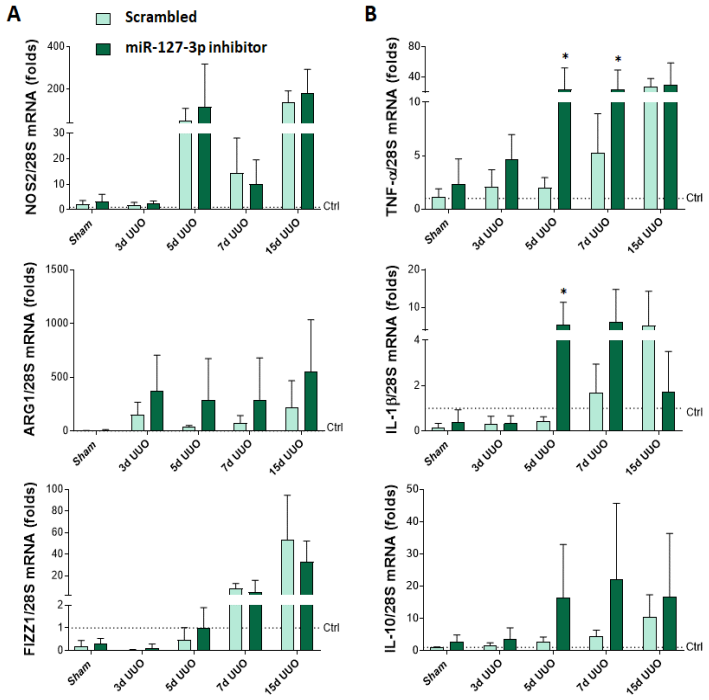

Figure 23. Macrophage polarization markers and related cytokines studied in kidney tissue from miR-127-3p inhibited and Scrambled mice. Data are presented as mean ± SD. UUO-mice N=8, *Sham*-mice N=5. Significant differences between experimental groups, miR-127-3p inhibited and Scrambled mice, as fold change values are indicated by *(P<0.05). **A)** Graphics show an induced expression levels of NOS2, ARG1 and FIZZ1 along UUO experimental model, but no differences between experimental conditions studied. **B)** TNFα and IL-1β pro-inflammatory cytokines are induced highly in miR-127-3p inhibited mice, at days 5 and 7 after UUO surgery, in comparison with Scrambled mice. IL-10, considered an anti-inflammatory cytokine, do not show differences between conditions along UUO experimental model.

The results demonstrate that miR-127-3p inhibition in the UUO mice model leads to an exacerbated inflammatory response including an increased presence of M2 macrophages within the renal parenchyma and inflammatory cytokines, in miR-127-3p-inhibited group compared to Scrambled one.

3.2.1 Renal function evaluation in urine and serum samples

To complete the role of miR-127-3p in UUO model, we studied the effect of the miRNA modulation in renal function by analyzing the following parameters: creatinine, urea, cystatin, uric acid, proteins, and phosphorous, in serum and urine (**Figure 24**) samples, taken into account that some renal function parameters in UUO experimental model have limitations, as it has been already explained in the material and methods section.

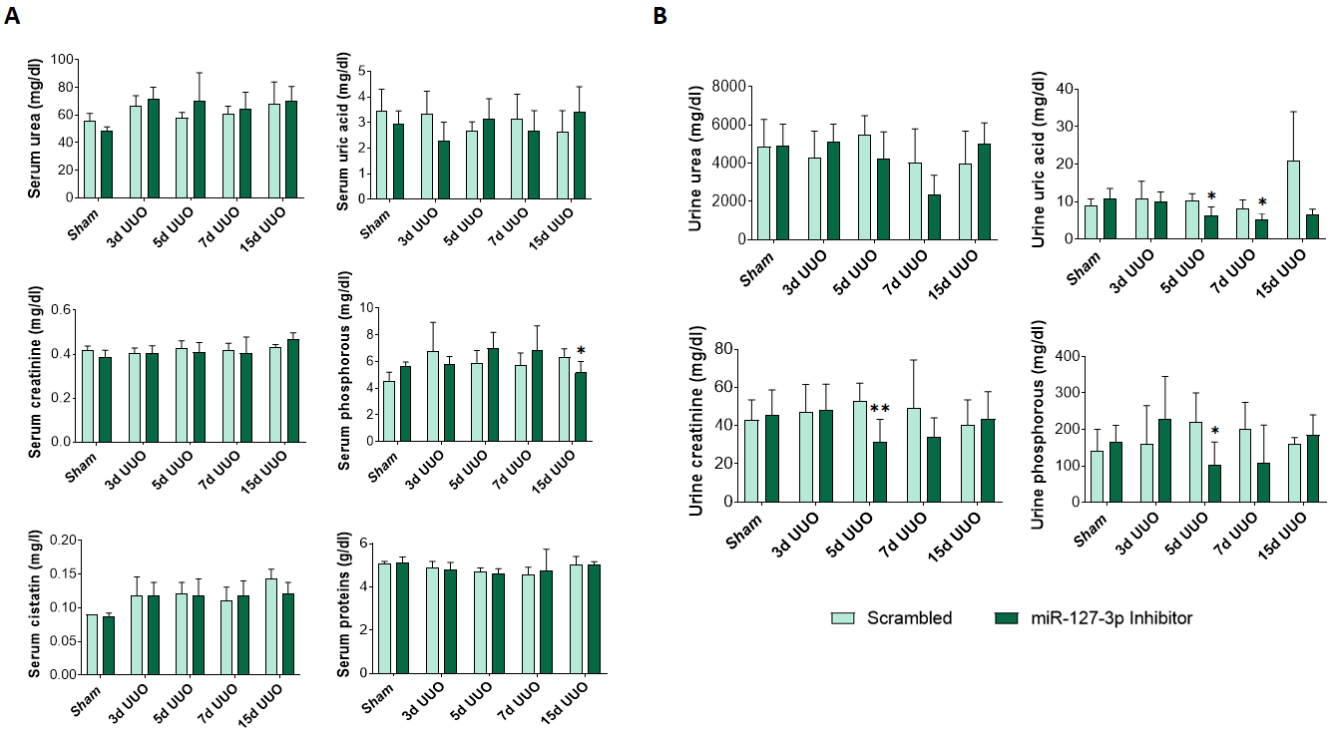

Figure 24. Analysis of serum and urine levels of renal function parameters used in clinical practice. A) Graphs show a decrease in serum phosphorous at day 15 after surgery in miR-127-3p inhibited mice, in comparison with Scrambled mice, and no differences were founded in the rest of the serum parameters evaluated. **B)** Urine parameters analyzed indicate that miR-127-3p inhibited mice excrete less uric acid and creatinine in urine than Scrambled mice, showing significant differences at days 5 and 7 post-surgery. Data are presented as mean ± SD. UUO-mice N=8, *Sham*-mice N=3. Significant differences from *sham* control group are indicated by *(P<0.05); **(P<0.01).

Our findings indicate that any serum parameter measured exhibited significant differences between groups, except phosphorous, which decreased at day 15 after surgery in miR-127-3p inhibited mice. Besides, urine markers analyzed showed that acid uric and creatinine were less excreted in miR-127-3p inhibited mice at days 5 and 7 after surgery, showing significant differences from Scrambled mice, and indicating that the modulation of miR-127-3p along the UUO mouse model affects renal function during the progression of renal disease.

Taken together, data obtained from miR-127-3p inhibition in UUO mice demonstrate that the block of miR-127-3p expression during the progression of chronic renal damage aggravates kidney injury and induces an exacerbated macrophage response within the renal parenchyma. The whole data made it conceivable that the induction of miR-127-3p expression in the early stages of kidney damage could be beneficial in delaying progression.

3.2 miR-127-3p over-expression in mice

After demonstrating that miR-127-3p inhibition during early stages of renal damage in UUO mouse model affects the progression of kidney disease and aggravates renal injury, the next step in this work was to investigate whether the induction of miR-127-3p expression along the experimental model could be used as a therapeutical intervention able to reduce or delay the progression of kidney injury.

To aim that, we tested different viral-based tools able to up-modulate gene expression in animals, as it was already explained in the material and methods section. In this work, we included the results obtained from the optimizing protocols for overexpression, all of them were performed in *sham* mice.

3.2.1 miR-127-3p over-expression test using adeno-associated viral particles

The first attempt in the searching of a successful tool able to induce miR-127-3p overexpression in kidney cells from mice was carried out by using adeno-associated particles labeled with GFP to monitor cell infection, provided by Doctor Chillón Rodríguez and his group (Viral Vectors Production Unit, UAB). For this purpose, we tried to find which of the 5 vectors are the most appropriate and have a higher kidney tropism and low distribution to other organs. For this purpose, we employed **one mouse per different construct tested** (a total of 5 mice) and they were sacrificed on day 11 after retro-orbital injection. A *sham* mouse in which the vehicle (sodium chloride) was administered by the same method, was used as a control to compare obtained results.

The images derived from the analyses of GFP signaling in mice performed under an IVIS device show how treated mice do not exhibit GFP fluoresce in kidney either in the rest of vital organs apart from the bladder, in comparison with the control mouse (**Figure 25A**). Moreover, isolated and OCT compound embedded kidneys from mice were analyzed under the microscope to visualize GFP fluoresce signaling. As a result, we included in **Figure 25B** an image in which we can observe that no GFP signaling from kidney cells was found, which indicates adeno-associated constructs do not successfully target the kidney and/or are able to infect cells.

A

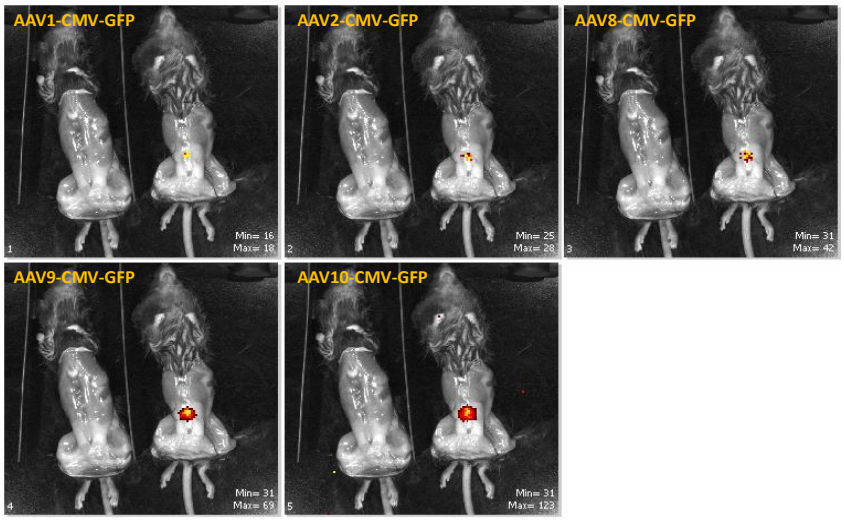

Figure 25. A) GFP signaling analysis to assess kidney tropism in retro-orbital adeno-associated injected mice. Fluoresce signaling was acquired by an IVIS device, and each adeno-associated animal was compared with a *sham* mouse as control. Any construct shows GFP fluorescence in the kidney or others vital organs. Signal detected is observed in bladder because of the clearance of viral particles in the urine. **B) GFP signaling analysis to study infection of Kidney cells in retro-orbital adeno-associated injected mice.** No GFP signaling was detected in kidney cells from mice (Image zoom: x400).

B

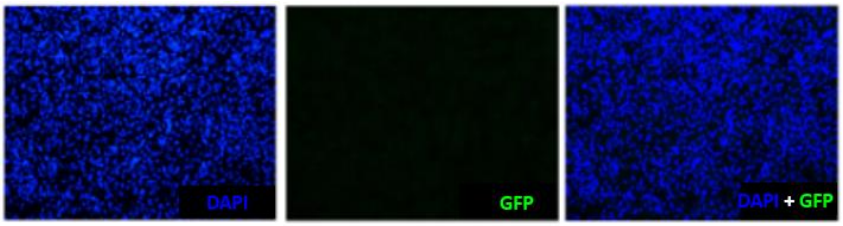

Based on the results obtained showing no fluoresce GFP signaling in the renal tissue from animals, any adeno-associated viral construct tested was selected to further explore the up-modulating miRNA experiments for the moment.

3.2.2 miR-127-3p over-expression test using lentiviral particles

For testing *in vivo* miRNA over-expression by lentiviral particles, different routes of administration were studied. We employed a total of 9 mice divided into the next groups: **miR-127-3p induced by renal-arterial administration**: 1 animal per sacrificed time established (3, 5, and 10 days after administration). **miR-127-3p induced by renal-parenchymal administration**: 1 animal per sacrificed time established (3, 5, and 10 days after administration). **miR-127-3p induced by retro-orbital administration**: 1 animal per sacrificed time established (5, 10, and 15 days after administration).

Same as adenovirus constructs tested, lentiviral vector purchased to generate lentiviral particles able to infect cells contains a copGFP promoter which is linked to the pre-miR-127-3p promoter to monitor infected cells expressing GFP, and therefore the miRNA induction. Based on that, we studied GFP expression in frozen kidney

sections from mice, embedded in OCT compound by fluorescence microscopy, to determine whether any experimental administration method achieves the induction of miR-127-3p expression in kidney cells from mice at the established times.

Results are shown in **Figure 26**, in which renal-arterial injected mice show GFP signaling in kidney cells located in the renal cortex at days 3 and 10 after lentivirus administration, indicating the presence of infected kidney cells at those times. Also parenchymal injected mice show GFP fluorescence at day 10 post-injection, but signaling was only detected in the left kidney's injection area while the rest of the renal cortex do not show expression. On the contrary, mice in which lentiviral particles were administered by retro-orbital injection do not show GFP signaling along the experiment.

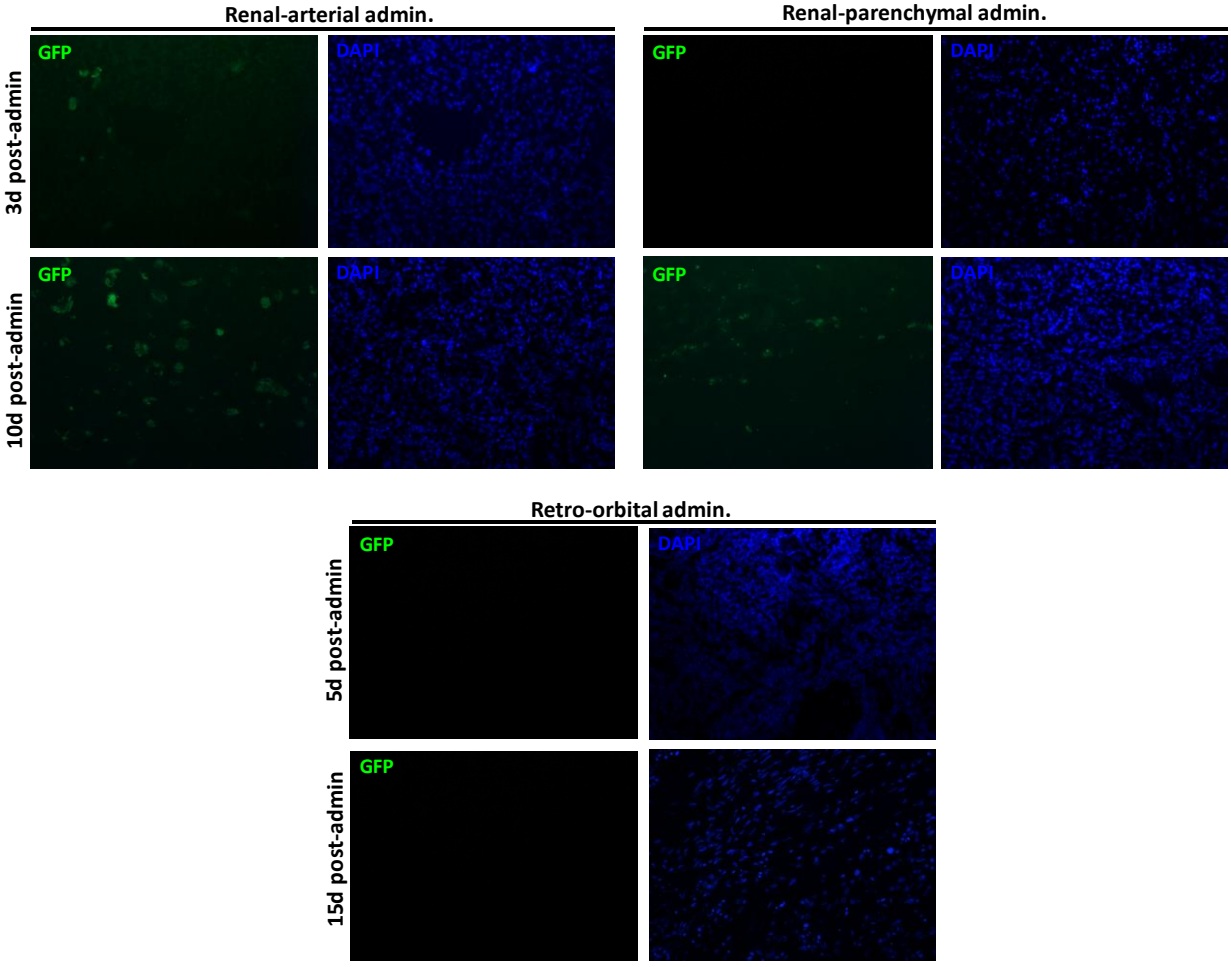

Figure 26. GFP florescence analysis to asses lentiviral infection able to induce miR-127-3p expression in kidney cells from mice. Image show GFP expression in the renal cortex cells of renal-arterial injected mice, at days 3 and 10 after lentiviral administration. Moreover, mice in which lentiviral particles were administered in the kidney by parenchymal injection also show GFP expression at day 10 after administration, but it is merely located in parenchymal cells. Finally, mice retro-orbitally injected do not show GFP expression during the experiment (Image zoom: x400).

Considering that kidney tissue presents high auto-fluorescence signaling, and trying to avoid overestimation, we decided to analyze miR-127-3p expression by qRT-PCR in kidney sections from mice to assess that the GFP signaling observed under the microscope corresponded with infected cells expressing GFP and thereby the miRNA. **Figure 27** discloses that miR-127-3p expression is higher in the intervened kidneys (left kidneys) of renal-arterial injected mice, at days 3 and 10 post-administration than in the non-intervened kidneys (right kidneys) of same mice, both in comparison with *sham* mice as control group. Nevertheless, intervened kidneys (left kidneys) from mice in which the lentivirus was directly administered in the renal parenchyma, do not exhibited higher expression of miRNA in a different manner than the non-intervened kidneys (right kidneys) from same mice group. Moreover, none of the kidneys from retro-orbital injected mice shows a wide difference miRNA expression from control mice at any time.

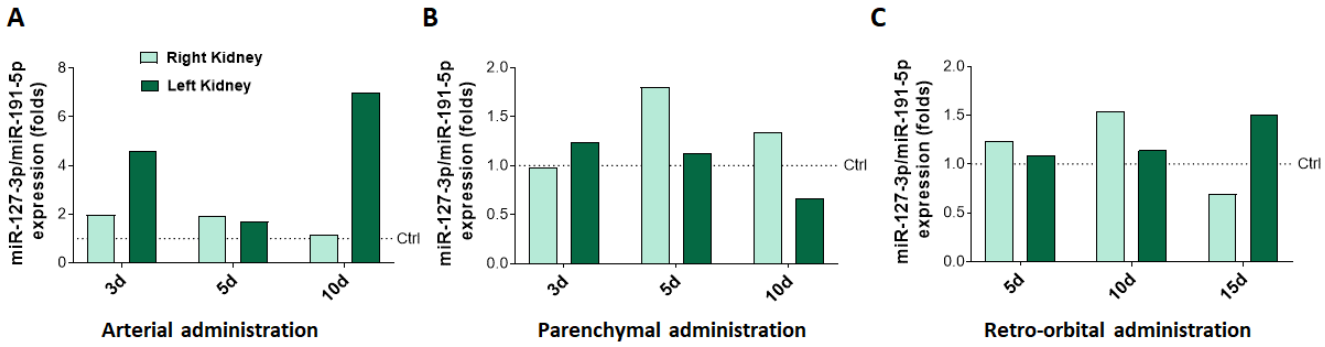

Figure 27. Analysis of miR-127-3p expression in kidney samples from differently lentiviral administration methods achieved in mice. Data are presented as mean ± SD. Arterial-administration mice (N=1/sacrificed time), parenchymal administration mice (N=1/sacrificed time), retro-orbital administration mice (N=1/sacrificed time) and S*ham* control group (N=3), used to obtain fold change values. **A)** miRNA expression is higher in intervened kidneys (left kidneys) of arterial-injected mice, at days 3 and 10 after administration. **B)** There are no miRNA expression differences in intervened (left kidneys) and non-intervened (right kidneys) kidneys, and control mice, in parenchymal administration mice samples. C) Retro-orbital injected mice do not show miR-127-3p expression differences in kidney samples along the experiment.

Summarizing, data indicate that the administration of lentiviral particles by renal parenchymal and retro-orbital injection do not successfully induce miR-127-3p expression in kidneys from mice. However, the renal-arterial injection method can induce miRNA expression in kidney cells since day 3, especially at day 10 after treatment, and the induction is located in the renal cortex, where chronic damage occurs.

4. *In vitro* study of miR-127-3p expression in macrophage polarization

Once we have observed that miR-127-3p is expressing in the kidney tissue along damage progression in the UUO mouse model and that its inhibition aggravates kidney injury and triggers an exacerbated macrophage response in mice, we were further in our study unmasking the role of this miRNA by studying its involvement in macrophage polarization, which is considered a key process in the development of the fibrosis underlying CKD. For this, we use murine macrophages naïves Mϕ[Non-stimulated] and different induced phenotypes (M1[LPS] and M2[IL-4]).

First, we studied the expression of NOS2 and ARG1, as pro-inflammatory and anti-inflammatory macrophage markers respectively, by qRT-PCR in the cells to evaluate the efficiency of the stimulation and if macrophages were polarized towards the required phenotype. Results are presented in **Figure 28**; in which we can observe that NOS2 is highly expressed in the M1[LPS] phenotype compared to Mϕ[Non-stimulated] macrophages. On the contrary, the M2[IL-4] phenotype, as an anti-inflammatory macrophage, expresses higher amounts of ARG1 compared to naïve macrophages (Mϕ[Non-stimulated]) and the pro-inflammatory phenotype (M1[LPS]). Therefore, stimulation successfully polarized macrophages towards different phenotypes consider relevant to be involved in the development and establishment of the CKD.

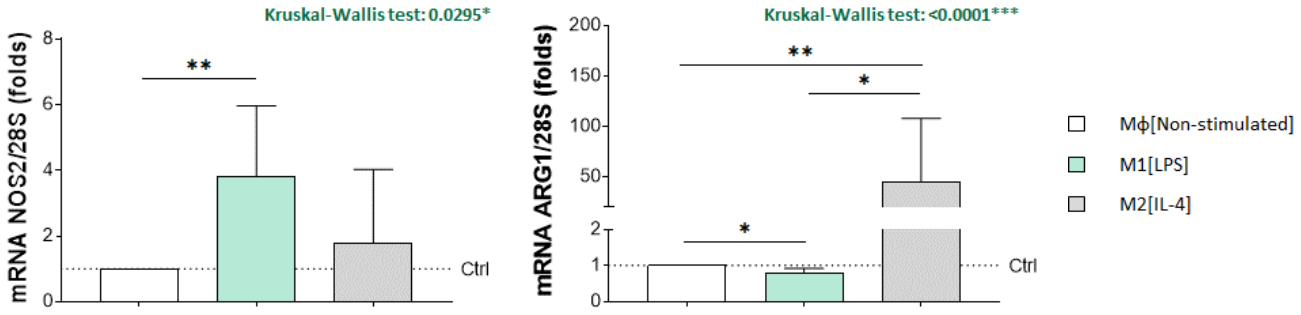

Figure 28. Macrophage polarization markers in different induced phenotypes (M1[LPS] and M2[IL-4]) compared to naïve macrophages Mϕ[Non-stimulated]. Graphics show an induced expression levels of NOS2 in the pro-inflammatory M1[LPS] phenotype in comparison with the Mϕ[Non-stimulated] macrophages. Conversely, ARG1 shows higher expression in the M2[IL-4] phenotype compared to both other experimental groups, as it was predictable. Data are presented as mean ± SD. M1[LPS] N=4, M2a[IL-4] N=6 and Mϕ[Non-stimulated] N=8. Significant differences between experimental groups are indicated, as fold change values by *(P<0.05), **(p<0.01).

Once we verified that macrophage polarization was successfully achieved, then we studied the expression of miR-127-3p by qRT-PCR in our experimental groups. Results are presented in **Figure 29** and reveal that the miRNA expression does not significantly change in the macrophages depending on the stimulus received.

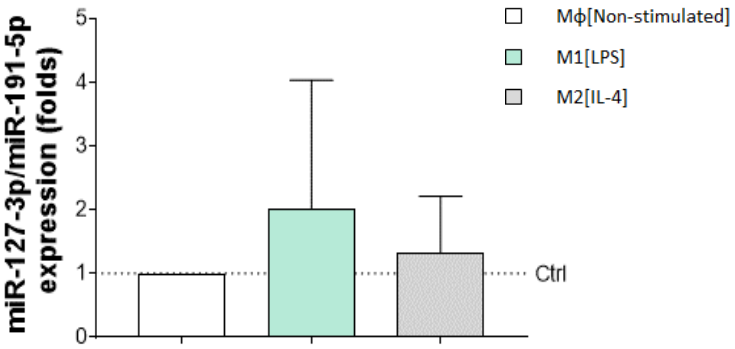

Figure 29. miR-127-3p expression in different induced phenotypes (M1[LPS] and M2[IL-4]) compared to naïve macrophages Mϕ[Non-stimulated]. As the figure shows, different stimulated macrophages do not express miR-127-3p in a different manner. Results from qRT-PCR are presented as mean ± SD, N=7. Significant differences from Non-stimulated as control group are indicated as fold change values by *(P<0.05).

Continuing with our study unmasking the role of miR-127-3p in the macrophage polarization process, the next step was to modulate the miRNA in the cells by transient transfection with Pre-miR-127-3p and Anti-miR-127-3p technology, to overexpress and to inhibit the miRNA, respectively, and using Pre-Negative and Anti-Negative sequences as control groups. **Figure 30** shows that miR-127-3p was significantly overexpressed in the cells treated with the Pre-miR-127-3p compared to the control group (Pre-Neg). As expected, cells treated with Anti-miR-127-3p didn´t show statistical significance in the inhibition of the miRNA expression compared to the control group (Anti-Neg), due to a possible blocking of miRNA function rather than its degradation, although we consider effective the miRNA.

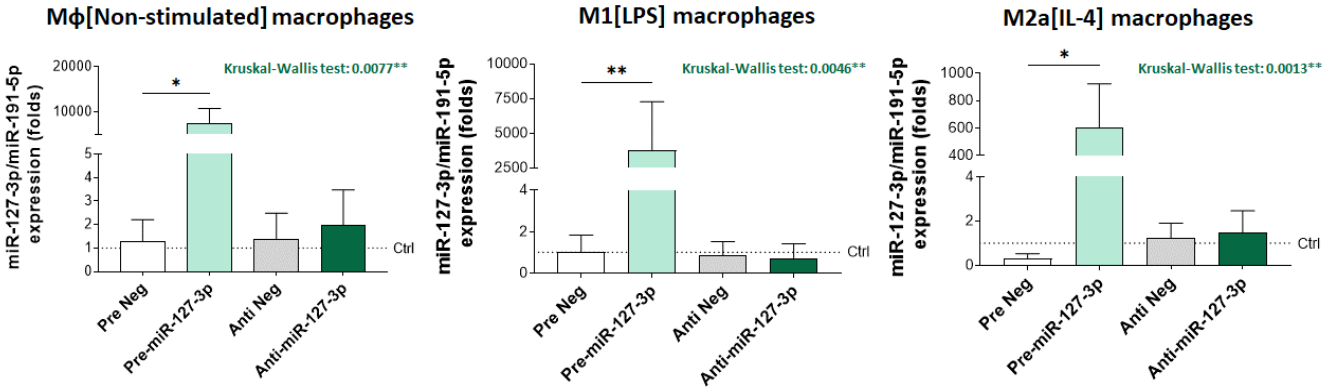

Figure 30. miR-127-3p analysis in naïve macrophages Mϕ[Non-stimulated] and different induced phenotypes (M1[LPS] and M2[IL-4]) after miR-127-3p modulation by transient transfection. As shown, the overexpression of miR-127-3p was successfully achieved compared to Pre-Neg as a control group. The inhibition of the miRNA didn´t show lower levels than its control group (Anti-Neg) with statistical significance. Results from qRT-PCR are presented as mean ± SD, N=4. Significant differences from Negative (Neg) groups are indicated as fold change values by *(P<0.05) and **(P<0.01).

Finally, we investigated whether NOS2 and ARG1 molecules change their expression between experimental groups (Mϕ[Non-stimulated], M1[LPS], and M2a[IL-4]) in which miR-127-3p expression was modulated (**Figure 31**).

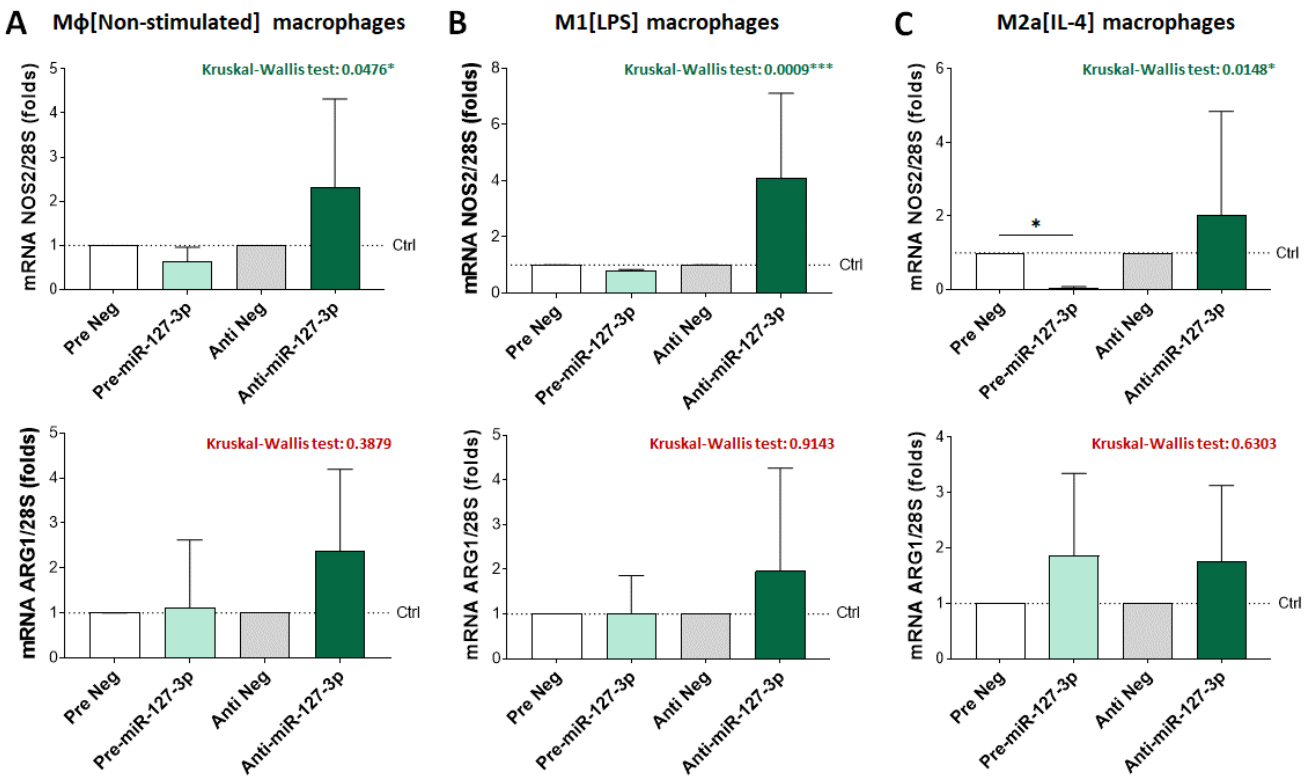

Figure 31. Macrophage phenotype markers analysis in naïve macrophages Mϕ[Non-stimulated] and different induced phenotypes (M1[LPS] and M2[IL-4]) after miR-127-3p modulation by transient transfection. All experimental groups show an induction of NOS2 in cells in which miR-127-3p was inhibited. Besides, the M2a[IL-4] phenotype significantly shows a lower expression of this pro-inflammatory marker in cells overexpressing miR-127-3p. On the contrary, the expression of ARG1 doesn't show significance between conditions. Results from qRT-PCR are presented as mean ± SD, N=4. Significant differences from Negative (Neg) groups are indicated as fold change values by *(P<0.05).

Graphics in **Figure 31** demonstrate that miR-127-3p over-expression in the M2a [IL-4] phenotype leads to a decrease in the expression of NOS2, as a pro-inflammatory macrophage marker. Moreover, an elevated tendency for NOS2 expression in miR-127-3p inhibited cells was found, regardless of the stimulus received, reproducing our *in vivo* data. All these results suggest that the induction of miR-127-3p expression along the kidney injury could be beneficial to delay disease progression, since it modulates macrophage polarization, among other cell processes.

5. Serum miRNAs as biomarkers of CKD and its related outcomes

As it has been mentioned in previous sections, the search for novel early renal injury biomarkers able to detect a premature condition of CKD, and capable of differentiating between stages has been turned into a significant challenge for the future. In this context, numerous studies have reported circulating miRNAs as potential useful biomarkers that associate with different pathologies and even indicate, stage and progression of many diseases (Huang W, 2017; O'Brien et al., 2018; Hanna et al., 2019). In order to demonstrate the value of microRNAs as biomarkers of disease in clinical practice, our lab has previously identified and published a set of serum miRNAs including miR-127-3p, able to diagnose AKI with a high sensibility and specificity and to reflect the persistence of cellular and tissue damage when renal function is apparently restored by classical parameters (Aguado-Fraile, Elia, Ph.D.Dissertation, 2013).

Based on that, we studied the expression of some of the miRNAs belonging to the renal damage set describe above: miR-127-3p, miR-126-3p, miR146a-3p, miR-26b-5p, miR-27a-3p, and miR-93-3p by qRT-PCR in a serum collection of CKD patients (PRONEDI cohort). Clinical settings of these patients can be found in detail in **Annex 1**. Then, we correlated the miRNAs expression results with CKD progression, estimated by KDIGO criteria (KDIGO

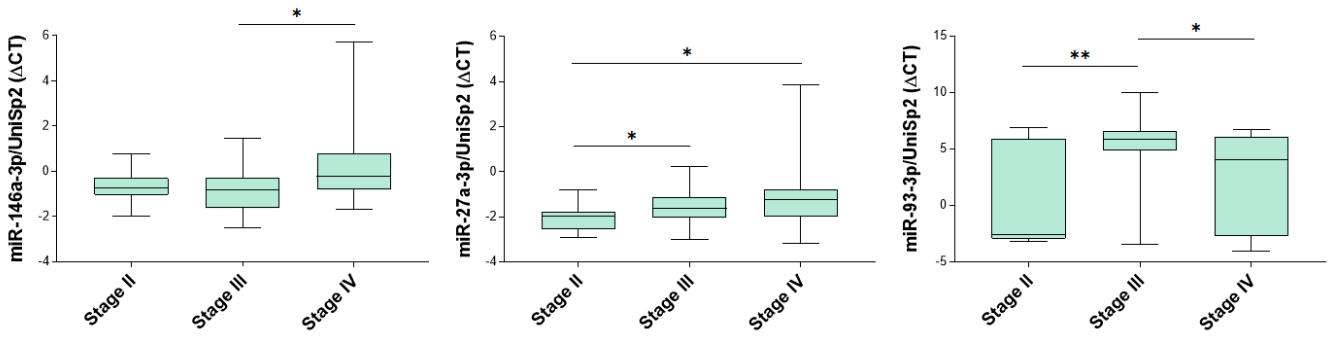

Guidelines) in different stages of kidney damage. Results in **Figure 32** demonstrate that serum levels of miR-146a-3p, miR-27a-3p, and miR-93-3p correlates with kidney damage severity. In fact, lower levels of those miRNAs (a higher ΔCT) are detected in serum from patients with along CKD progression. It is important to mention that for the statistical analysis miRNAs expression data were presented as ΔCTs, and higher values of ΔCT indicate lower amount of the miRNA.

Figure 32. Correlation between miRNAs expression in serum from patients and the progression of CKD. As graphics show, the expression of miR-146a-3p, miR-27a-3p, and miR-93-3p correlates with CKD severity determined by KDIGO classification in stages 2, 3, and 4. miRNAs expression levels are shown in ΔCTs values, which means that those miRNAs expression in serum decreases when kidney damage advances in patients. P-values showing statistical significance are indicated by *(P<0.05) and **(P<0.01).

Additionally, we also investigated the correlation between miRNAs expression levels in serum and associated renal damage parameters already collected from these patients. **Table 10** shows a summary of the variables studied and the strength and direction of the association (Spearman r, rS) obtained in the correlation study. Below, graphics from **Figure 33** shows the results that showed statistical significance (p-value<0.05).

Evaluated parameters		miR-127-3p	miR-126-3p	miR-146a-3p	miR-26b-5p	miR-27a-3p	miR-93-3p
PTH	p-value	0.9879	0.5234	0.6313	0.4533	0.9005	0.7695
	Spearman r	0.002147	-0.0905	-0.06813	-0.1063	0.01777	0.04163
FGF	p-value	0.2594	0.0574	0.6759	0.9209	0.3366	0.0601
	Spearman r	-0.1337	-0.2234	0.04976	0.01182	-0.1141	-0.2212
Klotho	p-value	0.2456	0.8448	0.3445	0.8719	0.2416	0.9273
	Spearman r	0.1376	0.02331	0.1122	-0.01921	0.1388	0.01087
Vitamin D	p-value	0.5927	0.1512	**0.009****	**0.0093****	0.6107	0.2653
	Spearman r	-0.06505	0.1734	**0.3099**	**0.3088**	0.0619	-0.135
PCR	p-value	0.5614	0.4765	0.1386	0.1139	0.7216	0.7243
	Spearman r	0.07278	0.08916	-0.1843	-0.1964	-0.04469	0.04424
IL-6	p-value	0.7488	0.8427	0.7101	0.7362	0.7014	0.5028
	Spearman r	-0.04548	-0.02821	-0.05281	-0.04786	-0.05446	-0.09502
TNFα	p-value	0.1492	0.3645	0.1173	0.154	0.1385	0.9447
	Spearman r	0.1839	-0.1162	-0.1994	-0.1817	-0.1887	-0.00891
OXID	p-value	0.6019	0.4331	0.8645	0.9751	0.166	0.096
	Spearman r	-0.0726	0.1089	-0.02377	0.004343	-0.1912	-0.2288
LPO	p-value	0.4697	0.3015	0.2856	0.8699	0.9457	0.1251
	Spearman r	0.1005	0.1432	0.148	-0.02283	0.009486	0.2113
GOT	p-value	**0.0267***	0.7071	0.1632	0.2809	0.1718	0.5572
	Spearman r	**0.2594**	0.04474	-0.1649	-0.1279	-0.1617	0.06983
GPT	p-value	**0.0024****	0.8762	0.345	0.2741	0.5393	0.2279
	Spearman r	**0.3527**	0.01868	-0.1129	-0.1306	-0.07354	0.1439
GGT	p-value	0.1431	0.7207	0.1544	**0.0066****	0.0871	0.4514
	Spearman r	0.2039	0.05027	-0.1984	**-0.3687**	0.2373	0.1057
FA	p-value	0.6018	0.4312	0.9371	0.2163	0.875	0.571
	Spearman r	-0.06441	-0.09702	0.009749	-0.1519	0.01943	0.06992
GFR	p-value	0.1094	0.4836	0.1284	0.1412	**0.0235***	0.2611
	Spearman r	0.1864	0.08213	-0.1772	-0.1715	**-0.2613**	-0.1314
DKK3	p-value	0.4548	0.788	0.3987	0.1802	0.4627	0.2154
	Spearman r	0.08761	0.03158	-0.09886	-0.1564	-0.08609	0.1447

Table 10. Correlation between miRNAs expression levels and clinical parameters of PRONEDI patients´ cohort. Table shows correlation between miR-127-3p and GOT and GPT measures, miR-146a-3p and miR-26b-5p and Vitamin D, miR-26b-5p and GGT, and miR-27a-3p and GFR. P-values were calculated comparing miRNA expression (ΔCTs) in serum samples with the values of the parameters measured for each PRONEDI cohort patient. Spearman r (rS) measures the strength and direction of association between the two ranked variables compared. Significant differences are indicated by *(P<0.05); **(P<0.01).

As can be observed in the table content, correlations between miR-127-3p, miR-146a-3p, miR-26b-5p, and miR-27a-3p with some of the parameters evaluated in serum samples from patients demonstrate statistical significance (*p-value<0.05; **p-value<0.01). Thus, data demonstrate that there is a positive relation (rS>0) between miR-127-3p expression (ΔCT) and GOT and GPT levels detected in serum from patients. Same situation than between miR-146a-3p and miR-26b-5p expression (ΔCT) and Vitamin D levels, which means a lower miRNAs expression (an upper ΔCT) detected when the respective parameter increases in serum from patients. On the

contrary, the correlation between miR-26b-5p expression level (ΔCT) and GGT measured in serum from patients shows a negative relationship, same than between miR-27a-3p and GFR measured in those patients, which means expression of miR-26b-5p and miR27a-3p decreases (an upper ΔCT) when the GGT and GFR also are lower in patients.

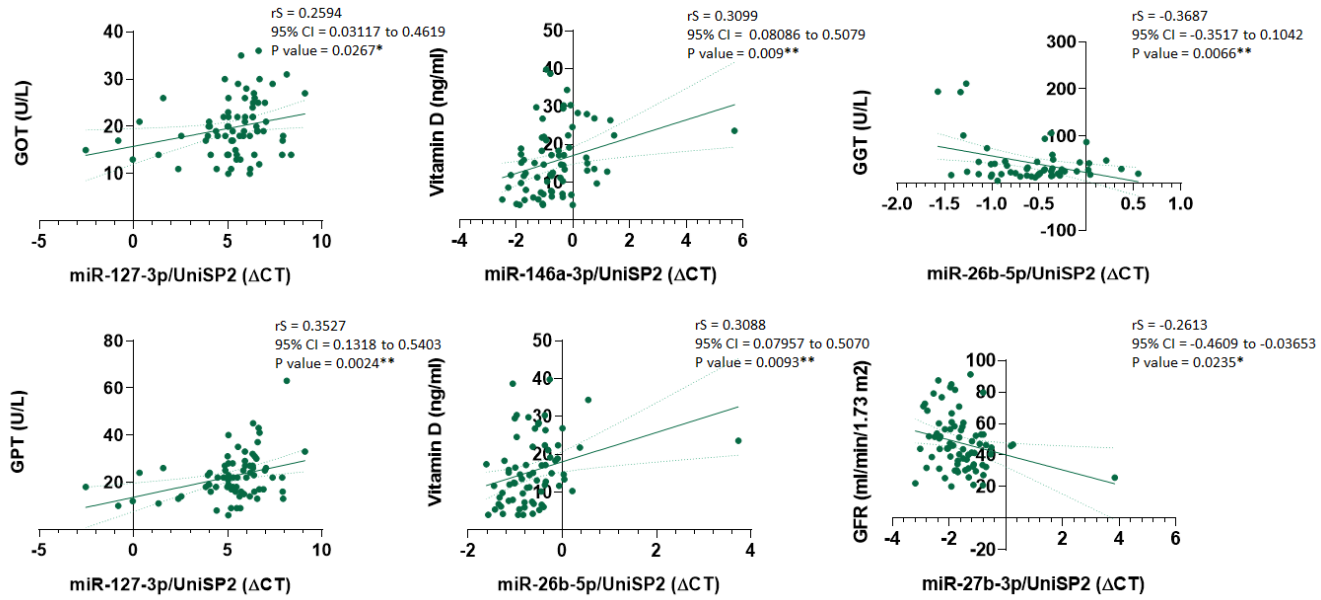

Figure 33. Graphics derived from Spearman's correlation coefficient between miRNAs expression levels and parameters evaluated with statistical significance. As graphics show, miR-127-3p expression (ΔCT) correlates with GOT and GPT, and miR-146a-3p and miR-26b-5p do it with Vitamin D, all of them in a positive manner (rS>0), indicating more ΔCT value of these miRNAs when those parameters increase in serum sample from patients. Inversely, miR-26b-5p expression (ΔCT) demonstrates a negative relationship with GGT levels detected (rS<0), same than miR-27-3p ΔCT with GFR, which means an upper miRNA ΔCT value when the parameter decreases. P-values are indicated by *(P<0.05) and **(P<0.01)

Both results suggest that miRNAs expression levels in serum samples could indicate liver affection in patent during CKD progression and alterations related to Vitamin D such as anemia or bone affection, both features well known associated with CKD outcome. These results demonstrate that the serum miRNA levels studied could be useful as accurate biomarkers of CKD progression and they can be also accurate tools for patient classification and management. In summary, our findings highlight the possible usefulness of serum miRNAs in clinical practice for CKD management.

Discussion

Identification of molecular mechanisms underlying renal injury and repair is essential for increasing our understanding of CKD pathophysiology and to develop novel therapeutic target tools and biomarkers able to significantly improve CKD patient management and their quality of life.

In this work, we have identified miR-127-3p as a key mediator involved in the progression of renal disease and its potential role as a therapeutic target tool for CKD treatment. We have established the Unilateral Ureteral Obstruction model in mice as a suitable experimental model to study the role of miR-127-3p during disease progression, which mimics human chronic obstructive nephropathy in an accelerated manner and produces the main features that lead to the progression of renal disease. Subsequently, we have evidenced that miR-127-3p expression is induced after kidney injury in UUO mice and concurs with the expression of tubular damage, fibrosis development markers, and also with the associated inflammatory response in which macrophages are key cells involved. In addition, we have demonstrated that the block of miR-127-3p expression in UUO mice accelerates the disease progression and exacerbates the associated macrophage response. Based on this finds, we have tried different viral-based particles and administration approaches, and finally, we have successfully induced miR-127-3p expression in the renal cortex of mice using lentiviral particles injected through the renal arteria. Moreover, we have demonstrated *in vitro* that miR-127-3p expression is not different in murine macrophages depending on the stimulus received, but its modulation by transient transfection in the cells induces changes in the expression of different macrophage phenotype markers. Finally, we have established that some of the serum miRNA levels studied belonging to a set previously identified in our lab, including miR-127-3p, able to diagnose AKI in patients and related with kidney damage, could be useful and accurate biomarkers of CKD progression, contributing to patient classification in different damage stages, and prematurely detect kidney injury outcomes allowing better patient management.

Numerous studies have identified different miRNAs as critical regulators involved in many pathophysiologic processes including CKD (Ichii & Horino, 2018; Zhao et al., 2019). Some of them have associated miR-127-3p with cellular processes intimately related to kidney damage, such as EndMT (Ghosh et al., 2012) and inflammation (Ying et al., 2015). Besides, previous results of our lab have demonstrated the implication of this miRNA in kidney response to I/R and AKI development (Aguado-Fraile et al., 2012; Conde et al., 2017). We also have results that revealed the pivotal role of miR-127-3p in maintaining renal homeostasis during a pro-fibrotic stimulus in HK-2 cells to be implicated in EMT, and showed an increased expression of this miRNA in human biopsies from CKD patients during early stages of disease (Martín-Gómez Laura, Ph.D. Dissertation, 2017). But up to our knowledge, this work is the first characterizing the role of miR-127-3p in CKD development and the macrophage polarization response associated to the renal disease progression.

As mentioned above, our results have demonstrated for the first time that miR-127-3p expression is induced after renal injury *in vivo* and concurs with damage severity along the progression of renal disease until the end of the experimental model, when fibrosis is totally established. Published results describe several miRNAs involved in the development of kidney damage in biopsies from CKD patients and kidney samples from UUO, including increased expression of miR-21, miR-192 miR-141 and miR-205, and downregulation of miR-200 family in IgA and diabetic nephropathies, both common etiologies of CKD. In the UUO mouse model miR-433, miR-382, miR-491, and miR-30c also was found increased in kidney tissue. But, miR-127-3p is not among them (Ichii & Horino, 2018; Rysz et al., 2017; Yu et al., 2019; Fierro-Fernández et al., 2020). However, miR-127-3p expression has been extensively associated with several cancers and pointed out as a tumor suppressor molecule that regulates cell proliferation, migration, and invasion (D. Wang et al., 2018; L. Wang et al., 2019; Jl et al., 2019; Tian et al., 2020; Umeh-Garcia et al., 2020). Aditionally, miR-127-3p has been involved in inflammation response and described as regulator of macrophage polarization underlying fibrosis in lung diseases (J. Shi et al., 2014; T. Xie et al., 2012; Ying et al., 2015).

To study the implication of miR-127-3p along CKD development we have set up the UUO model in mice. This experimental model has been widely described as the most appropriate *in vivo* model for investigating the molecular mechanisms that lead to renal fibrosis underlying chronic renal damage in an accelerated manner (Eddy et al., 2012; Martínez-Klimova et al., 2019b). We have characterized this experimental model in order to demonstrate that we are able to reproduced the main processes and effects observed and published by the scientific community using this model.

Renal samples evaluation from UUO mice revealed that obstructed kidneys exhibit a pathological medulla ablation and renal cortex narrowing since day 7 after surgery to the end of the experimental model compared to *sham* mice, which are considered very characteristic features of end-stage renal disease (Missbach-Guentner et al., 2018). Renal cortex remodeling in mice samples has included structural damage and fibrosis development along UUO, characterized by the appearance of inflammatory infiltrates, tubular atrophy, glomeruli rarefaction, interstitial distortion, and collagen deposits as a component of an abnormal ECM. All of them are described as regular processes that occur during CKD progression within the renal tissue and have been previously reported in the UUO experimental model (Martínez-Klimova et al., 2019). Correlating with that, we have confirmed fibroblasts activation into myofibroblasts from day 5 after injury in UUO mice samples. This process is intimately involved in the development of a pathological EMC that contributes to fibrosis development (Guzzi et al., 2019). However, TGFβ expression, as EMT marker, has increased in those samples earlier than the fibrosis markers evaluated, αSMA and FSP1, and at the same time as the expression of classical tubular damage markers evaluated, NGAL and KIM1, which indicates that in this work, the molecular mechanisms that contribute to structural damage have preceded

fibrogenesis, which faithfully reproduce CKD progression in humans (Mellado et al., 2015) and defines which could be a therapeutic window for treatment of kidney disease progression in this model.

It is important to discuss that NGAL and KIM1 molecules have been commonly reported as novel AKI biomarkers to be rapidly and robustly expressed in the kidney cells and released into the microenvironment in response to tubular damage against renal ischemic injury. Due to that, they are easily detected in blood and urine samples from patients (Vaidya et al., 2008) which makes them excellent minimum-invasive disease biomarkers. Advantageously, in recent years there is a growing literature suggesting that these molecules are also markers of kidney disease and severity, and they are inversely associated with the GFR, which could be used for a better diagnosis and prognosis of CKD patients (Devarajan, 2008; Soveri et al., 2020). Based on that, we decided to include them in this work as specific biomarkers of tubular injury that give us information about kidney damage progression along the UUO model, following some works already published (Humphreys et al., 2013; Nakagawa et al., 2015). Besides, we decided to study their expression in renal tissue from mice instead of fluids detection techniques as most of the published studies have done, since we have studied tissue samples from different time points along the experimental model while urine and blood samples were collected at the sacrificed time.

On the other hand, as it was described in the introduction of this work, there is an inflammatory response associated with the damage severity in CKD (Mihai et al., 2018) in which macrophages are key cells playing an important mediation for disease development through their polarization into different phenotypes (Guiteras et al., 2016; Mihai et al., 2018). In concordance with the bibliography, our results have pointed out that the inflammatory infiltrates within the renal parenchyma were highly composed of T lymphocytes and macrophages. Moreover, evaluation of classical molecules and cytokines related with macrophage phenotypes by IHQ and qRT-PCR, have suggested that M1 macrophages have been recruited to the local inflammation site to be the predominant phenotype population during early stages of kidney damage, but along the disease progression they have changed their phenotype toward M2, constituting a mixed macrophage population, a finding that has been extensively reported in the bibliography but which molecular mechanisms remained largely unknown (Kim et al., 2015; Guiteras et al., 2016; Parisi et al., 2018; Meng et al., 2019).

Unexpectedly, we also have found that YM1, studied in this work as an M2 macrophage marker, was also expressed in proximal tubular epithelial cells from *sham* mice and UUO mice in early stages of kidney damage, and that this expression was vanishing with the severity of the damage along the experimental model. Related to that, evidence indicates that YM1 is highly expressed in healthy kidney tissue and freely filtered by the glomerulus, but also secreted by activated macrophages in the kidney upon stress or damage (Ohno et al., 2015; Conroy et al., 2018) playing a crucial role having a chemotactic effect and regulating a variety of essential biological processes including oxidant injury, inflammasome activation, Th1/Th2 inflammatory balance, M2 macrophage

differentiation, TGFβ1 expression, ECM regulation, and parenchymal scarring (Kawada et al., 2007; Lee et al., 2011; Conroy et al., 2018). These published data perfectly match with our findings of YM1 expression and explain the expression pattern shown in our experiments from healthy tubules in *sham* mice to its vanishing along UUO experimental model in them, but appearing in peritubular cells.

Related to the UUO model, estimation of renal function in mice after ureteral obstruction, as a common biomarker used in clinic to detect CKD progression, has demonstrated that despite morphology alteration and fibrogenesis in kidney tissue from UUO mice, renal functionality has remained unaffected, as it would expect due to the compensation work of the non-operated kidney (CK). That issue has been previously indicated as an UUO experimental model disadvantage highly reported by the bibliography (H. C. Yang et al., 2010b). Nevertheless, we consider the UUO mouse model as the best experimental approach to unveil the role of miR-127-3p in the tubulointerstitial injury and fibrosis development along with renal damage since other existing models of CKD such as 5/6 nephrectomy or HIV-associated nephropathy (HIVAN) are also widely used, but commonly do it to elucidate mechanisms of glomerular disease. Interstitial fibrosis caused by folic acid also could be an option in our work but, although renal function can be assessed as a measure of CKD, the model takes much longer (around 28-42 days), and it is somewhat variable (H. C. Yang et al., 2010a).

Regarding miR-127-3p, we have observed induction of this miRNA after kidney injury in UUO mice. The highest expression was recorded on day 5 after surgery correlating with severe tubular damage and EMT evidence, fibroblasts activation into myofibroblasts, and with the increase of macrophage infiltration. However, miR-127-3p expression disappears at the end of the experimental model, when fibrosis is established. We also have confirmed that miRNA expression is localized in epithelial tubular cells from the renal cortex in UUO mice, as was expected from previous results of our lab in which miR-127-3p expression correlated with damage severity in biopsies from CKD patients (Martin-Gómez, Ph.D. Dissertation, October 2017). These results strongly indicate that miR-127-3p induction is involved in mechanisms underlying kidney damage progression during UUO experimental model.

Significantly, miR-127-3p expression has been previously reported to increase in lung and liver inflammation and fibrosis development (Tryndyak et al., 2009; Milosevic et al., 2012). Moreover, L. Shi and colleagues, published in 2017 that miR-127-3p expression was induced in lung adenocarcinoma promoting stem-like traits, increased resistance to the epidermal growth factor receptor inhibitor, and cells migration capacity. These works firmly indicate a relation between this miRNA induction and the pathological context, but are controversial with previous results of our lab already explained, which indicate the pivotal role of miR-127-3p in the maintenance of the epithelial phenotype in proximal tubules cells exposed to pro-fibrotic stimuli (Martín-Gómez, Laura, Ph.D.Dissertation, 2017) that have pointed out the modulation of this miRNA as a therapeutic strategy for renal disease treatment.

As a first approach in the proof-of-concept studies, we have inhibited miR-127-3p expression *in vivo* to study the implication of this miRNA in the progression of the renal disease along the UUO animal model. Our experiments have demonstrated as an innovative result that the blockage of miR-127-3p expression in UUO mice enhance structural kidney damage and fibrosis development, and exacerbates macrophage inflammatory response within the renal parenchyma along disease progression. These findings support the *in vitro* results previously obtained in our lab about the protector role of this miRNA during kidney disease and lead us to suggest probably miRNA expression at physiological amounts is not enough to block with the disease progression, by itself.

As it was described in the results, HE and Masson stains have confirmed an earlier tubular dilatation and atrophy, and more collagen fibers deposited in the renal interstitium demonstrating worse structural damage and fibrosis development in UUO mice in which miR-127-3p was inhibited. The increased expression of tubular damage and fibrosis development markers studied by qRT-PCR, including NGAL, KIM1, TGFβ, and FSP1, has supported this result. But despite these results, αSMA as a fibrosis marker determined by IHC, has increased its expression along disease development but has not showed differences between miR-127-3p inhibited mice and control ones, contrary to what was expected. On the one hand, this could be explained because the semi-quantitative character of the IHC technique requires bigger differences between experimental groups to reach statistical significance. Also, there are published results reporting that αSMA could not be a functional marker of fibrogenic cells that correlates positively with the level of collagen gene expression and the disease severity in skeletal muscle fibrosis (W. Zhao et al., 2018). On the other hand, miR-127-3p could be involved in molecular mechanisms underlying fibrosis development through other pathways not related to αSMA (Ina et al., 2011).

Regarding inflammatory response, macrophage characterization in kidney tissue has demonstrated that infiltration was higher in UUO mice in which the miRNA was inhibited compared to the Scrambled group. This result leads us to postulate an implication of miR-127-3p in this context along with kidney damage progression. Going further, the increased expression at day 7 after surgery of CD68 and YM1 molecules studied in kidney tissue by IHQ as an overall macrophage marker and M2 phenotype marker, respectively, has suggested a higher macrophage polarization towards M2 phenotype in those mice. However, macrophage markers studied by qRT-PCR also demonstrated expression of M1-related molecules since day 5 after surgery in UUO miR-127-3p inhibited mice. Taken these results together, it could be conceivable that there is an exacerbated macrophage response when miRNA is inhibited that results in the appearance of a mixed population in which both phenotypes are orchestrating the inflammatory response along kidney damage resulting in a worse progression of the disease. That agrees with the bibliography describing that different phenotypes can coexist in the same population in a determinate space and time and that polarization states can change or reverse responding to physiological conditions and the local cytokine milieu (Murray, 2017; Chen et al., 2019; Orekhov et al., 2019).

Up to now, there is no publication within the bibliography reporting this miRNA involved in kidney fibrosis. However, in this context, there are some publications that involve miR-127-3p expression in the development of lung inflammation and injury through macrophage polarization (Ying et al., 2015; Li et al., 2017). These works have demonstrated that the induction of miR-127-3p expression enhances the activation of JNK kinase which exaggerates a pro-inflammatory response promoting lung inflammation and injury, while its inhibition inactivates this pathway and suppresses the production of pro-inflammatory cytokines protecting against pathology in the lung. On the contrary, Xie T. and colleagues published in 2012 that a higher expression of this miRNA inhibits inflammation by targeting CD64 in macrophages which regulates cytokines release and reduces acute lung injury (T. Xie et al., 2012). The discrepancy in the results highlights the need to study the miR-127-3p role specifically in each pathological context.

In our work, miR-127-3p expression correlates along with the UUO model with the severity of the damage, which is in concordance with the results obtained by Ying et al., 2015, and Li et al., 2017 in the lung. But, our results by inhibiting miRNA expression in UUO mice, have demonstrated the opposite effects. Taking into account that renal damage was more severe in miR-127-3p inhibited UUO mice in comparison to the control ones, we could hypothesize that the induction of miR-127-3p expression could be beneficial for delaying renal injury progression in UUO mice, according to the results published by Xie and colleagues in 2012.

Related to that, our *in vitro* experiments have demonstrated in murine macrophages stimulated toward different phenotypes, that although miR-127-3p is not differently expressed in the cells depending on the stimulus received, the exogenous modulation of this miRNA by transient transfection in the cells affects the expression of the polarization markers studied. Particularly, inhibition of miR-127-3p expression induces an increased tendency to NOS2 expression, studied as a pro-inflammatory macrophage marker, in both M1[LPS] and M2a[IL-4] phenotypes. These results, strongly suggest that the inhibition of miR-127-3p exacerbates a pro-inflammatory response. Moreover, and regarding the potential protective role of miR-127-3p in which this work has been based on, the over-expression of miR-127-3p in the alternatively activated macrophages (M2[IL-4]) has led to a significant decrease of NOS2, which could enhance the functionality of this phenotype implicated in inflammation control and resolution. Indeed, miR127-3p participates in wound healing, and tissue repair and remodeling which is strongly related to inflammation resolution (Orekhov et al., 2019).

It is important to discuss that we have not found significant differences among experimental groups in the expression of ARG1 studied by qRT-PCR, as M2[IL-4] macrophage marker, when miR-127-3p was modulated in the cells. We could explain this finding because the transcription rate in primary cultured macrophages is very low, and some genes, such as ARG1, are poorly expressed, so large numbers of cells in each experiment are needed to

obtain enough mRNA to see the differences between conditions. Additionally, it is conceivable that miR-127-3p modulation is not involve in mechanisms that control ARG1 transcription.

Nevertheless, results from *in vitro* experiments have demonstrated that although miR-127-3p per se is not differentially expressed among different macrophage phenotypes it could be indirectly involved in macrophage polarization, which constitutes a cellular process strongly associated with CKD development (Guiteras et al., 2016; Pan et al., 2015; Parisi et al., 2018). In this sense, macrophages could be potential targets to ameliorate renal injury through manipulation of their polarization (Engel & Chade, 2019) and as it was largely described in the introduction of this work, miRNAs have been unleashed as novel therapeutic strategies for the treatment of diseases due to their key role in the regulation of cell function (O'Brien et al., 2018), which include macrophage polarization (Shapouri-Moghaddam et al., 2018; Orliaguet et al., 2020).

So far, all the results obtained in this work strongly confirm a relationship between miR-127-3p and the main cellular processes that contribute to the development of chronic kidney damage. Furthermore, our evidence has suggested that the overexpression of this miRNA in kidney tissue could have a beneficial role by regulating molecular mechanisms that underlie the progression of the disease. Thus, we also have tried to overexpress miR-127-3p in the UUO experimental model to determine whether this miRNA intervention could be a potential therapeutic strategy for CKD treatment.

Currently, the most common tool used to induce miRNAs expression *in vivo* experiments is by the administration of viral vehicles containing the pre-miR sequence. Many publications describe different methods, vias, and/or dosages to successfully achieve kidney cells, M. Kim et al., 2009; Park et al., 2010; Lan et al., 2012; Espana-Agusti et al., 2015, are some examples. Based on this knowledge, we have tried to target renal cortex cells by testing several adeno-associated particles provided by Dr. Chillón Rodríguez and his group (Viral Vectors Production Unit, UAB) and also, different lentiviral particles following the procedures described in some publications (H. H. Chen et al., 2016; D. Chen et al., 2017; Fierro-Fernández et al., 2020) and specified in the material and method section.

Unfortunately, any adeno-associated constructs tested induced the miRNA expression in the kidney cells, and we could not overexpress miR-127-3p by parenchymal and retro-orbital administration methods as we have expected, but renal-arterial injection successfully induced the miRNA expression in kidney cells since day 3, and especially at day 10 after treatment. Therefore, and because of these preliminary results, the overexpression approach is still an objective of our work. Additional experiments are necessary to improve the overexpression technique to define an adequate dose and time frame along the UUO experimental model to assure high levels of miRNA before the kidney damage is established and fibrosis became irreversible.

Besides, we are aware that this work lacks more studies devoted to identifying miRNA target genes and the signaling pathways triggered by miR-127-3p underlying this pathological context. These findings would strongly support our hypothesis and would allow us to point out miR-127-3p as a novel candidate molecule in the therapy of CKD.

In this sense, there are some validated and predicted target genes that could be downregulated by miR-127-3p expression and have a positive effect in the resolution of this pathological context. On the one hand, MMP13 has been validated in previous results of our lab as a miR-127-3p target molecule involved in the EMT process under TGFβ stimuli in proximal tubule cells, which contributes to matrix remodeling and promotes fibrosis development (Martín-Gómez, Laura, Ph.D.Dissertation, 2017). The relationship between MMP13 and miR-127-3p has been already described by Yang C and colleagues in hepatocellular carcinoma whose furthermore propose that during disease miR-127-3p expression is induced in the tissue maybe to play a protective role by downregulating this metalloproteinase, but is inhibited by c-Jun through TGFβ mediated ERK and JNK pathways which results in a worse progression of pathology (Z. Yang et al., 2013). That could explain what is happening during the progression of chronic kidney damage in which TGBβ is induced along with tubular damage and inflammation response. On the other hand, we have preliminary results indicating that Slug could be regulated by this miRNA interfering in the activation of fibroblasts, which is considered also a pivotal process for the development of CKD, however, more studies are necessary to demonstrate this fact. Besides, we have pointed out Lamtor1 as a target gene of miR-127-3p in macrophages to be an activator of the mTOR signaling pathway downstream PI3K-Akt pathway, and directly implicated in metabolism and many cellular processes including cell growth, proliferation, and apoptosis (Saxton & Sabatini, 2017). Several studies have confirmed that dysregulation of mTOR signaling disrupts renal cell homeostasis and results in kidney diseases through multiple pathways such as promoting EMT in tubular epithelial cells and fibroblast activation (Pérez, 2011; Márquez & Pascual, 2014; Gui & Dai, 2020). Regarding inflammatory response, it has been published that the amino acid–sensing pathway consisting of Lamtor1, mTORC1, and TFEB is involved in the regulation of innate immune response, including macrophage polarization (Hayama et al., 2018). All these works support the idea of Lamtor1 as a molecule involved in the establishment of kidney damage, possibly exerting its role as a target of miR-127-3p since the downregulation of this gene by the miRNA would result in the non-activation of the mTOR signaling pathway which has been demonstrated beneficial to attenuate kidney diseases development (Y. Liu, 2006; Márquez & Pascual, 2014). However, Kimura and colleagues published that Lamtor1 is essential for M2 macrophage polarization via the amino acid-sensing mTORC1-activating pathway and that loss of Lamtor1 promotes M1 polarization (Kimura et al., 2016) what is controversial with our hypothesis about the beneficial role of the downregulation of this gene through miR-127-3p in the development of chronic kidney disease and the obtained results of this thesis in which the inhibition of miR-127-3p accelerates kidney damage and exacerbate macrophage response.

As it was already mentioned, more studies are needed to elucidate the target genes and mechanisms regulated by miR-127-3p mediating into chronic kidney disease, and which strongly allow us to point out a potential therapeutic strategy for CKD treatment based on miR-127-3p modulation. Moreover, current therapies are limited and up to date, there is no cure for this disease. In fact, the majority of clinical trials ongoing are devoted to mitigate disease symptoms and improve patient management and their quality of life.

Another important feature in CKD is that the gold standard methods for diagnosis and classification of disease based on severity, are not able to identify kidney damage in the early stages of disease (Lopez-Giacoman S & Madero M, 2015; Rysz et al., 2017). Thus, CKD courses with a long clinically silent period, and therefore treatment could only be applied when kidney dysfunction is already established (Bidin et al., 2019). Because of that, the search for early renal injury biomarkers, as part of pathophysiological mechanisms and also capable of identifying severity, has been turned into a significant challenge for the future. As it was largely described in the introduction of this work, there are promising molecules that are being investigated as potential biomarkers of renal damage. However, none of them has already confirmed efficacy, sensitivity, and specificity.

In this regard, circulating miRNAs have demonstrated in the last decades that they could serve as accurate biomarkers of many pathological contexts (O'Brien et al., 2018; Hanna et al., 2019). Based on that, previous results of our lab identified a set of serum miRNAs including miR-127-3p able to diagnose AKI with a high sensibility and specificity and to reflect the persistence of cellular and tissue damage when renal function is restored by classical parameters (Aguado-Fraile, Elia, Ph.D.Dissertation, 2013). These findings highlight the value of miRNAs in clinical practice. For these reasons, in this work, we have also correlated the serum expression of some miRNAs, with the clinical settings of a CKD patient cohort, including severity.

As a novel result, we have demonstrated that the expression of miR-146-3p, miR-27a-3p, and miR-93-3p in serum samples significantly decreases when kidney damage progresses, and they can discriminate between patients in different stages of the disease, which could be useful to CKD diagnosis and patient stratification. Unexpectedly, miR-127-3p was not among them, even though our results strongly have demonstrated an implication of this miRNA in disease development. Interestingly, this could suggest that the dysregulation of miR-127-3p expression is not the result of kidney injury, but rather this miRNA is being regulated "on purpose" as part of the pathophysiological mechanism throughout the disease, might be with a protective effect inside renal tissue as our results strongly suggest. Thus, they are released to urine or blood could be tightly regulated or even avoided. Moreover, it is known that specific miRNAs can be deregulated in a tissue taking part in a molecular mechanism involved in the disease development, but not mandatory have to be the same that are released to urine or fluids and that we detect as circulating molecules (Zedan et al., 2018).

Moreover, miR146a-3p, miR-26-5p, miR-27a-3p, and also miR-127-3p serum expression correlates with some parameters evaluated in the patient cohort as CKD outcomes such as Vitamin D, transaminases, and GFR. Further studies should be performed in order to unveil the implications of these correlation but if miRNAs expression is related with CKD severity and progression, correlation with these parameters could be used to allow a better patient management. Remarkably, vitamin D levels and bone remodelation is tightly linked to CKD outcome, and liver homeostasis is also affected during CKD (Fernández-Juárez et al., 2013).

Related to that, many publications have described some of these miRNAs as renal damage biomarkers. Francesca C and colleagues published that miR-27a-3p correlates with the progression of Kidney Fibrosis in Diabetic Nephropathy in urine samples from patients (Conserva et al., 2019). Circulating miR-26b-3p and let-7g-5p were reported as potential biomarkers of chronic kidney disease (Berillo et al., 2018), and also urinary miR-26b-3p levels were associated with AKI induced by sepsis (J. Zhang et al., 2018). Moreover, miR-146a-3p has been unleashed as a potential marker of albuminuria in essential hypertension in urinary exosomes (Perez-Hernandez et al., 2018).

All of these taken together, reveals that although further investigations are necessary, serum miRNA levels including ours could be useful biomarkers for CKD patient management in many aspects and stages of disease progression and outcome, which is considered a major goal for CKD.

In this sense, it is important to recall that miRNAs studied in this work were selected from a panel published from our lab reporting that levels in serum from patients remained altered when AKI episode was clinically resolved and sCr values were restored (Aguado-Fraile et al., 2015). Thus, the miRNAs studied could be useful for identifying a potential risk for suffering CKD in the early stages of renal damage or detecting patients progressing to the next stage of kidney disease. That would allow better patient management and treatment since renal damage appears and avoiding patients to progress to a late-stage kidney damage disease (ESKD), which strongly would improve patient´s life quality and would reduce the cost for the health systems.

In summary, in this work, we have reported for the first time miR-127-3p in CKD, identifying this miRNA as a critical molecule involved in the progression of the disease. We have evidenced that miR-127-3p expression is induced after kidney injury in the cytoplasm of tubular cells in UUO mice and that this expression concurs with the main cellular processes underlying chronic kidney damage. Additionally, we have revealed that miR-127-3p inhibition aggravates tubular damage, fibrosis development, and exacerbates the associated macrophage response. Thus, our findings strongly suggest that the overexpression of this miRNA during the early stages of kidney damage could be a potential therapeutic strategy for CKD treatment. In this sense, we have performed preliminary experiments to demonstrate the beneficial role of this miRNA in this pathological context, but further investigation is needed,

as well as the identification of the target genes regulated by this miRNA along disease progression. Finally, we have established that the serum levels of renal-related miRNAs studied could be useful as accurate biomarkers of CDK progression and could contribute to an early patients' diagnosis and stratification in different stages by kidney damage severity.

This work constitutes an example of translational research from bench to the bedside in which studies of CKD molecular mechanisms in experimental *in vitro* and *in vivo* models, can be useful in this clinical context. Thus, miR-127-3p has been identified as a key mediator of renal responses in chronic kidney damage which could contribute to achieving one of the major goals in CKD: the identification of novel targets for efficient therapeutic intervention. Indeed, it is important to notice that some of our findings described in this work, are on the basis of an intellectual property application for the use of this miRNA as a therapy for CKD treatment already in PCT extension and wait for approval in different countries. This intellectual property protection will allow us to develop potential new therapeutic approaches to CKD that might be useful in patients after clinical trial.

Conclusions

1. miR-127-3p is induced in kidney tissue throughout the UUO experimental model. The increase in miR-127-3p expression throughout the model correlates with tubular damage, fibrosis development, and the increase in inflammatory infiltrate.

2. Inhibition of miR-127-3p in the murine model of UUO results in worsening kidney damage and increased inflammatory infiltrate, including an enlarged population of M2 macrophages. Besides, there is a higher expression of inflammatory cytokines within the renal tissue during experimental disease development.

3. The use of lentiviral vectors, containing the mature miR-127-3p sequence, administered via the renal artery seems to be the most effective method for overexpressing miR-127-3p in epithelial cells of the renal cortex in the murine model of UUO.

4. The expression of miR-127-3p in murine macrophages does not change depending on the M1 and M2 phenotype induced by treatment with LPS or IL4, respectively.

5. The overexpression of miR-127-3p in murine macrophages polarized to M2 by treatment with IL-4 leads to a decrease in the expression of NOS2, indicating that the exogenous up-regulation of miR127-3p in macrophages exacerbates and perpetuates an M2 phenotype.

6. Low levels of miR-146a-3p, miR-27a-3p, and miR-93-3p in the serum of patients diagnosed with Chronic Kidney Disease associate with more severe stages of CKD. Furthermore, the serum levels of miR-127-3p, miR-146a-3p, miR-27a-3p, and miR-26b-5p also associate with other clinical parameters, including liver function parameters and Vitamin D levels. This, indicates the potential usefulness of these miRNAs in the stratification and management of patients with CKD, in clinical practice.

Conclusiones

1. miR-127-3p se induce en el tejido renal a lo largo del modelo experimental UUO. El aumento de expresión de miR-127-3p a lo largo del modelo se correlaciona con el de daño tubular, el desarrollo de la fibrosis y el aumento de infiltrado inflamatorio.

2. La inhibición de miR-127-3p en el modelo murino de UUO resulta en un agravamiento del daño renal y una exacerbación de la respuesta inflamatoria que incluye un aumento de la población de macrófagos M2 y de la expresión de citoquinas inflamatorias.

3. La utilización de vectores lentivirales, conteniendo la secuencia de miR127-3p madura, administrados por vía arteria renal parece ser el método más efectivo para la sobreexpresión de miR-127-3p en células epiteliales de la corteza renal en el modelo murino de UUO.

4. La expresión de miR-127-3p en macrófagos murinos no cambia en función del fenotipo M1 o M2 inducidos mediante tratamiento con LPS e IL4, respectivamente.

5. La sobre-expresión de miR-127-3p en macrófagos murinos polarizados a M2 por tratamiento con IL-4 conduce a una bajada en la expresión de NOS2, indicando que niveles elevados de miR127-3p en macrófagos exacerba y perpetúa un fenotipo M2.

6. Bajos niveles de miR-146a-3p, miR-27a-3p y miR-93-3p en suero de pacientes diagnosticados de enfermedad renal crónica se asocian a estadios más graves de la ERC. Además, los niveles en suero de miR-127-3p, miR-146a-3p, miR-27a-3p y miR-26b-5p se asocian con otros parámetros clínicos, incluidos parámetros de función hepática y niveles de Vitamina D. Esto indica la potencial utilidad de estos miRNAs en la estratificación y el manejo de pacientes con ERC en la práctica clínica.

Bibliography

Aguado-Fraile, Elia, Ph.D.Dissertation, 2013). (2013). *Estudio De Micrornas Implicados En La Respuesta Renal a Isquemia-Reperfusión: Identificación Como Nuevos Biomarcadores De Daño Renal Agudo*. http://eprints.ucm.es/20779/1/T34388.pdf

Aguado-Fraile, E., Ramos, E., Conde, E., Rodríguez, M., Martín-Gómez, L., Lietor, A., Candela, Á., Ponte, B., Liaño, F., & Laura García-Bermejo, M. (2015). *A Pilot Study Identifying a Set of microRNAs As Precise Diagnostic Biomarkers of Acute Kidney Injury*. https://doi.org/10.1371/journal.pone.0127175

Aguado-Fraile, E., Ramos, E., Sáenz-Morales, D., Conde, E., Blanco-Sánchez, I., Stamatakis, K., Peso, L. del, Cuppen, E., Brüne, B., & Bermejo, M. L. G. (2012). miR-127 Protects Proximal Tubule Cells against Ischemia/Reperfusion: Identification of Kinesin Family Member 3B as miR-127 Target. *PLoS ONE*, *7*(9), e44305. https://doi.org/10.1371/journal.pone.0044305

Akchurin, O. M., & Kaskel, F. (2015). Update on inflammation in chronic kidney disease. *Blood Purification*, *39*(1–3), 84–92. https://doi.org/10.1159/000368940

Andrade-Oliveira, V., Foresto-Neto, O., Watanabe, I. K. M., Zatz, R., & Câmara, N. O. S. (2019). Inflammation in renal diseases: New and old players. *Frontiers in Pharmacology*, *10*(October), 1–19. https://doi.org/10.3389/fphar.2019.01192

Arvaniti, E., Moulos, P., Vakrakou, A., Chatziantoniou, C., Chadjichristos, C., Kavvadas, P., Charonis, A., & Politis, P. K. (2016). Whole-transcriptome analysis of UUO mouse model of renal fibrosis reveals new molecular players in kidney diseases. *Scientific Reports*, *6*(May), 1–16. https://doi.org/10.1038/srep26235

Banerjee, S., Xie, N., Cui, H., Tan, Z., Yang, S., Icyuz, M., Abraham, E., & Liu, G. (2013). MicroRNA let-7c Regulates Macrophage Polarization. *The Journal of Immunology*, *190*(12), 6542–6549. https://doi.org/10.4049/jimmunol.1202496

Barahona, A. R. (2019). *Estudios genéticos y fisiopatológicos para la búsqueda de nuevos biomarcadores y terapias en acidemia propiónica*.

Bartel, D. P. (2018). Metazoan MicroRNAs. *Cell*, *173*(1), 20–51. https://doi.org/10.1016/j.cell.2018.03.006

Berillo, O., Huo, K.-G., Richer, C., Fraulob-Aquino, J. C., Rehman, A., Briet, M., Boutouyrie, P., Lipman, M. L., Sinnett, D., Paradis, P., & Schiffrin, E. L. (2018). A3952 Circulating miR-26a-5p and let-7g-5p are potential biomarkers of chronic kidney disease. *Journal of Hypertension*, *36*. https://journals.lww.com/jhypertension/Fulltext/2018/10003/A3952_Circulating_miR_26a_5p_and_let_7g_5p_are.572.aspx

Bidin, M. Z., Shah, A. M., Stanslas, J., & Lim, C. T. S. (2019). Blood and urine biomarkers in chronic kidney disease: An update. *Clinica Chimica Acta*, *495*(January), 239–250. https://doi.org/10.1016/j.cca.2019.04.069

Bikbov, B., Purcell, C. A., Levey, A. S., Smith, M., Abdoli, A., Abebe, M., Adebayo, O. M., Afarideh, M., Agarwal, S. K., Agudelo-Botero, M., Ahmadian, E., Al-Aly, Z., Alipour, V., Almasi-Hashiani, A., Al-Raddadi, R. M., Alvis-Guzman, N., Amini, S., Andrei, T., Andrei, C. L., … Murray, C. J. L. (2020).

Global, regional, and national burden of chronic kidney disease, 1990–2017: a systematic analysis for the Global Burden of Disease Study 2017. *The Lancet*, *395*(10225), 709–733. https://doi.org/10.1016/S0140-6736(20)30045-3

Bonneau, E., Neveu, B., Kostantin, E., Tsongalis, G. J., & De Guire, V. (2019). How close are miRNAs from clinical practice? A perspective on the diagnostic and therapeutic market. *Electronic Journal of the International Federation of Clinical Chemistry and Laboratory Medicine*, *30*(2), 114–127.

Caescu, C. I., Guo, X., Tesfa, L., Bhagat, T. D., Verma, A., Zheng, D., & Stanley, E. R. (2015). Colony stimulating factor-1 receptor signaling networks inhibit mouse macrophage inflammatory responses by induction of microRNA-21. *Blood*, *125*(8), e1–e13. https://doi.org/10.1182/blood-2014-10-608000

Chen, D., Xiong, X. Q., Zang, Y. H., Tong, Y., Zhou, B., Chen, Q., Li, Y. H., Gao, X. Y., Kang, Y. M., & Zhu, G. Q. (2017). BCL6 attenuates renal inflammation via negative regulation of NLRP3 transcription. *Cell Death & Disease*, *8*(10), e3156. https://doi.org/10.1038/cddis.2017.567

Chen, H. H., Lan, Y. F., Li, H. F., Cheng, C. F., Lai, P. F., Li, W. H., & Lin, H. (2016). Urinary miR-16 transactivated by C/EBPβ reduces kidney function after ischemia/reperfusion-induced injury. *Scientific Reports*, *6*(February), 1–14. https://doi.org/10.1038/srep27945

Chen, Q., Wang, H., Liu, Y., Song, Y., Lai, L., Han, Q., Cao, X., & Wang, Q. (2012). Inducible microRNA-223 down-regulation promotes TLR-triggered IL-6 and IL-1β production in macrophages by targeting STAT3. *PLoS ONE*, *7*(8), 1–12. https://doi.org/10.1371/journal.pone.0042971

Chen, T., Cao, Q., Wang, Y., & Harris, D. C. H. (2019). M2 macrophages in kidney disease: biology, therapies, and perspectives. *Kidney International*, *95*(4), 760–773. https://doi.org/10.1016/j.kint.2018.10.041

Cobos Jiménez, V., Bradley, E. J., Willemsen, A. M., van Kampen, A. H. C., Baas, F., & Kootstra, N. A. (2014). Next-generation sequencing of microRNAs uncovers expression signatures in polarized macrophages. *Physiological Genomics*, *46*(3), 91–103. https://doi.org/10.1152/physiolgenomics.00140.2013

Conde, E., Giménez-Moyano, S., Martín-Gómez, L., Rodríguez, M., Ramos, M. E., Aguado-Fraile, E., Blanco-Sanchez, I., Saiz, A., & García-Bermejo, M. L. (2017). HIF-1α induction during reperfusion avoids maladaptive repair after renal ischemia/reperfusion involving miR127-3p. *Scientific Reports*, *7*(1), 41099. https://doi.org/10.1038/srep41099

Conroy, A. L., Hawkes, M. T., Elphinstone, R., Opoka, R. O., Namasopo, S., Miller, C., John, C. C., & Kain, K. C. (2018). Chitinase-3-like 1 is a biomarker of acute kidney injury and mortality in paediatric severe malaria NCT01255215 NCT. *Malaria Journal*, *17*(1), 1–11. https://doi.org/10.1186/s12936-018-2225-5

Conserva, F., Barozzino, M., Pesce, F., Divella, C., Oranger, A., Papale, M., Sallustio, F., Simone, S., Laviola, L., Giorgino, F., Gallone, A., Pontrelli, P., & Gesualdo, L. (2019). Urinary miRNA-27b-3p and miRNA-1228-3p correlate with the progression of Kidney Fibrosis in Diabetic Nephropathy. *Scientific Reports*, *9*(1), 1–11. https://doi.org/10.1038/s41598-019-47778-1

Devarajan, P. (2008). Neutrophil gelatinase-associated lipocalin (NGAL): A new marker of kidney disease. *Scand J Clin Lab Invest Suppl.*, *241*, 89–94. https://doi.org/10.1080/00365510802150158

Djudjaj, S., & Boor, P. (2019). Cellular and molecular mechanisms of kidney fibrosis. *Molecular Aspects of Medicine*, *65*(April), 16–36. https://doi.org/10.1016/j.mam.2018.06.002

Eddy, A. A., López-Guisa, J. M., Okamura, D. M., & Yamaguchi, I. (2012). Investigating mechanisms of chronic kidney disease in mouse models. *Pediatric Nephrology*, *27*(8), 1233–1247. https://doi.org/10.1007/s00467-011-1938-2

Engel, J. E., & Chade, A. R. (2019). Macrophage polarization in chronic kidney disease: A balancing act between renal recovery and decline? *American Journal of Physiology - Renal Physiology*, *317*(6), F1409–F1413. https://doi.org/10.1152/ajprenal.00380.2019

Espana-Agusti, J., Tuveson, D. A., Adams, D. J., & Matakidou, A. (2015). A minimally invasive, lentiviral based method for the rapid and sustained genetic manipulation of renal tubules. *Scientific Reports*, *5*(May), 1–8. https://doi.org/10.1038/srep11061

Essandoh, K., Li, Y., Huo, J., & Fan, G.-C. (2016). MiRNA-Mediated Macrophage Polarization and its Potential Role in the Regulation of Inflammatory Response. *Shock (Augusta, Ga.)*, *46*(2), 122–131. https://doi.org/10.1097/SHK.0000000000000604

Fernández-Juárez, G., Luño, J., Barrio, V., de Vinuesa, S. G., Praga, M., Goicoechea, M., Lahera, V., Casas, L., & Oliva, J. (2013). 25 (OH) vitamin D levels and renal disease progression in patients with type 2 diabetic nephropathy and blockade of the renin-angiotensin system. *Clinical Journal of the American Society of Nephrology*, *8*(11), 1870–1876. https://doi.org/10.2215/CJN.00910113

Fierro-Fernández, M., Miguel, V., Márquez-Expósito, L., Nuevo-Tapioles, C., Herrero, J. I., Blanco-Ruiz, E., Tituaña, J., Castillo, C., Cannata, P., Monsalve, M., Ruiz-Ortega, M., Ramos, R., & Lamas, S. (2020). MiR-9-5p protects from kidney fibrosis by metabolic reprogramming. *FASEB Journal*, *34*(1), 410–431. https://doi.org/10.1096/fj.201901599RR

Fierro-Fernández, M., Miguel, V., Márquez-Expósito, L., Nuevo-Tapioles, C., Herrero, J. I., Blanco-Ruiz, E., Tituaña, J., Castillo, C., Cannata, P., Monsalve, M., Ruiz-Ortega, M., Ramos, R., & Lamas, S. (2020). MiR-9-5p protects from kidney fibrosis by metabolic reprogramming. *The FASEB Journal*, *34*(1), 410–431. https://doi.org/10.1096/fj.201901599RR

Fu, X. D. (2014). Non-coding RNA: A new frontier in regulatory biology. *National Science Review*, *1*(2), 190–204. https://doi.org/10.1093/nsr/nwu008

Gajjala, P. R., Sanati, M., & Jankowski, J. (2015). Cellular and molecular mechanisms of chronic kidney disease with diabetes mellitus and cardiovascular diseases as its comorbidities. *Frontiers in Immunology*, *6*(JUN), 1–15. https://doi.org/10.3389/fimmu.2015.00340

Gebert, L. F. R., & MacRae, I. J. (2019). Regulation of microRNA function in animals. *Nature Reviews Molecular Cell Biology*, *20*(1), 21–37. https://doi.org/10.1038/s41580-018-0045-7

Ghosh, A. K., Nagpal, V., Covington, J. W., Michaels, M. A., & Vaughan, D. E. (2012). Molecular basis of

cardiac endothelial-to-mesenchymal transition (EndMT): Differential expression of microRNAs during EndMT. *Cellular Signalling*, *24*(5), 1031–1036. https://doi.org/10.1016/j.cellsig.2011.12.024

Golestaneh, L., Alvarez, P. J., Reaven, N. L., Funk, S. E., McGaughey, K. J., Romero, A., Brenner, M. S., & Onuigbo, M. (2017). All-cause costs increase exponentially with increased chronic kidney disease stage. *The American Journal of Managed Care*, *23*(10 Suppl), S163–S172. http://europepmc.org/abstract/MED/28978205

Gorostidi, M., Sánchez-Martínez, M., Ruilope, L. M., Graciani, A., de la Cruz, J. J., Santamaría, R., del Pino, M. D., Guallar-Castillón, P., de Álvaro, F., Rodríguez-Artalejo, F., & Banegas, J. R. (2018). Chronic kidney disease in Spain: Prevalence and impact of accumulation of cardiovascular risk factors. *Nefrologia*, *38*(6), 606–615. https://doi.org/10.1016/j.nefroe.2018.04.010

Guay C, Regazzi R. Circulating microRNAs as novel biomarkers for diabetes mellitus. Nat Rev Endocrinol. 2013 Sep;9(9):513-21. doi: 10.1038/nrendo.2013.86. Epub 2013 Apr 30. PMID: 23629540.

Gui, Y., & Dai, C. (2020). mTOR Signaling in Kidney Diseases. *Kidney360*, *1*(11), 1319–1327. https://doi.org/10.34067/kid.0003782020

Guiteras, R., Flaquer, M., & Cruzado, J. M. (2016). Macrophage in chronic kidney disease. *Clinical Kidney Journal*, *9*(6), 765–771. https://doi.org/10.1093/ckj/sfw096

Guzzi, F., Cirillo, L., Roperto, R. M., Romagnani, P., & Lazzeri, E. (2019). Molecular mechanisms of the acute kidney injury to chronic kidney disease transition: An updated view. *International Journal of Molecular Sciences*, *20*(19). https://doi.org/10.3390/ijms20194941

Hanna, J., Hossain, G. S., & Kocerha, J. (2019). The potential for microRNA therapeutics and clinical research. *Frontiers in Genetics*, *10*(MAY). https://doi.org/10.3389/fgene.2019.00478

Hayama, Y., Kimura, T., Takeda, Y., Nada, S., Koyama, S., Takamatsu, H., Kang, S., Ito, D., Maeda, Y., Nishide, M., Nojima, S., Sarashina-Kida, H., Hosokawa, T., Kinehara, Y., Kato, Y., Nakatani, T., Nakanishi, Y., Tsuda, T., Koba, T., … Kumanogoh, A. (2018). Lysosomal Protein Lamtor1 Controls Innate Immune Responses via Nuclear Translocation of Transcription Factor EB. *The Journal of Immunology*, *200*(11), 3790–3800. https://doi.org/10.4049/jimmunol.1701283

Hill NR, Fatoba ST, Oke JL, Hirst JA, O'Callaghan CA, et al. (2016) Global Prevalence of Chronic Kidney Disease – A Systematic Review and Meta-Analysis. PLOS ONE 11(7): e0158765. https://doi.org/10.1371/journal.pone.0158765

Hombach, S., & Kretz, M. (2016). *Biology and Functioning*. 171–181. https://doi.org/10.1007/978-3-319-42059-2

Huang W. MicroRNAs: Biomarkers, X, Vol. Diagnostics, and Therapeutics. Methods Mol Biol. 2017;1617:57-67. doi: 10.1007/978-1-4939-7046-9_4. PMID: 28540676.

Humphreys, B. D., Xu, F., Sabbisetti, V., Grgic, I., Naini, S. M., Wang, N., Chen, G., Xiao, S., Patel, D., Henderson, J. M., Ichimura, T., Mou, S., Soeung, S., McMahon, A. P., Kuchroo, V. K., & Bonventre, J. V. (2013). Chronic epithelial kidney injury molecule-1 expression causes murine kidney fibrosis. *Journal of Clinical Investigation*, *123*(9), 4023–4035. https://doi.org/10.1172/JCI45361

Ichii, O., & Horino, T. (2018). MicroRNAs associated with the development of kidney diseases in humans and animals. *Journal of Toxicologic Pathology*, *31*(1), 23–34. https://doi.org/10.1293/tox.2017-0051

Ina, K., Kitamura, H., Tatsukawa, S., & Fujikura, Y. (2011). Significance of α-SMA in myofibroblasts emerging in renal tubulointerstitial fibrosis. *Histology and Histopathology*, *26*(7), 855–866. https://doi.org/10.14670/HH-26.855

lma L. Saucedo, Marlene M. Perales-Quintana, David Paniagua-Vega, Concepcion Sanchez-Martinez, Paula Cordero-Perez and Noemi W. Minsky*, "Chronic Kidney Disease and the Search for New Biomarkers for Early Diagnosis", Current Medicinal Chemistry (2018) 25: 3719.

Jha, V., & Modi, G. K. (2018). Getting to know the enemy better—the global burden of chronic kidney disease. *Kidney International*, *94*(3), 462–464. https://doi.org/10.1016/j.kint.2018.05.009

Jl, L., Zhu, Z. N., He, C. J., & Shen, X. (2019). MiR-127-3p targets KIF3B to inhibit the development of oral squamous cell carcinoma. *European Review for Medical and Pharmacological Sciences*, *23*(2), 630–640. https://doi.org/10.26355/eurrev_201901_16877

K/DOQI clinical practice guidelines for chronic kidney disease: evaluation, classification, and stratification. (2002). *American Journal of Kidney Diseases : The Official Journal of the National Kidney Foundation*, *39*(2 Suppl 1), S1-266.

Kato, M., Zhang, J., Wang, M., Lanting, L., Yuan, H., Rossi, J. J., & Natarajan, R. (2007). *MicroRNA-192 in diabetic kidney glomeruli and its function in TGF- -induced collagen expression via inhibition of E-box repressors*.

Kawada, M., Hachiya, Y., Arihiro, A., & Mizoguchi, E. (2007). Role of mammalian chitinases in inflammatory conditions. *Keio Journal of Medicine*, *56*(1), 21–27. https://doi.org/10.2302/kjm.56.21

KDIGO 2017 Clinical Practice Guideline Update for the Diagnosis, Evaluation, Prevention, and Treatment of Chronic Kidney Disease-Mineral and Bone Disorder (CKD-MBD). (2017). *Kidney International Supplements*, *7*(1), 1–59. https://doi.org/10.1016/j.kisu.2017.04.001

Ketteler, M., Block, G. A., Evenepoel, P., Fukagawa, M., Herzog, C. A., McCann, L., Moe, S. M., Shroff, R., Tonelli, M. A., Toussaint, N. D., Vervloet, M. G., & Leonard, M. B. (2018). Diagnosis, Evaluation, Prevention, and Treatment of Chronic Kidney Disease-Mineral and Bone Disorder: Synopsis of the Kidney Disease: Improving Global Outcomes 2017 Clinical Practice Guideline Update. *Annals of Internal Medicine*, *168*(6), 422–430. https://doi.org/10.7326/M17-2640

Khalid U, Gilda Pino-Chavez, Prabhu Nesargikar, Robert H. Jenkins, Timothy Bowen, Donald J. Fraser, and Rafael Chavez. Kidney ischaemia reperfusion injury in the rat: the EGTI scoring system as a valid and reliable tool for histological assessment. Journal of Histology & Histopathology, 2016. ISSN 2055-091X, Vol. 3, Arti 1.

Kim, M., Chen, S. W. C., Park, S. W., Kim, M., D'agati, V. D., Yang, J., & Lee, H. T. (2009). Kidney-specific reconstitution of the A1 adenosine receptor in A1 adenosine receptor knockout mice reduces renal ischemia-reperfusion injury. *Kidney International*, *75*(8), 809–823.

Kim, M. G., Kim, S. C., Ko, Y. S., Lee, H. Y., Jo, S. K., & Cho, W. (2015). The role of M2 macrophages in the progression of chronic kidney disease following acute kidney injury. *PLoS ONE*, *10*(12), 1–17. https://doi.org/10.1371/journal.pone.0143961

Kimura, T., Nada, S., Takegahara, N., Okuno, T., Nojima, S., Kang, S., Ito, D., Morimoto, K., Hosokawa, T., Hayama, Y., Mitsui, Y., Sakurai, N., Sarashina-Kida, H., Nishide, M., Maeda, Y., Takamatsu, H., Okuzaki, D., Yamada, M., Okada, M., & Kumanogoh, A. (2016). Polarization of M2 macrophages requires Lamtor1 that integrates cytokine and amino-acid signals. *Nature Communications*, *7*, 1–15. https://doi.org/10.1038/ncomms13130

Kramer, H. (2019). Diet and Chronic Kidney Disease. *Advances in Nutrition*, *10*(8), S367–S379. https://doi.org/10.1093/advances/nmz011

Kriegel, A. J., Liu, Y., Cohen, B., Liu, Y., & Liang, M. (2020). MiR-382 targeting of kallikrein 5 contributes to renal inner medullary interstitial fibrosis. *Physiol & Genomics*, *44*, 259–267. https://doi.org/10.1152/physiolgenomics.00173.2011

Lan, Y.-F., Chen, H.-H., Lai, P.-F., Cheng, C.-F., Huang, Y.-T., Lee, Y.-C., Chen, T.-W., & Lin, H. (2012). MicroRNA-494 reduces ATF3 expression and promotes AKI. *Journal of the American Society of Nephrology : JASN*, *23*(12), 2012–2023. https://doi.org/10.1681/ASN.2012050438

Lee, C. G., Silva, C. A. Da, Cruz, C. S. Dela, Ahangari, F., Ma, B., Kang, J., He, C., Takyar, S., & Elias, J. A. (2011). Role of chitin and chitinase/chitinase-like proteins in inflammation, tissue remodeling, and injury. Annual review of physiology. *Annual Review of Pharmacology and Toxicology*, *73*, 1–28. https://doi.org/10.1146/annurev-physiol-012110-142250.Role

Lee, K. Y. (2019). M1 and M2 polarization of macrophages: a mini-review. *Medical Biological Science and Engineering*, *2*(1), 1–5. https://doi.org/10.30579/mbse.2019.2.1.1

Levey, A. S., De Jong, P. E., Coresh, J., Nahas, M. El, Astor, B. C., Matsushita, K., Gansevoort, R. T., Kasiske, B. L., & Eckardt, K. U. (2011). The definition, classification, and prognosis of chronic kidney disease: A KDIGO Controversies Conference report. *Kidney International*, *80*(1), 17–28. https://doi.org/10.1038/ki.2010.483

Levey, A. S., Eckardt, K. U., Tsukamoto, Y., Levin, A., Coresh, J., Rossert, J., De Zeeuw, D., Hostetter, T. H., Lameire, N., Eknoyan, G., & Willis, K. (2005). Definition and classification of chronic kidney disease: A position statement from Kidney Disease: Improving Global Outcomes (KDIGO). *Kidney International*, *67*(6), 2089–2100. https://doi.org/10.1111/j.1523-1755.2005.00365.x

Li, Q., Ge, Y. L., Li, M., Fang, X. Z., Yuan, Y. P., Liang, L., & Huang, S. Q. (2017). miR-127 contributes to ventilator-induced lung injury. *Molecular Medicine Reports*, *16*(4), 4119–4126. https://doi.org/10.3892/mmr.2017.7109

Li, R., Chung, A. C. K., Dong, Y., Yang, W., Zhong, X., & Lan, H. Y. (2013). The microRNA miR-433 promotes renal fibrosis by amplifying the TGF-β/Smad3-Azin1 pathway. *Kidney International*, *84*(6), 1129–1144. https://doi.org/10.1038/ki.2013.272

Liu, F., Li, Y., Jiang, R., Nie, C., Zeng, Z., Zhao, N., Huang, C., Shao, Q., Ding, C., Qing, C., Xia, L., Zeng, E., & Qian, K. (2015). miR-132 inhibits lipopolysaccharide-induced inflammation in alveolar macrophages by the cholinergic anti-inflammatory pathway. *Experimental Lung Research*, *41*(5),

261–269. https://doi.org/10.3109/01902148.2015.1004206

Liu, Y. (2006). Rapamycin and chronic kidney disease: beyond the inhibition of inflammation. *Kidney International*, *69*(11), 1925–1927. https://doi.org/10.1038/sj.ki.5001543

Lopez-Giacoman S, Madero M. Biomarkers in chronic kidney disease, from kidney function to kidney damage. World J Nephrol 2015; 4(1): 57-73

Lorenzen, J. M., Haller, H., & Thum, T. (2011). MicroRNAs as mediators and therapeutic targets in chronic kidney disease. *Nature Publishing Group*, *7*(5), 286–294. https://doi.org/10.1038/nrneph.2011.26

Márquez, E., & Pascual, J. (2014). Inhibición de mTOR, proteínas Akt y enfermedad renal crónica. *Nefrologia*, *34*(4), 425–427. https://doi.org/10.3265/Nefrologia.pre2014.Apr.12381

Martín-Gómez, Laura, Ph.D.Dissertation, 2017). (2017). *Caracterización de miR-127 como nuevo mediador de la fibrosis renal (Ph.D. Dissertation)*.

Martínez-Klimova, E., Aparicio-Trejo, O. E., Tapia, E., & Pedraza-Chaverri, J. (2019a). Unilateral ureteral obstruction as a model to investigate fibrosis-attenuating treatments. *Biomolecules*, *9*(4). https://doi.org/10.3390/biom9040141

Martínez-Klimova, E., Aparicio-Trejo, O. E., Tapia, E., & Pedraza-Chaverri, J. (2019b). Unilateral Ureteral Obstruction as a Model to Investigate Fibrosis-Attenuating Treatments. *Biomolecules*, *9*(141). https://doi.org/10.3390/biom9040141

Matthew, B. D., & Katalin, S. (2016). The next generation of therapeutics for chronic kidney disease. *Nature Reviews Drug Discovery*, *15*(8), 568–588. https://doi.org/10.1038/nrd.2016.67.THE

Mellado, M., Jankowski, J., Reddy Gajjala, P., & Sanati, M. (2015). Cellular and molecular mechanisms of chronic kidney disease with diabetes mellitus and cardiovascular diseases as its comorbidities. *Front. Immunol*, *6*, 340. https://doi.org/10.3389/fimmu.2015.00340

Meng, X. M., Mak, T. S. K., & Lan, H. Y. (2019). Macrophages in Renal Fibrosis. In *Advances in Experimental Medicine and Biology* (Vol. 1165). Springer Singapore. https://doi.org/10.1007/978-981-13-8871-2_13

Mihai, S., Codrici, E., Popescu, I. D., Enciu, A. M., Albulescu, L., Necula, L. G., Mambet, C., Anton, G., & Tanase, C. (2018). Inflammation-related mechanisms in chronic kidney disease prediction, progression, and outcome. *Journal of Immunology Research*, *2018*. https://doi.org/10.1155/2018/2180373

Milosevic, J., Pandit, K., Magister, M., Rabinovich, E., Ellwanger, D. C., Yu, G., Vuga, L. J., Weksler, B., Benos, P. V, Gibson, K. F., McMillan, M., Kahn, M., Kaminski, N., & Simmons, R. P. (2012). Profibrotic Role of miR-154 in Pulmonary Fibrosis. *American Journal of Respiratory Cell and Molecular Biology*, *47*. https://doi.org/10.1165/rcmb.2011-0377OC

Missbach-Guentner, J., Pinkert-Leetsch, D., Dullin, C., Ufartes, R., Hornung, D., Tampe, B., Zeisberg, M., & Alves, F. (2018). 3D virtual histology of murine kidneys -high resolution visualization of pathological alterations by micro computed tomography. *Scientific Reports*, *8*(1), 1407. https://doi.org/10.1038/s41598-018-19773-5

Mohr, A. M., & Mott, J. L. (2015). Overview of microRNA biology. *Seminars in Liver Disease*, *35*(1), 3–11. https://doi.org/10.1055/s-0034-1397344

Morizane, R., Fujii, S., Monkawa, T., Hiratsuka, K., Yamaguchi, S., Homma, K., & Itoh, H. (2014). MiR-34c attenuates epithelial-mesenchymal transition and kidney fibrosis with ureteral obstruction. *Scientific Reports*, *4*, 1–9. https://doi.org/10.1038/srep04578

Murray, P. J. (2017). Macrophage Polarization. *Annual Review of Physiology*, *79*, 541–566. https://doi.org/10.1146/annurev-physiol-022516-034339

Nakagawa, S., Nishihara, K., Miyata, H., Shinke, H., Tomita, E., Kajiwara, M., Matsubara, T., Iehara, N., Igarashi, Y., Yamada, H., Fukatsu, A., Yanagita, M., Matsubara, K., & Masuda, S. (2015). *Molecular Markers of Tubulointerstitial Fibrosis and Tubular Cell Damage in Patients with Chronic Kidney Disease*. https://doi.org/10.1371/journal.pone.0136994

Nogueira, A., Pires, M. J., & Oliveira, P. A. (2017). Pathophysiological mechanisms of renal fibrosis: A review of animal models and therapeutic strategies. *In Vivo*, *31*(1), 1–22. https://doi.org/10.21873/invivo.11019

O'Brien, J., Hayder, H., Zayed, Y., & Peng, C. (2018). Overview of microRNA biogenesis, mechanisms of actions, and circulation. *Frontiers in Endocrinology*, *9*(AUG), 1–12. https://doi.org/10.3389/fendo.2018.00402

Ohno, M., Bauer, P. O., Kida, Y., Sakaguchi, M., Sugahara, Y., & Oyama, F. (2015). Quantitative real-time PCR analysis of YKL-40 and its comparison with mammalian Chitinase mRNAs in normal human tissues using a single standard DNA. *International Journal of Molecular Sciences*, *16*(5), 9922–9935. https://doi.org/10.3390/ijms16059922

Orecchioni, M., Ghosheh, Y., Pramod, A. B., & Ley, K. (2019). Macrophage polarization: Different gene signatures in M1(Lps+) vs. Classically and M2(LPS-) vs. Alternatively activated macrophages. *Frontiers in Immunology*, *10*(MAY), 1–14. https://doi.org/10.3389/fimmu.2019.01084

Orekhov, A. N., Orekhova, V. A., Nikiforov, N. G., Myasoedova, V. A., Grechko, A. V., Romanenko, E. B., Zhang, D., & Chistiakov, D. A. (2019). Monocyte differentiation and macrophage polarization. *Vessel Plus*, *2019*. https://doi.org/10.20517/2574-1209.2019.04

Orliaguet, L., Dalmas, E., Drareni, K., Venteclef, N., & Alzaid, F. (2020). Mechanisms of Macrophage Polarization in Insulin Signaling and Sensitivity. *Frontiers in Endocrinology*, *11*(February), 1–23. https://doi.org/10.3389/fendo.2020.00062

Pan, B., Liu, G., Jiang, Z., & Zheng, D. (2015). Regulation of renal fibrosis by macrophage polarization. *Cellular Physiology and Biochemistry*, *35*(3), 1062–1069. https://doi.org/10.1159/000373932

Parisi, L., Gini, E., Baci, D., Tremolati, M., Fanuli, M., Bassani, B., Farronato, G., Bruno, A., & Mortara, L. (2018). Macrophage Polarization in Chronic Inflammatory Diseases: Killers or Builders? *Journal of Immunology Research*, *2018*. https://doi.org/10.1155/2018/8917804

Park, S. W., Chen, S. W. C., Kim, M., Brown, K. M., D'Agati, V. D., & Lee, H. T. (2010). Protection against

acute kidney injury via A1 adenosine receptor-mediated Akt activation reduces liver injury after liver ischemia and reperfusion in mice. *Journal of Pharmacology and Experimental Therapeutics*, *333*(3), 736–747. https://doi.org/10.1124/jpet.110.166884

Perez-Hernandez, J., Olivares, D., Forner, M. J., Ortega, A., Solaz, E., Martinez, F., Chaves, F. J., Redon, J., & Cortes, R. (2018). Urinary exosome miR-146a is a potential marker of albuminuria in essential hypertension. *Journal of Translational Medicine*, *16*(1), 1–9. https://doi.org/10.1186/s12967-018-1604-6

Pérez, J. C. R. (2011). El papel de los inhibidores de mTOR en las enfermedades renales. *Nefrologia*, *31*(3), 251–255. https://doi.org/10.3265/Nefrologia.pre2011.Apr.10947

Rysz, J., Gluba-Brzózka, A., Franczyk, B., Jablonowski, Z., & Cialkowska-Rysz, A. (2017). Novel biomarkers in the diagnosis of chronic kidney disease and the prediction of its outcome. *International Journal of Molecular Sciences*, *18*(8). https://doi.org/10.3390/ijms18081702

Saliminejad, K., Khorram Khorshid, H. R., Soleymani Fard, S., & Ghaffari, S. H. (2019). An overview of microRNAs: Biology, functions, therapeutics, and analysis methods. *Journal of Cellular Physiology*, *234*(5), 5451–5465. https://doi.org/10.1002/jcp.27486

Salloum-Asfar, S., Satheesh, N. J., & Abdulla, S. A. (2019). Circulating miRNAs, Small but Promising Biomarkers for Autism Spectrum Disorder. *Frontiers in Molecular Neuroscience*, *12*, 253. https://doi.org/10.3389/fnmol.2019.00253

Saxton, R. A., & Sabatini, D. M. (2017). mTOR Signaling in Growth, Metabolism, and Disease. *Cell*, *169*(2), 361–371. https://doi.org/10.1016/j.cell.2017.03.035

Shanmugam, A., Nagarajan, A., & Pramanayagam, S. (2017). Non-coding DNA – a brief review. *Journal of Applied Biology & Biotechnology*, *October*. https://doi.org/10.7324/jabb.2017.50507

Shapouri-Moghaddam, A., Mohammadian, S., Vazini, H., Taghadosi, M., Esmaeili, S. A., Mardani, F., Seifi, B., Mohammadi, A., Afshari, J. T., & Sahebkar, A. (2018). Macrophage plasticity, polarization, and function in health and disease. In *Journal of Cellular Physiology* (Vol. 233, Issue 9). https://doi.org/10.1002/jcp.26429

Sheedy, F. J. (2015). Turning 21: Induction of miR-21 as a key switch in the inflammatory response. *Frontiers in Immunology*, *6*(JAN), 1–9. https://doi.org/10.3389/fimmu.2015.00019

Shi, J., Xia, Z., Lu, H., Wang, F., Xu, L., Hangjie, Y., Kang, Y., Zhang, H., & Zhao, D. (2014). *JNK Pathway Inflammation and Injury by Activating the Polarization and Promotes Lung MiR-127 Modulates Macrophage*. https://doi.org/10.4049/jimmunol.1402088

Shi, L., Wang, Y., Lu, Z., Zhang, H., Zhuang, N., Wang, B., Song, Z., Chen, G., Huang, C., Xu, D., Zhang, Y., Zhang, W., & Gao, Y. (2017). miR-127 promotes EMT and stem-like traits in lung cancer through a feed-forward regulatory loop. *Oncogene*, *36*(12), 1631–1643. https://doi.org/10.1038/onc.2016.332

Sohel, M. H. (2016). Achievements in the Life Sciences Extracellular / Circulating MicroRNAs : Release Mechanisms , Functions and Challenges. *ALS*, *10*(2), 175–186.

Soveri, I., Helmersson-Karlqvist, J., Fellström, B., & Larsson, A. (2020). Day-to-day variation of the kidney proximal tubular injury markers urinary cystatin C, KIM1, and NGAL in patients with chronic kidney disease. *Renal Failure*, *42*(1), 400–404. https://doi.org/10.1080/0886022X.2020.1757463

Sun, Yang, Li, Q., Gui, H., Xu, D. P., Yang, Y. L., Su, D. F., & Liu, X. (2013). MicroRNA-124 mediates the cholinergic anti-inflammatory action through inhibiting the production of pro-inflammatory cytokines. *Cell Research*, *23*(11), 1270–1283. https://doi.org/10.1038/cr.2013.116

Sun, Yingqing, Koo, S., White, N., Peralta, E., Esau, C., Dean, N. M., & Perera, R. J. (2004). Development of a micro-array to detect human and mouse microRNAs and characterization of expression in human organs. *Nucleic Acids Research*, *32*(22). https://doi.org/10.1093/nar/gnh186

Thulin, P., Wei, T., Werngren, O., Cheung, L., Fisher, R. M., Grandér, D., Corcoran, M., & Ehrenborg, E. (2013). MicroRNA-9 regulates the expression of peroxisome proliferator-activated receptor δ in human monocytes during the inflammatory response. *International Journal of Molecular Medicine*, *31*(5), 1003–1010. https://doi.org/10.3892/ijmm.2013.1311

Tian, P., Tao, L., Wang, Y., & Han, X. (2020). MicroRNA-127 Inhibits the Progression of Melanoma by Downregulating Delta-Like Homologue 1. *BioMed Research International*, *2020*. https://doi.org/10.1155/2020/8523465

Tomson, C., & Duffy, S. (2019). Management of chronic kidney disease. *Medicine (United Kingdom)*, *47*(9), 567–575. https://doi.org/10.1016/j.mpmed.2019.06.011

Tryndyak, V. P., Ross, S. A., Beland, F. A., & Pogribny, I. P. (2009). Down-regulation of the microRNAs *miR-34a* , *miR-127* , and *miR-200b* in rat liver during hepatocarcinogenesis induced by a methyl-deficient diet. *Molecular Carcinogenesis*, *48*(6), 479–487. https://doi.org/10.1002/mc.20484

Turner, J. M., Bauer, C., Abramowitz, M. K., Melamed, M. L., & Hostetter, T. H. (2012). Treatment of chronic kidney disease. *Kidney International*, *81*(4), 351–362. https://doi.org/10.1038/ki.2011.380

Umeh-Garcia, M., Simion, C., Ho, P.-Y., Batra, N., Berg, A. L., Carraway Iii, K. L., Yu, A., & Sweeney, C. (2020). A Novel Bioengineered MicroRNA-127 Prodrug Suppresses The Growth And Metastatic Potential Of Triple Negative Breast Cancer Cells. *Cancer Research*, *February 0*(80(3)), 418–429. https://doi.org/10.1158/0008-5472.CAN-19-0656

Vaidya, V. S., Ferguson, M. A., & Bonventre, J. V. (2008). Biomarkers of acute kidney injury. In *Annual Review of Pharmacology and Toxicology* (Vol. 48, pp. 463–493). NIH Public Access. https://doi.org/10.1146/annurev.pharmtox.48.113006.094615

Vanholder, R., van Laecke, S., Glorieux, G., Verbeke, F., Castillo-Rodriguez, E., & Ortiz, A. (2018). Deleting death and dialysis: Conservative care of cardio-vascular risk and kidney function loss in chronic kidney disease (CKD). *Toxins*, *10*(6). https://doi.org/10.3390/toxins10060237

Vergadi, E., Vaporidi, K., Theodorakis, E. E., Doxaki, C., Lagoudaki, E., Ieronymaki, E., Alexaki, V. I., Helms, M., Kondili, E., Soennichsen, B., Stathopoulos, E. N., Margioris, A. N., Georgopoulos, D., & Tsatsanis, C. (2014). Akt2 Deficiency Protects from Acute Lung Injury via Alternative Macrophage Activation and miR-146a Induction in Mice. *The Journal of Immunology*, *192*(1), 394–406.

Wahid, F., Shehzad, A., Khan, T., & Kim, Y. Y. (2010). MicroRNAs: Synthesis, mechanism, function, and recent clinical trials. *Biochimica et Biophysica Acta - Molecular Cell Research*, *1803*(11), 1231–1243. https://doi.org/10.1016/j.bbamcr.2010.06.013

Wang, D., Tang, L., Wu, H., Wang, K., & Gu, D. (2018). MiR-127-3p inhibits cell growth and invasiveness by targeting ITGA6 in human osteosarcoma. *IUBMB Life*, *70*(5), 411–419. https://doi.org/10.1002/iub.1710

Wang, L., Wang, X., & Jiang, X. (2019). MiR-127 suppresses gastric cancer cell migration and invasion via targeting Wnt7a. *Oncology Letters*, *17*(3), 3219–3226. https://doi.org/10.3892/ol.2019.9955

Wang, N., Liang, H., & Zen, K. (2014). Molecular mechanisms that influence the macrophage M1-M2 polarization balance. *Frontiers in Immunology*, *5*(NOV), 1–9. https://doi.org/10.3389/fimmu.2014.00614

Wang, Y., Smith, W., Hao, D., He, B., & Kong, L. (2019). M1 and M2 macrophage polarization and potentially therapeutic naturally occurring compounds. *International Immunopharmacology*, *70*(January), 459–466. https://doi.org/10.1016/j.intimp.2019.02.050

Webster, A. C., Nagler, E. V., Morton, R. L., & Masson, P. (2017). Chronic Kidney Disease. *The Lancet*, *389*(10075), 1238–1252. https://doi.org/10.1016/S0140-6736(16)32064-5

Xie, T., Liang, J., Liu, N., Wang, Q., Li, Y., Noble, P. W., & Jiang, D. (2012). miRNA-127 Inhibits Lung Inflammation by Targeting IgG Fcγ Receptor I. *Journal of Immunology Research*, *March 1*(188(5)), 2437–2444. https://doi.org/10.4049/jimmunol.1101070

Xie, Y., Bowe, B., Mokdad, A. H., Xian, H., Yan, Y., Li, T., Maddukuri, G., Tsai, C. Y., Floyd, T., & Al-Aly, Z. (2018). Analysis of the Global Burden of Disease study highlights the global, regional, and national trends of chronic kidney disease epidemiology from 1990 to 2016. *Kidney International*, *94*(3), 567–581. https://doi.org/10.1016/j.kint.2018.04.011

Yang, H. C., Zuo, Y., & Fogo, A. B. (2010a). Models of chronic kidney disease. *Drug Discovery Today: Disease Models*, *7*(1–2), 13–19. https://doi.org/10.1016/j.ddmod.2010.08.002

Yang, H. C., Zuo, Y., & Fogo, A. B. (2010b). Models of chronic kidney disease. *Drug Discovery Today: Disease Models*, *7*(1–2), 13–19. https://doi.org/10.1016/j.ddmod.2010.08.002

Yang, J., Lim, S. Y., Ko, Y. S., Lee, H. Y., Oh, S. W., Kim, M. G., Cho, W. Y., & Jo, S. K. (2019). Intestinal barrier disruption and dysregulated mucosal immunity contribute to kidney fibrosis in chronic kidney disease. *Nephrology Dialysis Transplantation*, *34*(3), 419–428. https://doi.org/10.1093/ndt/gfy172

Yang, Z., Zhang, Y., & Wang, L. (2013). A Feedback Inhibition between miRNA-127 and TGFβ/c-Jun Cascade in HCC Cell Migration via MMP13. *PLoS ONE*, *8*(6).

Ying, H., Kang, Y., Zhang, H., Zhao, D., Xia, J., Lu, Z., Wang, H., Xu, F., & Shi, L. (2015). MiR-127 Modulates Macrophage Polarization and Promotes Lung Inflammation and Injury by Activating the JNK Pathway. *The Journal of Immunology*, *194*(3), 1239–1251.

Yu, J., Yu, C., Feng, B., Zhan, X., Luo, N., Yu, X., & Zhou, Q. (2019). Intrarenal microRNA signature related to the fibrosis process in chronic kidney disease: Identification and functional validation of key miRNAs. *BMC Nephrology*, *20*(1), 1–13. https://doi.org/10.1186/s12882-019-1512-x

Zarjou, A., Yang, S., Abraham, E., Agarwal, A., & Liu, G. (2011). *Identification of a microRNA signature in renal fibrosis : role of miR-21*. 793–801. https://doi.org/10.1152/ajprenal.00273.2011.

Zedan, A. H., Hansen, T. F., Assenholt, J., Pleckaitis, M., Madsen, J. S., & Osther, P. J. S. (2018). MicroRNA expression in tumour tissue and plasma in patients with newly diagnosed metastatic prostate cancer. *Tumor Biology*, *40*(5), 1–11. https://doi.org/10.1177/1010428318775864

Zhang, J., Wang, C.-J., Tang, X.-M., & Wei, Y.-K. (2018). Urinary miR-26b as a potential biomarker for patients with sepsis-associated acute kidney injury: a Chinese population-based study. *European Review for Medical and Pharmacological Sciences*, *22*(14), 4604–4610. https://doi.org/10.26355/eurrev_201807_15518

Zhang, W., Liu, H., Liu, W., Liu, Y., & Xu, J. (2015). Polycomb-mediated loss of microRNA let-7c determines inflammatory macrophage polarization via PAK1-dependent NF-κB pathway. *Cell Death & Differentiation*, *22*(2), 287–297. https://doi.org/10.1038/cdd.2014.142

Zhang, Y., Zhang, M., Zhong, M., Suo, Q., & Lv, K. (2013). Expression profiles of miRNAs in polarized macrophages. *International Journal of Molecular Medicine*, *31*(4), 797–802. https://doi.org/10.3892/ijmm.2013.1260

Zhao, H., Ma, S. X., Shang, Y. Q., Zhang, H. Q., & Su, W. (2019). microRNAs in chronic kidney disease. *Clinica Chimica Acta*, *491*(November 2018), 59–65. https://doi.org/10.1016/j.cca.2019.01.008

Zhao, W., Wang, X., Sun, K. H., & Zhou, L. (2018). A-Smooth Muscle Actin Is Not a Marker of Fibrogenic Cell Activity in Skeletal Muscle Fibrosis. *PLoS ONE*, *13*(1), 1–16. https://doi.org/10.1371/journal.pone.0191031

Zhou, Q., Fan, J., Ding, X., Peng, W., Yu, X., Chen, Y., & Nie, J. (2010). TGF-β-induced MiR-491-5p expression promotes Par-3 degradation in rat proximal tubular epithelial cells. *Journal of Biological Chemistry*, *285*(51), 40019–40027. https://doi.org/10.1074/jbc.M110.141341

Publications, patents, and meetings

ARTICLES

The data described in this work have generated the following articles:

PRINCIPAL AUTHOR: **Giménez-Moyano, Sara**
TITLE: miR-127-3p as a novel mediator in fibrosis development and macrophage polarization in Chronic Kidney Disease.
(In preparation).

Moreover, the author has contributed to the following publications:

AUTHORS: Paula Martínez de la Cruz, Amir Shabaka, Xabier Mielgo-Rubio, Carmen Guerrero-Márquez, **Sara Giménez-Moyano**, Gema Fernández-Juárez.
TITLE: Concomitant Acute Tubular Necrosis and Acute Interstitial Nephritis Induced by Tipifarnib in a Patient with Squamous Cell Carcinoma of the Lung.
JOURNAL: **American Journal of the Medical Sciences**. 2021 Apr 16; S0002-9629(21)00133-6.
DOI: 10.1016/j.amjms.2021.04.003.

AUTHORS: Ruperto, Mar; Rodríguez Mendiola, Nuria; Díaz Domínguez, Martha; **Giménez Moyano, Sara**; García Bermejo, María Laura; Fernández Lucas, Milagros.
TITLE: Effect of oral administration of docohexanoic acid on anemia and inflammation in hemodialysis patients: A randomized controlled clinical trial.
JOURNAL: **Clinical Nutrition ESPEN**. 2021, volume 41, February 01, pages 129-135.
DOI: https://doi.org/10.1016/j.clnesp.2020.12.004.

AUTHORS: Villacorta, Javier; Lucientes, Laura; Goicoechea, Elena; Acevedo, Mercedes; Cavedo, Teresa; Sánchez Cámara, Luis; Díaz Crespo, Francisco; **Giménez Moyano, Sara**; García Bermejo, Laura; Fernández Juárez, Gema.
TITLE: Urinary soluble CD163 as a biomarker of disease activity and relapse in antineutrophil cytoplasm antibody-associated glomerulonephritis.
JOURNAL: **Clinical Kidney Journal**. 2021, volume 14, issue 1, January, pages 212–219.
DOI: https://doi.org/10.1093/ckj/sfaa043. Impact factor: **3.388**.

AUTHORS: Herrera, Alberto; Herrera, Mercedes; Guerra Pérez, Natalia; Galindo, Cristina; Ferreiro Monteagudo, Reyes; Larriba, MJ; Muñoz, Alberto; García, Vanesa; Gil, Beatriz; García Bermejo, Laura; **Giménez Moyano, Sara**; Veguillas, Pilar; Candía, Antonio; Peña, Raúl; García De Herreros, Antonio; Pinto, Jesús; Bonilla, Félix; Carrato, Alfredo; Peña Maroto, Cristina.
TITLE: Endothelial cell activation on 3D-matrices derived from PDGF-BB Stimulated fibroblasts is mediated by Snail1.
JOURNAL: **Oncogenesis**. 2018, volume 7(76).
DOI: https://doi.org/10.1038/s41389-018-0085-z.

AUTHORS: Conde E; **Giménez-Moyano S**; Martín-Gómez L; Rodríguez M; Ramos ME; Aguado-Fraile E; Blanco-Sánchez I; Saiz A; García-Bermejo ML.
TITLE: HIF-1α induction during reperfusion avoids maladaptive repair after renal ischemia/reperfusion involving miR127-3p.
JOURNAL: **Scientific Reports**. 2017, volume 7(41099).
DOI: https://doi.org/10.1038/srep41099.

PATENTS

The data described in this work have generated the following Patent Application:

INVENTORS: García Bermejo, Laura; Conde Moreno, Elisa; **Giménez Moyano, Sara**; Martín Gómez, Laura.
TITLE: miR-127 agents for use in the treatment of renal fibrosis.
APPLICATION NUMBER:
European Application: 16382399.0.
International Application: PCT/EP2017/070223August2017.
ENTITY HOLDING: Fundación para la Investigación Biomédica del Hospital Ramón y Cajal.

COMMUNICATION TO SCIENTIFIC MEETINGS

International Meetings

AUTHORS: **Giménez Moyano, Sara**; Conde, Elisa; Rodríguez, Macarena; Ramos, Edurne; Marín Gómez, Laura; Rodríguez, Eulalia; Villar, María Luisa; García Bermejo, María Laura.
TITLE: "**miR-127 modulates macrophage polarization in renal fibrosis".**
TYPE OF PRESENTATION: Oral communication.
CONGRESS: International Congress of Immunology (ICI) 2016.
VENUE: Melbourne, Australia.
DATE: August 21-26th, 2016.

AUTHORS: Martín Gómez, Laura; Aguado Fraile, Elia; Ramos, Edurne; Conde, Elisa; Rodríguez Serrano, Esperanza Macarena; **Giménez Moyano, Sara**; Jiménez Álvaro, Sara; Liaño, Fernando; García Bermejo, María Laura.
TITLE: "**MiRNAs as novel biomarkers and therapeutic target in Chronic kidney disease"**.
TYPE OF PRESENTATION: Poster.
CONGRESS: American Society of Nephrology (ASN) Meeting, kidney Week 2015.
VENUE: San Diego, USA.
DATE: November 3-8th, 2015.

AUTHORS: Rodríguez Serrano, Esperanza Macarena; Galeano, Cristina; Ramos, Edurne; Conde, Elisa; Martín Gómez, Laura; **Giménez Moyano, Sara**; Liaño, Fernando; García Bermejo, María Laura.
TITLE: "**MiRNAs as novel biomarkers for transplanted patient's evolution"**.
TYPE OF PRESENTATION: Poster.
CONGRESS: American Society of Nephrology (ASN) Meeting, kidney Week 2015.
VENUE: San Diego, USA.
DATE: November 3-8th, 2015.

National Meetings

The data described in this work and collaborations have generated the following congress communications:

AUTHORS: **Giménez-Moyano S**., Blanco C., Crespo L., Salinas-Muñoz L., Rodríguez E.M., Serrano-Huertas S., Ramos E., Conde-Moreno E, García-Bermejo L.
TITLE: "**miR127 as a novel mediator in fibrosis development and macrophage polarization in Chronic Kidney Disease".**
TYPE OF PRESENTATION: Poster.
CONGRESS: CNIC PhDay 2019.
VENUE: Madrid, Spain.
DATE: November 22nd, 2019.

AUTHORS: **Giménez Moyano, Sara**; Crespo, Lorena; Salinas, Laura; Blanco Agudo, Carolina; Rodríguez, Esperanza Macarena; Ramos, Edurne; Serrano Huertas, Silvia; Conde, Elisa; García Bermejo, María Laura.
TITLE: "**miR127 as a critical mediator in Chronic Kidney Disease (CKD) role in macrophage polarization".**
TYPE OF PRESENTATION: Poster.
CONGRESS: 2nd Congress of the Spanish Society of Biochemistry and Molecular Biology (SEBBM).
VENUE: Madrid, Spain.
DATE: July 16-19th, 2019.

AUTHORS: Díaz Crespo, Francisco Javier; Velásquez Villarroel, MA; **Giménez Moyano, Sara**; Acevedo Ribó, Mercedes; García Bermejo, Laura; Fernández Juárez, Gema; Villacorta Pérez, Javier.
TITLE: "**Diferencias en el infiltrado de macrófagos CD163^{+} entre los diferentes subtipos histológicos de pacientes con vasculitis renal asociada a ANCA y su correlación clínica".**
TYPE OF PRESENTATION: Poster.
CONGRESS: XXIX Congreso Nacional de la Sociedad Española de Anatomía Patológica, XXIV Congreso Nacional de la Sociedad Española de Citología y V Congreso Nacional del Sociedad Española de Patología Forense.
VENUE: Granada, Spain.
DATE: May 22-24th, 2019.

AUTHORS: Díaz Crespo, Francisco Javier; Velásquez Villarroel, MA; **Giménez Moyano, Sara**; Acevedo Ribó, Mercedes; García Bermejo, Laura; Fernández Juárez, Gema; Villacorta Pérez, Javier.
TITLE: "**Expresión del óxido nítrico sintasa endotelial (eNOS) en vasculitis renal asociada a ANCAS y su correlación clínico-patológica".**
TYPE OF PRESENTATION: Poster.
CONGRESS: XXIX Congreso Nacional de la Sociedad Española de Anatomía Patológica, XXIV Congreso Nacional de la Sociedad Española de Citología y V Congreso Nacional del Sociedad Española de Patología Forense.
VENUE: Granada, Spain.
DATE: May 22-24th, 2019.

AUTHORS: Velásquez Villarroel, MA; **Giménez Moyano, S**; Villacorta Pérez, J; Díaz Crespo, F; Acevedo, M; Conde, E; Cases, C; Sánchez Álamo, B; García Bermejo, L; Fernández Juárez, G.
TITLE: "**Expresión del óxido nítrico sintasa endotelial (eNOS) en vasculitis renal asociada a ANCAS y su correlación clínico-patológica".**
TYPE OF PRESENTATION: Poster.
CONGRESS: XLVIII Congreso y de la Sociedad Española de Nefrología (SEN) y IX Congreso Iberoamericano de Nefrología.
VENUE: Madrid, Spain.
DATE: November 19th, 2018.

Annexes

Annex 1. Baseline clinical settings of PRONEDI cohort

Characteristics	PRONEDI (n=100)	P-value
Age - yr	68 ±8	0.55
Male sex – no. (%)	81 (80)	0.80
BMI - kg/m^2	30.9 ±5.0	0.12
Blood pressure – mmHg		
Systolic	148 ±17	0.22
Diastolic	79 ±10	0.44
Serum creatinine - mg/dL	1.58 ±0.47	0.69
HbA1C - (%)	7.1 ±1.3	0.61
PTH - pg/mL	72±58	0.36
c-LDL - mg/dL	101 ±31	0.04

Chronic Kidney Disease (CKD) is worldwide recognized as a priority health problem because of its high prevalence and incidence. It courses with a long clinically silent period, therefore diagnosis and treatment occur during advanced stages of the disease. Identification of molecular mechanisms underlying chronic renal injury and searching for early biomarkers of CKD are essential for improving our understanding of CKD pathophysiology and patient management.

microRNAs (miRNAs) are key regulators of gene expression that have emerged as a novel therapeutic target and useful biomarkers for pathology. In our lab we identified a set of miRNAs, including miR-127-3p, that remain altered after an AKI episode. We also demonstrated the protector role of miR-127-3p against ischemic injury in renal tubular cells. Moreover, bibliography has described miR-127-3p as a mediator in macrophage polarization during lung fibrosis. For all above, we aim to investigate the role of miR-127-3p in macrophage polarization during renal fibrosis underlying CKD and its modulation as a novel therapeutic strategy for the disease.

For this, we have studied miR-127-3p expression in a mouse model of renal fibrosis (UUO), and the effect of its exogenous modulation during disease development. We have demonstrated miR-127-3p increases along disease progression in proximal tubules, correlating with fibrosis and the inflammatory response in which macrophages are key cells involved. Besides, we have demonstrated that inhibition of miR-127-3p expression in UUO mice aggravates disease progression and exacerbates associated inflammatory response, including macrophages. Moreover, we have studied the expression of miR-127-3p and the effect of its modulation in naïve murine macrophages (Mϕ) and different induced phenotypes (M1[LPS] and M2[IL-4]). Results have shown that the expression of miR-127-3p does not change depending on the stimulus received. However, NOS2 expression, as a M1 macrophage marker, shows a positive tendency when the miRNA is inhibited in the cells. On the other hand, miRNA over-expression in the M2a [IL-4] phenotype leads to a decrease of NOS2, which suggests that the induction of miR-127-3p expression along the kidney injury modulate macrophages response and contribute to disease outcome. Based on these findings, we have tried different viral-based particles and administration approaches, and finally, we have successfully induced miR-127-3p expression in the renal cortex of mice using lentiviral particles injected through the renal arteria.

Finally, decreased serum levels of miR-146a-3p, miR-27a-3p, and miR-93-3p have been associated with CKD progression. Whereas miR-127-3p, miR-146a-3p, miR-27a-3p, and miR-26b-5p serum levels have demonstrated correlation with renal damage parameters.

In summary, all these results have revealed that miR-127-3p is involved in renal fibrosis as an important mediator of CKD development by affecting macrophages polarization, and therefore its modulation could be a potential therapeutic approach for CKD. Moreover, some studied miRNAs could serve as a useful and minimum-invasive biomarkers that contribute to stratification and patient management.